

AD-A260 762



DTIC
ELECTE
FEB 13 1993
S C D

(1)

Small Satellites and RPAs in Global-Change Research

UNCLASSIFIED STATEMENT A
Approved for public release
Distribution Unlimited

MITRE

93-02518

REPORT DOCUMENTATION PAGE			Form Approved OMB No. 0704-0188	
Public reporting burden for this collection of information is estimated to average 1 hour per response, including the time for reviewing instructions, searching existing data sources, gathering and maintaining the data needed, and completing and reviewing the collection of information. Send comments regarding this burden estimate or any other aspect of this collection of information, including suggestions for reducing this burden, to Washington Headquarters Services, Directorate for Information Operations and Reports, 1215 Jefferson Davis Highway, Suite 1204, Arlington, VA 22202-4302, and to the Office of Management and Budget, Paperwork Reduction Project (0704-0188), Washington, DC 20503.				
1. AGENCY USE ONLY (Leave blank)	2. REPORT DATE December 1, 1992	3. REPORT TYPE AND DATES COVERED		
4. TITLE AND SUBTITLE Small Satellites and RPAs in Global-Change Research			5. FUNDING NUMBERS PR - 8503A	
6. AUTHOR(S) P. Banks, J. Cornwall, F. Dyson, N. Fortson, P. Garwin, S. Koonin, C. Max, G. MacDonald, S. Ride, M. Ruderman, S. Treiman, J. Vesecky, R. Westervelt, F. Zachariasen				
7. PERFORMING ORGANIZATION NAME(S) AND ADDRESS(ES) The MITRE Corporation JASON Program Office A10 7525 Colshire Drive McLean, VA 22102			8. PERFORMING ORGANIZATION REPORT NUMBER JSR-91-330 ✓	
9. SPONSORING / MONITORING AGENCY NAME(S) AND ADDRESS(ES) Department of Defense Washington, DC 20301-7100			10. SPONSORING / MONITORING AGENCY REPORT NUMBER JSR-91-330	
11. SUPPLEMENTARY NOTES				
12a. DISTRIBUTION / AVAILABILITY STATEMENT Approved for public release; distribution unlimited.			12b. DISTRIBUTION CODE	
13. ABSTRACT (Maximum 200 words) This report contains an investigation of those global change science problems that can be addressed by remotely piloted aircraft or by small satellites, including the relationship to the NASA EOS program. New types of measurements that could be made possible by such satellite or aircraft platforms are pointed out. Issues of technical feasibility and cost are examined, as well as the role of new technology developed through DOD and other programs. Possible joint DOD/Global Science satellite missions are also discussed.				
14. SUBJECT TERMS remotely piloted aircraft, cloud albedo, oxidants, imaging IR detectors, LIDARS			15. NUMBER OF PAGES	
			16. PRICE CODE	
17. SECURITY CLASSIFICATION OF REPORT UNCLASSIFIED	18. SECURITY CLASSIFICATION OF THIS PAGE UNCLASSIFIED	19. SECURITY CLASSIFICATION OF ABSTRACT UNCLASSIFIED	20. LIMITATION OF ABSTRACT SAR	

Abstract

This report contains an investigation of those global change science problems that can be addressed by remotely piloted aircraft or by small satellites, including relationship to the NASA EOS program. New types of measurements that could be made possible by such satellite or aircraft platforms are pointed out. Issues of technical feasibility and cost are examined, as well as the role of new technology developed through DOD and other programs. Possible joint DOD/Global Science satellite missions are also discussed.

Contents

1	SMALL SATELLITES AND RPAs: SUMMARY AND CONCLUSIONS	1
1.1	Scientific Scope of the Study	2
1.2	Remotely Piloted Aircraft	3
1.2.1	Potential Advantages of RPAs	4
1.2.2	Issues to be Resolved	6
1.2.3	Instrumentation and Measurement Requirements	7
1.3	Small Satellites	9
1.3.1	Potential Advantages and Disadvantages	9
1.3.2	Lightweight Support Hardware and Instrumentation	10
1.3.3	Specific Small-Satellite Missions and Instruments	12
1.4	A DARPA Joint Global Change/Surveillance Satellite	14
1.4.1	Visible/IR Cloud, Radiation, and Surveillance	14
1.4.2	Dual-Purpose Lidar	15
1.5	Role of DOD Science and Technology	16
1.6	Recommendations	17
2	SCIENTIFIC OBJECTIVES OF GLOBAL CHANGE RESEARCH	21
2.1	General Types of Observational Missions	21
2.2	Major Scientific Issues in Global Change Research	23
3	CLOUDS AND RADIATION	29
3.1	Introduction	29
3.2	Simple Model of Cloud Optical Properties	35
3.3	Cloud Forcing	39
3.4	Factors Affecting the Radiation Balance of Clouds	43
3.5	Global Warming	46
4	THE USE OF RPAs IN SUPPORT OF THE ATMOSPHERIC RADIATION MEASUREMENT PROGRAM	51
4.1	Small RPA Instrument Packages for ARM Measurements	52
4.2	RPA Platform Requirements	56
4.3	Manned Aircraft vs. Existing and Proposed RPAs	62
4.4	FAA Requirements	67

4.5	Conclusions Regarding RPAs in ARM	68
4.6	Data Management	70
4.7	A Role for Balloon Flights: Instrument Testing and Development	72
5	INFLUENCING CLOUD ALBEDO FOR PROCESS DIAGNOSTICS	77
5.1	Introduction	77
5.2	Cloud Albedo	78
5.3	Seeding Droplet Growth	79
5.4	Observed Cloud Condensation Nuclei	87
5.5	Sea Surface Sulfur Emission and Oxidants	90
5.6	Cloud Process Experiments	91
6	OZONE DEPLETION	97
6.1	Present Situation in the Arctic	97
6.2	Obtaining better information	99
7	IR DETECTORS FOR RPAs AND SMALL SATELLITES	105
7.1	Classes Of Imaging IR Detectors	105
7.2	Applications Of Imaging IR Detectors For Radiation Measurements	109
8	POTENTIAL USES FOR SMALL SATELLITES IN THE STUDY OF GLOBAL CLIMATE	115
8.1	Process studies	115
8.2	Long-term Monitoring	118
8.2.1	Precursors to EOS	118
8.2.2	Adjuncts to EOS (satellites which could fly simultaneously with EOS)	119
9	CANDIDATE SCIENCE MISSIONS FOR SMALL SATELLITES	121
9.1	Introduction	121
9.2	Specific Proposed Missions	122
10	ISSUES IN THE CHOICE OF ORBITAL COVERAGE FOR SMALL SATELLITES	129
10.1	Flexible Space-Time Coverage	129

10.2 Implications of Diurnal Variability	134
10.2.1 The Context of Diurnal Variability	134
10.2.2 An Important Role For Small Satellites	136
11 SMALL SATELLITE INSTRUMENTS TO ADDRESS PROBLEMS FACING PRESENT EOS-CLASS EXPERIMENTS	147
11.1 Solid-state Lasers for LIDARS and Laser Rangers	147
11.2 Synthetic Aperture Radars (SARs)	148
11.3 A High Resolution Imaging Spectrometer (HIRIS)	152
12 SOME POSSIBILITIES FOR JOINT SURVEILLANCE /GLOBAL CHANGE SMALL SATELLITES	157
12.1 Surveillance vs Global Change	158
12.2 Visible/IR Satellite	161
12.3 Dual-Mode Lidar Satellite	164
12.4 The DARPA Proposal	167
A PRE-1998 EARTH SYSTEM SCIENCE EXPERIMENTS CURRENTLY PLANNED FOR SATELLITES	171
B MULTIPLE SATELLITE PERFORMANCE FOR EOS MISSION: (Presentation Made by R.L. Garwin to the EOS Engineering Review Advisory Committee, La Jolla, CA, July 1991)	185
B.1 Coincidence in Space and Time	185
B.2 Pointing	189
B.3 Pointing Accuracy and Stability	190

1 SMALL SATELLITES AND RPAs: SUMMARY AND CONCLUSIONS

JASON has now conducted two studies on the use of small satellites and remotely-piloted aircraft (RPAs) in global change research, with special reference to the DOE Atmospheric Radiation Measurement (ARM) program and to DARPA's Small Satellite program. The studies centered around two meetings, one in January and the other in June, 1991, to which we invited representatives of most areas of the global change program and of the DOD satellite science and technology community. We have already issued a report on the Winter Study. Here we present a more comprehensive report based mainly on our Summer Study. In this first section, we summarize the main themes and results, leaving a more complete discussion to later sections devoted to each major topic.

The charge from DOE and DARPA to JASON was to elucidate global change science problems that can be answered by small satellites and RPAs; investigate the role of DOD technology in global change research; and (for DARPA) propose small satellite sensor packages which simultaneously address a remote-sensing mission of interest to DOD and a related one of interest in global change science. In addition, we were asked to brief the EOS Engineering Review on our findings.

The Winter Study served to introduce people from a variety of technological communities to one another's problems and possible mutual interests. Our report on this study was itself introductory, dealing in broad terms with the technology of RPAs, small satellites, their instrumentation and support

hardware, and the scientific issues they could address. It was clear during the Winter Study that the involved communities' knowledge of each other's needs was not necessarily as great as their interest in each other.

At the Summer Study we found that many of the participants had made progress since the Winter Study and could, for example, make definite and quantitative proposals for small lightweight instruments for RPAs and small satellites. Our Summer Study report in turn deals as quantitatively as we now can with the issues first raised in the Winter Study and their further evolution as of the summer of 1991.

1.1 Scientific Scope of the Study

We investigated those parts of global change research which are reasonably closely connected with the ARM program. This DOE program is devoted to surface-based site studies of cloud and radiation dynamics (with possible aircraft and satellite support, as we discuss in this report), with an eye toward understanding processes and providing input for global circulation models (GCMs). We divide the scientific scope of the study into three areas:

1. Cloud and radiation dynamics, including radiation budgets and cloud radiative feedback processes.
2. Precipitation, water vapor column content and profiles, cloud formation.

3. Upper tropospheric and stratospheric dynamics and constituents, including greenhouse gases, aerosols, and polar stratospheric clouds.

For the most part we will be concerned with studies of the natural environment, but we also discuss an active modification experiment (sulfur aerosol seeding over the ocean) which could profitably be studied with small satellite and RPA sensors.

1.2 Remotely Piloted Aircraft

We have looked closely at airborne measurements that fit within the scientific scope of our study, such as those required for understanding clouds and the cloud/radiation interaction as part of the ARM program. We find that RPAs could make a vital—perhaps essential—contribution to ARM through continuous measurements above a CART site to obtain accurate vertical profiles of upper tropospheric radiation, water vapor, water droplets, ice particles, aerosols, and cloud structure, to complement the surface-based measurements. We also find a compelling case for using RPAs to study ozone depletion in the stratosphere.

Why should RPAs be used instead of ordinary aircraft for the measurements we are considering? There are great potential advantages relating to: cost, endurance aloft, altitude ceiling, and pilot safety. It is important to note that these potentialities have not been fully realized, but the technology to turn them into realities seems to be mainly straightforward and near-term. The significant issues that still remain unresolved are: high altitude reciprocating-engine development, RPA crash rate, and FAA approval

for flights in the US. In addition, since economics heavily favors small RPAs (at least in the near future), light-weight science instrumentation must be developed, especially for the visible and IR radiation measurements. We discuss all these questions in the next three subsections.

1.2.1 Potential Advantages of RPAs

RPAs have benefited from advances during the past decade in design codes (for operating at ceiling between stall and Mach divergence), strong and light composite structures, turbocharged engines, and miniaturization of control systems, giving such aircraft important advantages for global change research:

1. Cost. Economically, small RPAs are the only potentially feasible possibility for nearly continuous airborne measurements within ARM, the more so if two or more aircraft are to be flown simultaneously for accurate radiation divergence measurements. The operating costs for the manned higher altitude research aircraft currently in use or planned (ER-2, Sabreliner, WB 57F) average over \$4000/hr, far too expensive for a complete ARM mission. The vendors of small RPAs with performance suitable for ARM suggest RPA acquisition costs of \$1M or less, and hourly operating costs of \$500/hr. Of course, it remains to be seen whether these costs can actually be realized. Uncertainties in high altitude engine development and especially in RPA crash rate (each discussed in Section 1.2.2 below) affect any overall cost estimate.

Aurora's estimate of \$20M-\$25M total cost, exclusive of scientific

instrumentation, for a 5-year ARM program using a Perseus B system seems reasonable enough for the assumptions they made: a range of loss rates up to 1 every 200 missions, no expensive developmental problems with the high altitude engine, and one aircraft aloft continuously. Flying two or more aircraft together for radiation divergence measurements would of course either add to the cost or subtract from the fraction of time covered. To this estimate must be added the total cost of the instrumentation, including the instrument-loss appropriate for a given RPA crash rate.

2. Endurance Aloft. RPAs can fly for 24 hours at a time or longer. A diurnal cycle of actual measurement time is necessary for most missions. As just one example, changes in cirrus clouds between day and night are important for the radiation budget but have not been measured yet.
3. Altitude. RPAs are expected to operate at higher altitudes (> 20 km) than manned aircraft, which is crucial for studying ozone depletion and other stratospheric processes. To be useful for ARM they need operate only in the upper troposphere, from about 8 to 18 km, though only one RPA (the Boeing Condor, which is huge and very expensive) has actually done this yet.
4. Pilot Safety. RPAs eliminate the issue of pilot risk, which otherwise can complicate or prevent extended or dangerous oceanic, polar, or night flights. Missions with risk of RPA loss at the level of one per 200 flights may be tolerable economically, but such risk is far too high when a pilot's life is involved.

1.2.2 Issues to be Resolved

RPA's certainly hold much promise, but there remain important uncertainties affecting their cost and utility:

1. High Altitude Engine. The Amber aircraft have been tested up to about 8 km, but the performance of light RPA's at higher altitudes is not yet validated. It is straightforward and cheap to build a high-altitude airframe for a small RPA, and the existing avionics—which is an expensive part of an RPA—can be used with little change. The uncertain part is developing reciprocating engines, either multiply turbocharged or carrying onboard oxidizers. The recirculating engine now under construction for operation at stratospheric altitudes onboard Perseus A will be tested soon. The airbreathing, doubly turbocharged engines currently under consideration for ARM, which must operate over a wide range of pressure differentials up through the troposphere, remain to be developed.
2. Crash Rate. RPA's have a history of much higher crash rates than manned aircraft. The RPA's envisioned here could follow flight paths that avoid weather hazards and should have sufficient endurance (> 40 hours) to carry out a diurnal mission and still remain at high altitudes when necessary to ride out storms. At an ARM site in the western US it should be possible to operate takeoff and landing between storms, and maintain nearly continuous measurement time aloft. Nevertheless, we find it difficult to predict the crash rate in advance of some operational flight tests.

3. FAA Approval. Such approval will be required for flights above the US ARM site, or an expensive manned chase aircraft may be required at some altitudes. Developing safe protocols for assuring flight safety without any manned aircraft seems possible, but remains an unresolved issue.

1.2.3 Instrumentation and Measurement Requirements

A 100-200 kg instrument package must be developed for a complete set of RPA-based measurements for ARM. The standard PMS instruments should be adequate for *in situ* droplet and ice particle sampling. The 60-foot wingspan and light weight of the proposed Perseus B or Gnat 750-93L permit speeds as low as 80 m/s at upper troposphere altitudes, which are slow enough for accurate sampling of sub-100 μm particles (a major difficulty with the high speeds of the manned aircraft now in use). A reliable measure of the total H_2O content is also necessary. If the Lyman α photofragmentation technique proves inadequate, one might consider microwave sounding (perhaps in conjunction with a ground-based transmitter).

The visible/IR instruments could utilize recent improvements in detector technology, focal plane arrays, and miniaturization of support hardware, and have the potential (with some modifications) for also meeting requirements of small satellites for instruments of similar weight and capability. The proposal from the combined DOE Labs (radiometer, multispectral imager, camera, and lidar) is a promising first step in such a design. For high precision radiance measurements, position and pointing accuracy become important. To meet these requirements it should be sufficient to locate the position of

the RPAs within 100 m by GPS and to mount the radiometers on gimbals and point them to within 10^{-2} rad with compact gyros.

Assuming RPAs were to be deployed, we have investigated using them for some possible active experiments such as seeding a local ARM site with sulfides and/or oxidants, and detecting the effects on cloud droplets and albedo with the RPAs. Distributing about a ton of sulfur in one week within a 20-km region would suffice to study important details of the aerosol/droplet process.

Higher altitude (20-30 km) RPAs would be the best platforms for studying the mechanism of ozone depletion and other processes in the stratosphere. One essential task is to study the chemistry and transport of Cl and N, and the formation of polar stratospheric clouds in the northern hemisphere that could lead to an Arctic ozone hole similar to the Antarctic hole if greenhouse gases begin to cool the stratosphere. It might be possible to combine important stratospheric and tropospheric missions of RPAs at the proposed Arctic ARM site.

In comparing RPAs with small satellites, we note that even though some instruments may have much in common, there is a great difference between the overall cost of a small satellite program and an RPA program. Moreover, as described above, RPAs add crucially to the ARM program, making measurements at altitudes beyond the range of the surface-based ARM remote sensors. Many of these measurements cannot be made from satellites (for example, radiation flux as a function of altitude, in situ measurements, etc.). For these reasons, RPAs should have priority over small satellites in the ARM program.

1.3 Small Satellites

Satellites of all sizes will continue to be the major sensor platforms for many global change missions within the scope of our study, and as such are important to ARM. However, for a number of reasons the time is ripe to develop several small satellites for cloud, radiation, and other atmospheric studies, and we will discuss these independently of their direct connection to ARM. It is unlikely in any case that the ARM program, even with an augmented budget, would allow for the full development of a small satellite program, but ARM could contribute much by, e.g., supporting the development of small lightweight instruments.

We also address the DARPA charge to JASON to propose small-satellite concepts for joint tactical surveillance and global-change missions.

Our purpose here is to evaluate small satellite technologies and the need for particular missions. We do not make recommendations on which government agencies should be given responsibility for the specific missions we discuss.

1.3.1 Potential Advantages and Disadvantages

Small satellites are interesting because they should allow fast and flexible response to changing requirements and new developments; a smooth budget cycle; and make it possible to field constellations to meet certain coverage requirements. For example, measuring the radiation budget to a pre-

cision of $< 1\%$ requires at least three satellites in orbit at the same time for proper diurnal coverage. On the other hand, small satellites may have some disadvantages: higher cost per payload pound, because of multiplication of satellite support hardware; and failure to meet simultaneity requirements for numerous instruments to be at the same place at the same time.

Our judgment for satellites is that meeting many of the science needs within the scope of our study (including the need for constellations) can be done with small satellites without violating any fundamental requirements of simultaneity, and that the current and near-term programs for miniaturization of satellite support hardware, such as DARPA's Small Sat program, and of sensors, makes it very attractive to develop a small-satellite program for global change. This, of course, would go well beyond the scope of the ARM program, and participation of agencies such as DARPA would be of material assistance.

1.3.2 Lightweight Support Hardware and Instrumentation

The DARPA Small Sat program has already gone a long way toward developing lightweight satellite support technology, including guidance and control systems; on-board computers; inflatable solar arrays; and a common small-satellite bus. Lightweight support hardware is the way to get a high payload-to-total mass fraction, thus reducing the launch cost per payload pound. DARPA's goal is to push the payload-to-total mass fraction up to about 0.7, which will be spectacular if it is achieved.

The next step will be to develop lightweight instruments, which is a less well-developed technology thrust. We have looked at several proposals in this direction, including some Livermore-Los Alamos-Sandia concepts for radiometers, imaging IR spectrometers, and lidars and similar ideas for a Livermore Brilliant Eyes small-satellite constellation. For the most part, these and other concepts for lightweight sensors are serious and interesting, and well worth further investigation and selection of some for full-scale engineering design. We have already mentioned that such concepts will also be important in the development of RPAs for global change research.

Current versions of instruments with similar functions, developed by NASA and NOAA, are heavy by comparison. As one example, the MODIS-N imaging IR spectrometer for NASA's EOS-A satellite, which is intended to measure ocean color and other surface properties, and cloud properties as well, weighs 200 kg, while newly proposed imaging spectrometers, designed mainly just for cloud properties, are supposed to be closer to 20 kg. While the NASA/NOAA instruments in most cases have a proven space-flight heritage that the new proposals do not, and there are reasons for the NASA/NOAA sizes and weights, there are no reasons we know of which one could use to dismiss easily the light-weight instrument concepts for scientific missions of great interest, and we urge support for their development. In this connection, one should avoid the trap of obsession with exceedingly small size and weight. The idea is to do one's reasonable best in meeting the goals of small size and weight, but let the science objectives determine the overall satellite size. There is a lot of room between a Pegasus-class (~ 200 kg) payload and a Titan-IV or Shuttle payload ($> 12,000$ kg).

1.3.3 Specific Small-Satellite Missions and Instruments

Three specific small-satellite missions we propose, each tied to one element of the science scope defined in Section 1.2 are:

1. Earth Radiation Budget: Includes a radiometer in the NASA CERES class, plus a lightweight imaging IR spectrometer (generically, an IIRS). CERES itself is not very heavy (80 kg), but requires a co-flying IIRS for cloud information to attain the desired accuracy of $\leq 1\%$ in the regional monthly average radiation budget, and then only when there are three such satellites in orbit at the same time. The need could be met by a small IIRS with spatial resolution of 1 km, which could weigh less than 30 kg (when scaled to 800 km altitude) according to designs we have seen, allowing a Pegasus-class payload. With accelerated funding for CERES, and development of a suitable lightweight IIRS (possibly within DOE), a mid-decade launch seems possible. This is an important mission for connecting with earlier ERBE data, for laying a baseline for later measurements, and particularly for overlapping with ARM and FIRE; and we urge that a constellation of three satellites be considered for the earliest possible start.
2. Global Humidity and Precipitation: A microwave nadir sounder and an IIRS optimized for this mission should fit in a 200 kg payload, and could measure surface temperature and column-integrated humidity, but would provide only $\pm 50\%$ rainfall accuracy. Better measurement of precipitation requires a rain-radar such as the 400 kg instrument to be tested on aircraft for the tropical rainfall (TRMM) satellite scheduled for 1997, and also planned for the JEOS satellite. We believe small

satellites have a future role to play here, building on what is learned during TRMM and providing sufficient coverage for complete tropical and possibly global precipitation, now one of the major unknowns in global science. The exact size of satellites for this mission depends upon progress in developing small radars.

3. Satellite Limb-Scanning: Includes an IR (and possibly also a microwave) limb sounder; an IIRS optimized for limb viewing; possibly solar/lunar occultation limb scanners, a solar irradiance monitor. Polarimetry would be useful for aerosols.

In addition to these specific missions we propose the development of lightweight lidars and radars for use in many global-change applications:

Lightweight Lidars. We suggest that individual, small solid-state lasers could be separately optimized for preliminary investigation of several missions proposed for the EOS Geoscience Laser Ranging System (GLRS). For example, separate small satellite Lidars could begin testing ice-sheet altimetry, along track cloud profiles, and cloud backscatter cross sections. These mission goals, if taken one-by-one, may be feasible with present technology developed in DOD and DOE programs.

Synthetic Aperture Radars (SARs). Capabilities of dual-polarization or dual-frequency SARs can be developed on small satellites (as a complement to brief shuttle flights). A design for a Pegasus-launched dual-polarization SAR illustrates that it is feasible for such an instrument (340 kg satellite total mass) to collect a dual-polarization SAR image every other orbit, and to store four such images prior to down link. As with the Lidar, such a small SAR could provide a way to push along the development of larger,

EOS-class instruments without requiring such a costly initial investment or lengthy development cycle.

1.4 A DARPA Joint Global Change/Surveillance Satellite

DARPA requested JASON to come up with some concepts for such a satellite, and has proposed one of its own which we will discuss later. Before going into our concepts, we note that the spatial and spectral resolution requirements of passive sensors, and the power requirements for, e.g., lidars, are generally rather different for global change research and for surveillance. As an example, one might want spatial resolution as fine as 1 m for surveillance, while anything finer than 250 m or even 1 km is not needed for global change. Conversely, good spectral resolution ($\Delta\lambda/\lambda \sim 10^{-2}$) and carefully-calibrated precision might be needed for science, but not necessarily for surveillance (although the added value of well-calibrated irradiances may be helpful for DOD missions as well).

1.4.1 Visible/IR Cloud, Radiation, and Surveillance

(This is an area in which DARPA has also made a proposal; the ideas developed here are our independently developed approach.) The main sensors are a visible CCD focal-plane array (FPA) with 30-cm optics aperture, capable of 1 m resolution from low-earth orbit (LEO); and an IR bolometer focal-plane array (FPA) of the type described in Section 1.5 below, say of

size 512×512 and capable of $\lesssim 100 \mu\text{rad}$ resolution. Adequate spectral resolving power for global change could be gotten with a circular variable filter or linear wedge filter, or even a Michelson interferometer if necessary. The IR FPA would be used as a multi-pixel array for high spatial resolution and low spectral resolution, but could be used as a single- (or few-) pixel detector for the converse conditions. The main aperture would scan to arrive at a desired swath coverage.

1.4.2 Dual-Purpose Lidar

DARPA and ONR are working on a small-satellite-mounted Nd:YAG lidar, to be used for ocean-surface observation for a classified purpose. The needed lidar is quite powerful, and only runs on a 5% duty cycle (using solar arrays and batteries). ONR proposes to run the lidar at its fundamental wavelength of $1.06 \mu\text{m}$ with a silicon CCD array, but it is probably just as good to frequency-double the laser, in part because of the much greater quantum efficiency of silicon at $0.53 \mu\text{m}$. The same lidar, run at ~ 0.1 mJ/pulse at 40 Hz, with frequency-doubling and perhaps tripling, would be very useful in global change research for measuring cloud heights and structure; ice sheet height; and properties of atmospheric aerosols (cf. the NASA instrument SWIRLS, proposed for EOS-B). We propose, therefore, that the DARPA-ONR lidar be capable of dual-power operation, presumably by adjustment of the diode laser pumping power, and that it would then serve usefully its surveillance function as well as atmospheric and earth-sensing functions.

1.5 Role of DOD Science and Technology

Various DOD agencies and services, including DARPA, SDIO, the Army and Air Force, have an increasing interest in and commitment to both small-satellite technology and to sensors which might play a role in global change research. We have already mentioned a number of examples: the DARPA Small-Sat program, lidars, small SARs, IR FPAs. These last are being developed for the Army as tactical night-vision sensors, but have a good potential for use in global change research; they consist of large numbers of, e.g., vanadium-oxide bolometers some $50 \mu\text{m}$ square on a silicon chip. Their detectivity and FPA uniformity are in a range of interest for climate research.

While small-satellite support hardware is of immediate use for global-change satellites, and is rather near-term technology for the most part, the requirements for DOD sensors are typically different from those used for global change. For example, DOD needs passive IR sensors for space use that look at small 300°K bodies in a few spectral bands against a space background or high limb, or at thrusting boosters; or for tactical (i.e., background-limited) night-vision sensors with good spatial resolution, low or no spectral resolution, with good but not exceptional ($< 1\%$) pixel uniformity. There is some need for calibration, but not at the level ($< 1\%$) needed for the radiation budget. (However, we were pleased to note that at least one spectrometer designed for space viewing with a circular variable filter has been calibrated to an absolute accuracy of $\sim 2\%$ against a blackbody from 5 to $24 \mu\text{m}$.) As a result, there are no DOD instruments which can be directly used in global change research, with its emphasis on spectral resolving power and calibrated precision, and lack of interest in high spatial resolution. Nor, in

fact, are many of the current DOD sensors made to be especially small and light.

Nonetheless, there is much of value in current DOD sensor and small-satellite technology that can be transferred to the global-change community, and, as we have said, increasing interest in participating in the global-change mission through such vehicles as SERDP (Strategic Environmental Research and Development Program). Unfortunately, the past and current level of effort in this technology transfer is too small to be successful, and should be increased substantially, both on the part of DOD and non-DOD agencies. One still finds that the civilian and military communities misunderstand one another; for example, there is a certain resistance on the part of the NASA-oriented research community to the thought of multi-pixel (let alone full focal-plane) arrays, in part for reasons of unacceptable non-uniformity and need for individual pixel calibration, although multiple pixels (not necessarily a full FPA) are certainly very helpful in evaluating radiation measurements. On the other hand, for the DOD community to argue for full FPAs without meeting the requirements of pixel uniformity and precision would not be helpful. There is much room for fruitful compromise here, either with dual-use FPAs (see point 1.4 above), or with multi-pixel arrays that do not contain many thousands of detectors, each one of which must be individually calibrated, but perhaps only a few dozen.

1.6 Recommendations

1. Lightweight instruments and support hardware may be essential for the successful use of RPAs and small satellites in global-change research.

We recommend that both DOE and DARPA (see point 5 below) support programs in these areas, with near-term instrument emphasis on cloud and radiation sensors. Other DOD agencies can play vital roles and should be asked to participate at a significant level of effort. These are very appropriate projects for SERDP funding.

2. Development of RPAs and their instruments should be the first priority for augmenting the ARM program. It will also be necessary to construct a comprehensive measurement strategy for RPAs in ARM, including measurement accuracies needed, flight paths, implications for aircraft performance, mix of manned, unmanned aircraft and balloons, and the impact on the ARM plans for data management.
3. Aside from lightweight instruments, it will be necessary for DOE to participate in the evolutionary development of RPAs themselves. This includes using existing RPAs, such as Amber, if possible, for mid-altitude tests and missions, and using near-term high-altitude RPAs such as Perseus A for high altitude tests. DOE should participate in support of high-altitude long-endurance engine development, such as a two-stage turbocharged engine.
4. Small satellites are important adjuncts to ARM, and could be essential in carrying out near-term cloud and radiation studies of broader scope. We strongly urge that DOE participate (with other agencies) in fielding by the mid-nineties a fleet of at least three concurrent cloud and radiation satellites, carrying a radiometer (CERES or lightweight follow-on) and a lightweight IR imaging spectrometer. Some of the participating satellites can be already-planned flights with add-on instruments. The goal is to have the satellites in orbit during the ARM measurement period, and to shorten the gap between ERBE cloud/radiation studies

and NASA radiation budget programs of the next century.

5. We recommend that DARPA carry out an engineering and science design study of a small satellite for tactical surveillance, components of which might then be of use for a global change mission. If judged successful, this study should lead to joint DARPA support, with other agencies, of the necessary lightweight instrument and support hardware development. Any satellite launched under this program is likely to have its greatest impact if it is flown while ARM is operating, within the next decade.

6. In this report we point out several earth-monitoring missions (in addition to radiation measurements) that could benefit from sensors on small satellites, in some cases with multiple platforms. These include: a limb scanning mission to study the stratosphere, mesosphere, and upper troposphere; a global precipitation - water vapor mission; a solid-state LIDAR mission; a small SAR mission; a high-resolution imaging spectrometer mission. We recommend that the potentialities of these missions for small satellite platforms be explored in more detail.

2 SCIENTIFIC OBJECTIVES OF GLOBAL CHANGE RESEARCH

Earth system studies have an increased urgency because of the realization that anthropogenic influences can produce major global changes, such as greenhouse warming and ozone depletion. Studies related to global change have three fundamental scientific objectives: to describe accurately the physical, chemical, and biological processes that can be observed on this planet and influence its climate; to incorporate these processes into models that attempt to predict changes in climate, whether natural or anthropogenic; and to continuously monitor the climate system to detect such changes. These objectives will best be achieved by a balanced program of ground-based, airborne, and satellite observations. This report focuses on how RPA's and small satellites can make important contributions to this program.

2.1 General Types of Observational Missions

Missions to make detailed process studies and missions to monitor long term changes are each essential parts of Global Change research.

Process studies can be distinguished by the scale of the observations. The Earth system encompasses an enormous range of scales, with sizes ranging from the micron radii of cloud drops to the 10000 km of global weather features, and with times ranging from the minutes of thunderstorms to the millenia of ocean circulation. In any model there is a need to parameterize accurately, but simply, the effects of "sub-grid-scale" phenomena too small or

too rapid to be resolved. Thus there is a need for "intrinsic" process studies involving short-term observations over a limited spatial area. As examples of important intrinsic process studies, we note here some related to clouds and radiation:

- -Cloud formation and precipitation
- -Radiation transport inside, outside, and between clouds
- -Relations between convection, cloud formation, relative humidity, and windshear
- -Durability and radiative properties of different cloud types
- -Interactions involving radiation, clouds, and aerosols

Beyond intrinsic process studies, there is also a need for "extrinsic" process studies that involve relatively short-time observations of broader areas. These provide data crucial to calibrating and validating models. Examples of extrinsic process studies include:

- -Interactions between the ocean and the atmosphere
- -Synoptic scale motions of ozone, trace gases, water vapor, and clouds
- -Observations of snow cover and earth albedo
- -Observations of stratospheric conditions and chemistry

The other kind of observational mission, monitoring, is for the purpose of detecting secular trends in the Earth system. Climate is intrinsically noisy with a great natural variability even in the absence of anthropogenic perturbations. Monitoring must therefore be carried out over long times

with good stability to average out the noise and detect long-term changes. There are many important variables to be monitored, such as CO₂ and ozone concentrations, surface temperature, polar stratospheric temperature, cloud albedo, precipitation, trace gases, etc. Some may be sensitive telltales of global change, but it is not clear yet which are the best variables for detecting changes; some highly responsive variables could also turn out to be among the noisest.

Monitoring and intrinsic and extrinsic process missions will have different requirements of coverage in space and time, stability, accuracy, and precision. RPA's are natural platforms for intrinsic process studies, while satellites are well suited for monitoring. Depending upon specifics, extrinsic process studies could employ either type of platform.

2.2 Major Scientific Issues in Global Change Research

Among the scientific issues that must be addressed are the following:

A. Clouds and radiation

By scattering, emitting, and absorbing short-wave and long-wave radiation, clouds control the intake and exhaust of the great climate heat engine. As clouds are diverse and highly variable, they are difficult to parameterize in GCMs. The treatment of clouds and radiation is widely considered to be the greatest uncertainty in current atmospheric models. A better understanding can come from intrinsic measurements included in the DOE's ARM program. At the initial ARM site in Oklahoma, RPAs could be coupled with ground-based measurements. The tropical Western Pacific is another impor-

tant ARM locale with a larger spatial scale. Here, satellites and/or RPAs seem essential for unravelling and predicting the ENSO (el Nino/Southern Oscillation) phenomenon and understanding the role of high cirrus clouds in changing the albedo.

B. Carbon budget

A complete accounting of carbon fluxes in the earth system is important to understanding the connection between observations of increasing CO₂ and the burning of fossil fuels. Present estimates of these fluxes are out of balance by 40%. A recent analysis by P. Tans [Nature] based on the 3 ppm inter-hemispheric difference in CO₂ suggests a major unknown sink of carbon in the northern hemisphere. Observations of the biosphere (land types, vegetation, etc.) are important here. Long term measurements of the oxygen depletion in the atmosphere as suggested by Bonin [Princeton] can also help in understanding the carbon budget.

C. Methane

Methane is the third most important greenhouse gas (after water vapor and CO₂) and will account for 25% of the expected anthropogenic increase in radiative forcing. It is also important as a source of stratospheric water at high latitudes and as a component of the carbon budget. The boreal wetlands and tropical rice paddies are important sources of methane. The availability of hydroxyl radicals is the limiting step in the destruction of atmospheric methane and there is a clear need to quantify and monitor this factor. The largest potential source of methane is the solid methane hydrate that may be buried under Arctic permafrost and may become unstable as temperatures rise. It has been suggested by Nisbet that methane outbursts from the Bering

Sea caused sudden warmings at the ends of the last two ice ages.

D. Ozone

Ozone is both a greenhouse gas (in the troposphere) and a cooling agent (in the stratosphere). The depletion of ozone by CFCs in the antarctic stratosphere is now well documented and the mechanism by which it occurs is fairly well understood; *in-situ* aircraft observations played a very important role in these latter studies. Recent measurements have documented a smaller seasonal depletion of ozone in the arctic, and data from the TOMS instrument suggest a secular depletion at mid-latitudes in the northern hemisphere. Low winter stratospheric temperatures and the presence of stratospheric clouds are crucial to the mechanism of ozone destruction in the polar regions. These processes are likely to be studied best by RPAs.

As the stratospheric temperature is sensitive to the amount of stratospheric CO₂, a change in this temperature may be the most immediate and scientifically demonstrable deleterious effect of increasing CO₂. At the bottom of the atmosphere, CO₂ makes a minor addition to the greenhouse produced by water vapor. In the stratosphere, water vapor is negligible and the effects of CO₂ are dominant. Small satellites are probably the best platforms for rapid and accurate monitoring of stratospheric temperatures. Indeed, the Voyager spacecraft was able to perform such measurements at Uranus, using radio waves propagating around the limb of the planet.

E. Water cycle

Considering the central role of water in the climate system, it is disappointing that present estimates of global water fluxes fail to balance by about

50%. The atmospheric component of the water cycle can be understood best through intrinsic studies using airborne and ground-based instruments and by large scale rainfall measurements using satellites, especially with radars sensitive to clouds and rain. Water on the land surface, in vegetation, and in the oceans involves extrinsic measurements that may be difficult to make from satellites. A combination of ARM-site local measurements and global ground-based samplings will be required.

F. The oceans

The circulation, salinity, temperature, and chemical composition of oceans are important variables influencing variation of the climate system on time scales longer than a year. The sea surface temperature is the only oceanic variable that can be measured from satellites or RPAs. Without the ability to make continuous measurements throughout the ocean, our understanding of the global climate system will remain incomplete.

This is by no means an exhaustive list. Stratosphere-troposphere exchange and properties of the planetary boundary layer are equally important scientific issues that offer interesting potential applications for the platforms we are considering. In the sections that follow, we explore some of the scientific issues in greater detail, and investigate how they may be addressed by RPA's and small satellites.

REFERENCES FOR SECTION 2

1. K. D. Bonin, "A Precision Measurement of Atmospheric Oxygen using Frequency Modulation Interferometry," Princeton University Physics Department Preprint (1991).
2. E. G. Nisbet, "The End of the Ice Age," University of Saskatchewan, Department of Geological Sciences Preprint (1990).
3. P. P. Tans, I. Y. Fung and T. Takahashi, "Observational Constraints on the Global Atmospheric CO₂ Budget," *Science*, **247**, 1431-1438 (1990).

3 CLOUDS AND RADIATION

It is our purpose here to review enough of basic cloud physics and of the cloud/radiation interaction to be able to set forth a minimal set of processes which must be included in a GCM with predictive power about Global Change, and to discuss the main issues in the current understanding of the role of cloud forcing in the Earth's radiation budget. Our goal is to find out what present day measurements will be required to understand the cloud/radiation interaction well enough, particularly within the ARM program, and the degree to which RPAs and small satellites would make a significant difference.

3.1 Introduction

Clouds influence climate in two major ways: they reflect incident short wavelength solar radiation thus preventing it from reaching the earth's surface and heating it, and they absorb outgoing long wavelength radiation from the earth thus reducing the earth's ability to cool itself. Which of these two opposing effects dominates is a sensitive function of the interaction of clouds with radiation, which is itself a sensitive function of the processes going on within various kinds of clouds.

Solar radiation is (to a good approximation) a black-body spectrum at 5780° K, which peaks in the visible at a wavelength of about 0.5 μm . At the earth's orbit the flux of solar radiation is 1370 watts/m², and due to the existence of day and night and because the earth is a sphere, the average

solar energy incident at the top of the atmosphere is one fourth of this, or 340 Watts/m². The average earth albedo is .3, so 30% of the incident radiation is reflected, leaving 240 watts/m² to be absorbed by the earth's surface and atmosphere.

Radiation emitted from the earth is (to a relatively poor approximation) a black-body spectrum at 255°K, which peaks in the infrared at about 10μm. There is essentially no overlap between the solar spectrum and the earth's spectrum. As the outgoing IR radiation passes through the atmosphere, some of it is absorbed and reradiated back toward the earth, but of course the net IR radiation escaping into space from the top of the atmosphere is also 240 watts/m², since the earth is (essentially) in equilibrium.

The black-body spectra, and the principal atmospheric absorption bands, are shown in Figure 3-1.

The albedo of the earth's surface (insofar as it can be measured from satellites) is no more than .15. The average cloud cover over the earth is observed to be 60% (65% over the ocean and 50% over the land). Hence, to make up the average albedo of .3, the albedo of clouds is about .45. Clouds are therefore the most important component in the amount of reflected sunlight, and their existence is crucial in determining the surface temperature of the earth. In fact, (if other parameters were held constant) a change of albedo by 0.02 would warm the earth's surface by 1°C. Evidently, the modeling of clouds in climate models must be done very accurately.

To outgoing long wave IR radiation most clouds are essentially black. Therefore the outgoing flux is largely determined by the temperature of the cloud tops, or, if the sky is clear by the temperature of the earth's surface

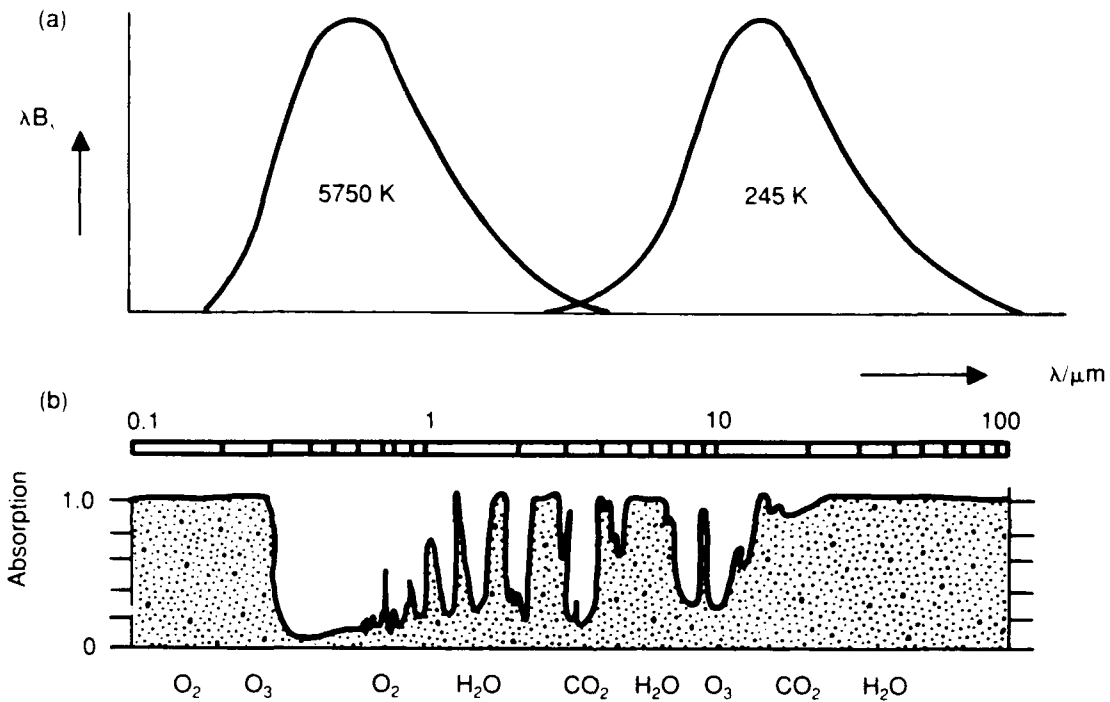


Figure 3-1. Curves of black-body energy B_λ at wavelength λ for 5750 K (approximating to the sun's temperature) and 245 K (approximating to the atmosphere's mean temperature). The curves have been drawn of equal areas since integrated over the earth's surface and all angles the solar and terrestrial fluxes are equal. (b) Absorption by atmospheric gases for a clear vertical column of atmosphere. The positions of the absorption bands of the main constituents are marked. (From Houghton, 1977)

Clouds are composed of water droplets and/or ice crystals, which form on cloud condensation nuclei (CCN). In principle, condensation of water vapor can occur whenever the humidity is above 100%, but because the equilibrium vapor pressure increases with the curvature of the surface at which condensation occurs, in practice humidities of above 300% are needed for pure water vapor to condense. Therefore actual cloud formation takes place because of the presence of relatively large aerosols and occurs when the humidity reaches a value not much above 100%. These aerosols constitute CCN. (See Section 5 for a thorough discussion of CCN and droplet formation.)

Clouds occur in several different forms, depending on their altitude, formation mechanisms, hydrodynamic properties, etc. Table 3-1 shows the distribution of the various forms over land and ocean. The relative amounts of these types often have diurnal variations which are of considerable importance. For example, the ratio of Stratus to Stratocumulus varies from less than 20% at local noon to nearly 30% in the early morning, while cumulonimbus peaks at 30% in late afternoon or evening and vanishes early in the morning.

Different cloud species contain water droplets and/or ice particles in differing ratios and with differing size distributions. One such distribution is shown in Figure 3-2. Cirrus clouds are essentially 100% ice crystals. The way in which the cloud interacts with radiation depends on the particle size in the cloud and on the wavelength of the radiation.

Finally, we point out that the definitions of a "cloud" and of its spatial dimensions are important in operationally defining cloud-free regions. While

Table 3-1

**AVERAGE % OF SKY COVER OVER { OCEAN
LAND
OF VARIOUS CLOUD TYPES**

Cumulus	12
	5
Cumulonimbus	6
	4
Stratus and Stratocumulus	34
	18
Nimbostratus	6
	6
Altostratus and Altocumulus	22
	21
Cirrus	13
	23

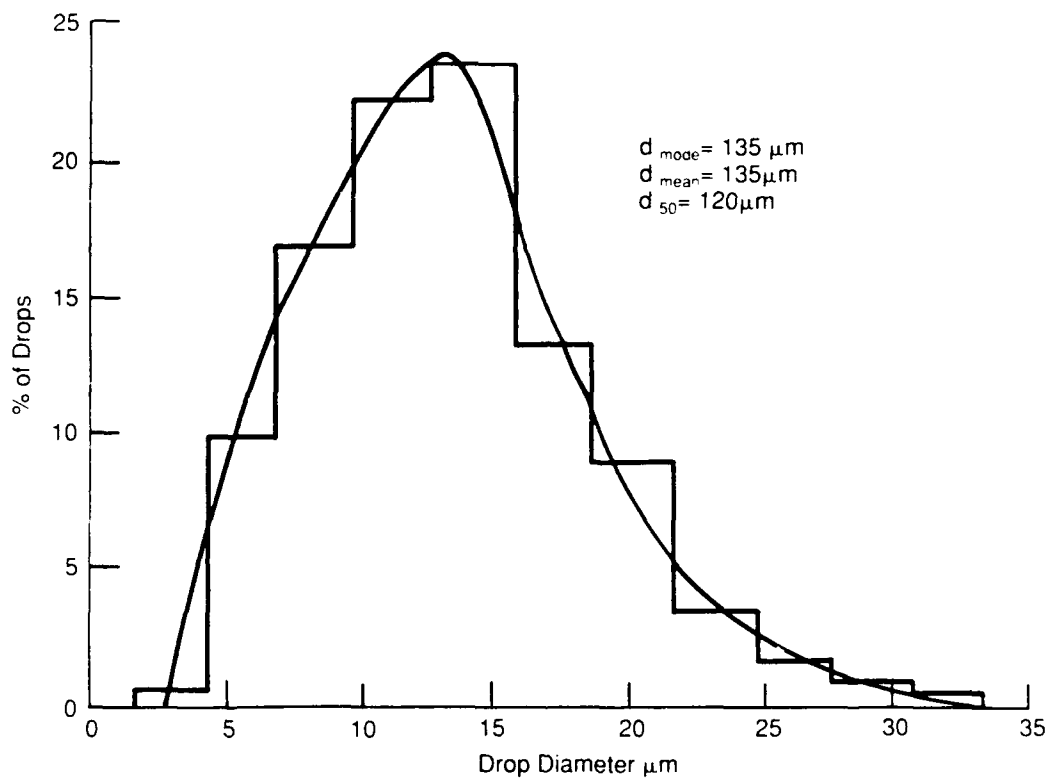


Figure 3-2. Average drop size spectrum for arctic stratus clouds.

the common-sense definition is straight forward, the technical definition is not. The presence or absence of a cloud is determined by an arbitrary threshold set on optical depth. (See the following section for a discussion of cloud optical depth.) For example, the optical depth of a cloud depends on such microscopic parameters as the spatial distribution of water density and the variation in size, shape, etc., of particles. The extreme inhomogeneity of clouds across a very large spatial spectrum makes cloud boundaries and, hence, the amount of cloud cover, dependent on the scale of the observing system; clouds appear to be fractal over a wide range of spatial scales.

3.2 Simple Model of Cloud Optical Properties

For incident solar radiation, emission is irrelevant because at $\lambda \sim 0.5\mu\text{m}$, the black body spectrum at the earth's temperature of around 270°K contributes essentially zero. So only scattering and absorption count. To a first approximation, let us neglect scattering into the beam, and assume the incident solar radiation suffers only losses due to clouds. Thus the radiation intensity $I_\lambda(\hat{k}, z)$ of photons of wavelength λ travelling in the direction \hat{k} satisfies

$$dI_\lambda(\hat{k}, z) = -(\sigma_\lambda^{\text{abs}}(z) + \sigma_\lambda^{\text{scatt}}(z))N(z)I_\lambda(\hat{k}, z)dz \quad (3-1)$$

where σ are absorption and scattering cross sections and N is particle density. Therefore,

$$I_\lambda(\hat{k}, z_2) = I_\lambda(\hat{k}, z_1)e^{\tau(z_2, z_1)} \quad (3-2)$$

where the (dimensionless) optical depth τ is

$$\tau(z_2, z_1) = \int_{z_1}^{z_2} \sigma_{\lambda}^e(z) N(z) dz \quad (3-3)$$

and

$$\sigma^e \equiv \sigma^{\text{abs}} + \sigma^{\text{scatt}} \quad (3-4)$$

is the extinction cross section.

Each type of cloud has, at a given height z_1 , a distribution $n(r, z)$ of sizes of particles of radius r (ice crystals are of course not spherically symmetric, though their absorption cross section does not differ markedly from that of liquid water droplets). In general, the cross section σ will also depend on the particle size. For wavelengths small compared to the particle size, as is typically the case for solar radiation (see Figure 3-2) the cross section is twice geometrical: $\sigma = 2\pi r^2$. Thus (if we take z_1 to be the top of the cloud where $\tau = 0$) the optical depth at height z is

$$\tau(z) = 2\pi \int_z^{\text{top}} dz' \int dr r^2 n(r, z'). \quad (3-5)$$

and $n(r, z')$ is the droplet size distribution, so that $N(z') = \int_0^{\infty} n(r, z') dr$. This equation is usually re-expressed in terms of the liquid water content (LWC) of the cloud, defined by

$$\text{LWC}(z) = \frac{4\pi}{3} \rho_w \int r^3 n(r, z) dr \quad (3-6)$$

where $\rho_w = 10^6 \text{g/m}^3$ is the density of water. The effective radius is defined by

$$\frac{\text{LWC}(z)}{r_{\text{eff}}(z)} = \frac{4\pi}{3} \rho_w \int r^2 n(r, z) dr. \quad (3-7)$$

Therefore one finally writes the optical depth in the form (assuming that r_{eff} does not vary with z)

$$\tau(z) = \frac{3}{2} \frac{1}{\rho_w r_{eff}} \int_z LWC(z') dz'. \quad (3-8)$$

If z is below the cloud, then the total optical thickness of the cloud is

$$\tau^* = \frac{3}{2} \frac{LWP}{r_{eff} \rho_w} \quad (3-9)$$

where the liquid water path is

$$LWP = \int_{\text{bottom}}^{\text{top}} LWC(z') dz'. \quad (3-10)$$

Crudely, then, $LWP = LWC \cdot t$, where t is the cloud thickness. The liquid water content varies greatly with cloud type, as shown in Table 3-2, as does the mean cloud thickness. Finally, when all of this is put together, and the average solar zenith angle of 60° is included, the previously inferred average cloud albedo of .45 results from an average optical thickness $\tau^* = 6$, assuming a simple geometry of plane parallel clouds. Since in fact clouds are horizontally variable, and there is some absorption, this value is actually a lower bound. For very thick clouds, diffuse radiation will dominate and the above model does not work.

Experimentally measured cloud albedos vary greatly, as a function of type, latitude, solar zenith angle, and other parameters. But overall, they are not inconsistent with the inferred value of .45. Therefore, we may have some confidence in the value of τ^* obtained above.

From the formula for τ^* , we see that it varies inversely with the effective droplet radius. Thus a cloud having the same LWP as another, but a larger number of smaller droplets, will have a larger τ^* and therefore a larger albedo.

Table 3-2

	LWC (g/m ³)	t (km)
Cumulus	.4	2
Cumulonimbus		
Tropical	1.0	5
Trade Wind	1.5	2
Midlatitude	1.5	2.5
Polar	1.5	2
Altostratus/Altostratus	.1	.5
Stratus/Stratocumulus	.2	1
Nimbostratus	.1	3

If one asks, therefore, what changes may take place in cloud albedo (to which, as we've remarked earlier, the earth's surface temperature is extremely sensitive) due to man's activities, we must concentrate on r_{eff} . For example, an increase in r_{eff} of 10% (which corresponds to a decrease in N of 30%) reduces the albedo enough so that ΔT at the surface = 1.3°C. Or, as another example, reducing N by a factor of 2 is equivalent to doubling the CO₂ concentration in the atmosphere.

A further effect of reducing droplet size, while keeping the total LWC constant, is likely to be an increase in cloud lifetime, and consequently of average cloud cover. As shown in Figure 3-2, typical droplet sizes now are

5-10 μ m. These do not rain out until they coalesce to form larger drops of 50 μ m diameter or more. Therefore if the mean droplet size were to decrease, the time to coalesce to a size which can rain will grow, thus increasing average cloud lifetime.

N and r_{eff} are largely determined by the number of CCN available. These vary widely between land and water (Figure 3-3).

Overall, the message from the simplified discussion of cloud albedo is that before any model can purport to predict global climate change due to greenhouse gas forcing, or anything else, it must first include such parameters as the fractional surface areas of the earth covered by clouds, the liquid water content of the clouds, the droplet effective radius, the droplet number, and the number and type of CCN.

These are stringent requirements on GCMs, and on computing capacity. Many of these parameters are not included yet in present models.

3.3 Cloud Forcing

Satellite observations have been used very effectively to obtain estimates of the effect of cloud cover on the net radiation balance. The key step in these investigations is determining the difference between the mean flux at the top of the atmosphere for all conditions and the mean flux for cloud-free conditions (taking into account that the definition of a cloud as discussed at the end of Section 3.1, is highly sensitive to the threshold set for optical

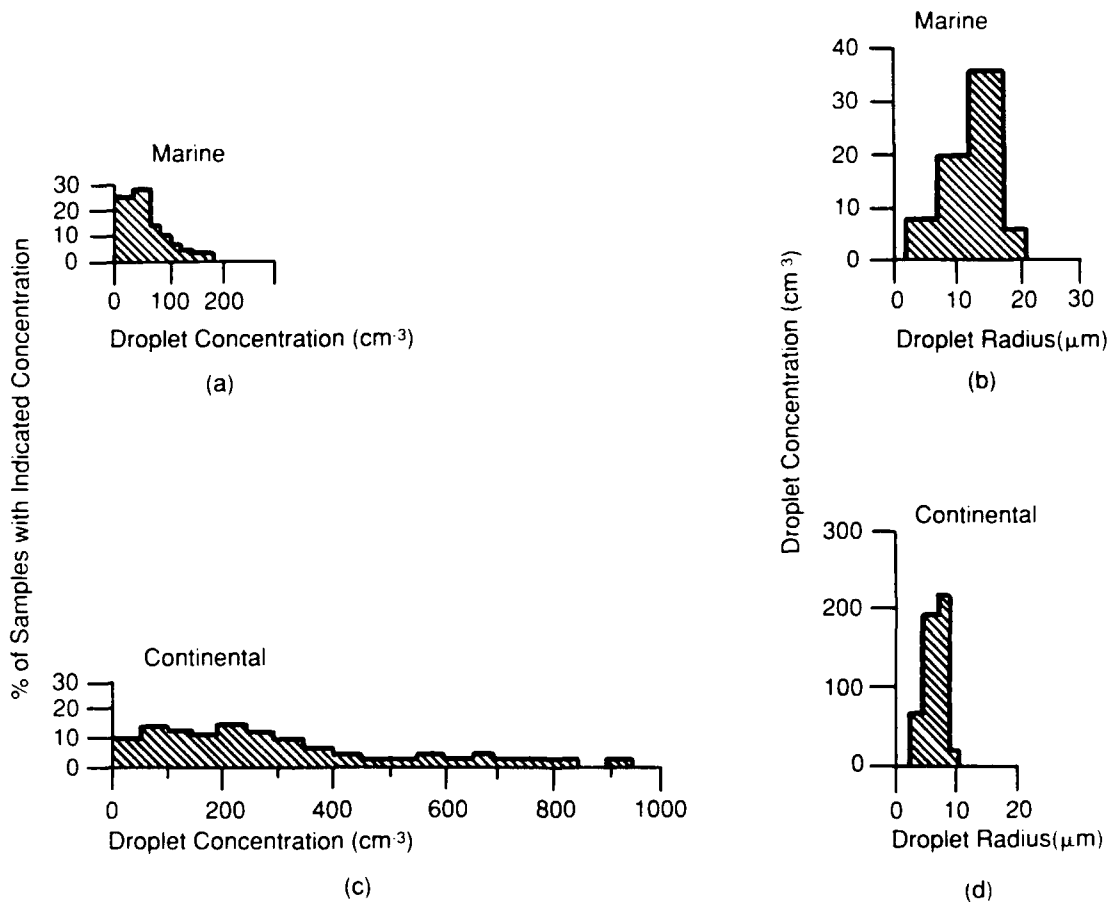


Figure 3-3. (a) Percentage of marine cumulus clouds with indicated concentrations. (b) Droplet size distributions in a marine cumulus cloud. (c) Percentage of continental cumulus clouds with indicated droplet concentrations. (d) Droplet size distributions in a continental cumulus cloud. Note change in ordinate from (b). [From *Tellus* 10. 258-259 (1958).]

thickness). This difference is now commonly referred to as cloud forcing, and can be expressed in the form

$$C_{LW} = F_0 - F \quad (3-11)$$

$$C_{SW} = Q - Q_0.$$

F is the net outgoing infrared flux at the top of the atmosphere, and Q is the net incoming solar radiation. F and Q are averaged over the spatial and temporal domains. The subscript 0 denotes the same average for cloud-free conditions. The effect of clouds on the net radiation field is then

$$C = C_{SW} + C_{LW}. \quad (3 - 12)$$

Ramanathan et al. (1989) obtained the geographic distribution of long-wave, short-wave, and net cloud forcing parameters from ERBE satellites. They used an algorithm that, when applied to ERBE measurements, determined whether the measurements corresponded to cloud-free or overcast conditions. In this way, they obtained

$$C_{LW} = 31W/m^2 \quad (3-13)$$

$$C_{SW} = -48W/m^2$$

$$C = -17W/m^2.$$

The negative value for the cloud forcing (C) indicates that the net effect of clouds is to decrease the amount of radiative energy trapped within the atmosphere; thus, clouds tend to cool the planet.

An alternative approach to determining the cloud forcing has been presented by Ardanuy et al. (1991), who start with the relationship

$$F = F_0 + A_C(F_C - F_0). \quad (3 - 14)$$

The cloud fraction A_C is taken from the THIR/THOMS Cloud Data Set compiled by Stowe et al. (1989). F_0 and F_C , the mean flux for overcast conditions, were estimated based on clear sky and cloud top temperatures that were also compiled in the THIR/THOMS data set. Using this alternative approach, Ardanuy et al. obtained $24W/m^2$, compared with the $31 W/m^2$ obtained by Ramanathan et al. The origin of the difference, $7W/m^2$, is not yet understood. The results of Ramanathan et al. are based only on measurements of ERBE, while Ardanuy et al. used a regression technique with a combination of Nimbus-7 ERB and THIR/THOMS measurements in an attempt to account for the effects of "other parameters."

An important issue concerning the reliability of the satellite observations is diurnal variability, which we discuss in Section 10, together with the potential use of small satellites in providing complete diurnal coverage.

A fundamental problem in using satellite observations alone to establish the cloud forcing is that these observations are limited to measuring the radiative flux at the top of the atmosphere. The stratosphere, lying above the tropopause, has its own radiative budget; in terms of climate change, that budget is dominated by the cooling due to increased carbon dioxide concentration. Studies of alterations in radiative flux due to changes in greenhouse gas concentrations have shown that the stratosphere reacts rapidly, on a time scale of months, while the troposphere reacts on a time scale measured in decades because of the high thermal inertia of the oceans. Since most clouds form in the troposphere, for problems of climate change, the main concern of ARM, the cloud forcing should be evaluated at the top of the troposphere, not

the top of the atmosphere. Since continuous observations of the tropopause flux over a full diurnal cycle can be made by instruments based on RPAs, these vehicles deserve special consideration and will be discussed in Section 4.

One of the assumptions in the above analysis of cloud forcing is that the radiation field where clouds are absent is similar to that in which clouds are present. However, the ambient conditions when clouds are absent are not likely to be the same as when clouds are present, for the simple reason that clouds develop only under conditions favorable for their formation. These conditions involve temperature and humidity, as well as winds and vertical velocity. Therefore, a strict determination of clear sky flux would include the environmental effects that are correlated with clouds. It would also seem that the larger the cloud-free area, the larger the *environmental difference*. One critical goal of the RPA-based program discussed in Section 4 would be to provide data on the environmental conditions under which clouds form and those for cloud-free areas, and determine the impact of these environmental parameters on the radiative flux.

3.4 Factors Affecting the Radiation Balance of Clouds

An important aim of global change research is to determine how cloud forcing is related to average cloud amount, and how both are related to the large-scale environmental parameters of the atmosphere, including the velocity, temperature, and humidity fields, the fluxes of energy and moisture

between clouds and environment, and-what now appears to be particularly important-the chemical composition of the atmosphere, both gaseous and particulate.

The environmental parameters determine the nature of the clouds and their altitude. For each cloud type, there is a delicate balance between long-wave and short-wave radiation. Cirrus clouds are especially important because of their ubiquity and highly variable properties, in response to both types of radiation. In the case of cirrus, the long-wave effect is large because of the high temperature contrast between cloud and earth-surface, while the short-wave effect is smaller because of the cloud's low optical thickness. But as cirrus clouds thicken, this warming effect can turn to cooling.

The effect of clouds also depends on their latitude and, very importantly, on whether they form at night or during the daytime. During the day, a cloud affects both the short- and long-wave radiation, but at night the impact is only on the long-wave radiative flux. A shift in climate that produces more daytime than nighttime clouds will result in cooler temperatures than a regime in which nighttime cloudiness increases more than daytime cloudiness. The day-to-night variation in cloud geometry could have strong effects on the radiation budget. For example, a cirrus sheet that was thin during the day, but thicker at night, would lead to warming, since it would be relatively transparent to short-wave radiation during the day, while at night it would blanket long-wave radiation.

The chemical composition of the atmosphere can have a significant effect on a cloud's optical properties by determining the type and size of the

aerosols which form cloud condensation nuclei. Twomey (1977) examined how pollutant CCNs can alter the effect of clouds on the earth's radiation budget. He showed that moderately thick clouds would increase in brightness with increasing CCN concentration even if the aerosols which make up the CCN are heavily absorbing. Only as the clouds become thicker, and contain more highly absorbing particles, would cloud brightness begin to decrease with CCN concentration.

More recently, Charlson et al. (1987) have postulated that over the oceans a major source of CCN is dimethylsulfide (DMS), which is produced by phytoplankton in sea water. DMS oxidizes in the atmosphere to form sulfate particles, which then act as CCN. While the CCN concentration over the remote oceans varies by a factor of ten, there is no observational evidence at this point showing that clouds respond to changes in DMS concentration or that there is a relationship between DMS and sea surface temperature.

Schwartz (1988) points out that anthropogenic emissions of sulfur dioxide are more than twice as large as those associated with marine DMS, and that these emissions have developed over the past 100 years. Since it takes a short time for sulfur dioxide to be oxidized and rained out as sulfuric acid, the anthropogenic sulfur dioxide effect would be confined largely to the Northern Hemisphere, where it is produced. Observations indeed indicate a large excess of sulfate particles in the Northern Hemisphere, but the cloud albedo data reveals no enhancement of cloud albedo in the Northern Hemisphere compared to the Southern Hemisphere. The long-term temperature trends in both hemispheres are also approximately equal, which would not

be expected if man-made aerosols had an impact on cloud cover.

In Section 5 we will discuss questions about the formation and role of sulfate particles in greater detail.

3.5 Global Warming

Possible feedback mechanisms which may take place when the earth begins to warm are changes in average cloud cover, changes in the altitude and hence temperature of cloud tops, and changes in the IR absorption of clear air because of the changed chemical composition of the atmosphere. If as the earth heats, the fraction of cirrus increases, or if the clouds move upward and their tops cool, the total outgoing radiation flux will decrease with the consequences of further warming the surface.

Based on the discussion throughout this section, we may now try to list the essential parameters which must be measured to understand the important feedback processes affecting cloud forcing, and hence influencing the effect of clouds on climate and, in particular, on Global Warming.

- i. Average total cloud cover, by type, must be known and the changes which may be induced by increasing greenhouse gases must be understood. The same is true for average cloud thickness and cloud geometry (e.g., aspect ratio and cloud top height) as well.
- ii. Cloud albedo must be understood. This requires knowing

cloud droplet number and size distribution as a function of cloud type and location, and it is crucial to understand what feedback mechanisms may cause global warming to alter these distributions. This is a very difficult subject which, as we have discussed, may well reach into the realm of marine biology since over the oceans CCN are apparently produced primarily by various types of phytoplankton. [Though outside the scope of this report, the impact of changes in temperature on the behavior of these animals must also be understood.] To get at possible changes in cloud albedo over land also requires us to understand the impact of anthropogenic aerosols, since these also serve as CCN. Present GCMs normally assume there are sufficient CCN present so that any increase in humidity will result in increased droplet number. Over land this may be true; over much of the ocean it probably is not. To understand cloud albedo also requires an understanding of the liquid water path in the cloud, and, as usual, what feedback mechanisms may change this. Increased humidity resulting from increased surface temperature will no doubt increase LWP. Increased cloud size may too.

- iii. Cirrus clouds need to be understood much better than they are now. They are after all responsible for a good part of the outgoing IR radiation. If global warming changes the distribution and temperature of cirrus, there will be a feedback effect which, given our present state of knowledge, could be of either sign.

- iv. Measurements of the pressure, temperature, water vapor and velocity fields as functions of space and time will be required. In particular the quantities involved in the vertical convection of mass and moisture associated with cumulus convection should be measured, together with the horizontal spreading and consequent formation of large areas of cirrus anvils extending from the tops of the convection columns. From these fields vertical profiles of temperature and the other relevant parameters can be obtained.
- v. To verify the calculations made by models using the input parameters listed above, ARM must also measure radiation fluxes, as functions of wavelength, height, and angle. In the same spirit, the average effect of cloud forcing on the Earth's radiation budget must be measured reliably and compared with model predictions.

As discussed in the rest of this report, both RPAs and small satellites have vital roles to play in these measurements. In the next section we consider RPAs and how they are needed to complement the ground-based observations of the ARM program.

REFERENCES FOR SECTION 3

1. Ardanuy, P., L. Stowe, A. Gruber, and M. Weiss (1991), Shortwave, longwave, and net cloud-radiative forcing as determined from Nimbus-7 operations. *J. Geophys. Res.* (in press).
2. Charlson, R., J. Lovelock, M. Andreae, and S. Warren (1987) Oceanic phytoplankton, atmospheric sulfur, cloud albedo and climate. *Nature* 326, 655-661.
3. Ramanathan, V., R. Cess, E. Harrison, P. Minnis, B. Barkstrom, E. Ahmand, and D. Hartmann (1989) Cloud radiative forcing and climate: Results from the earth radiation budget experiment. *Science* 243, 57-63.
4. Schwartz, S. (1988) Are global cloud albedo and climate controlled by marine phytoplankton? *Nature* 336, 441-445.
5. Stowe, L., H. Yeh, C. Wellmeyer, H. Kyle, and the Nimbus-7 Cloud Data Processing Team (1989) Nimbus-7 global cloud climatology. Part II: First year results. *J. Climate* 2, 671-709.
6. Twomey, S. (1977) The influence of pollution on the shortwave albedo of clouds. *J. Atmos. Sci.* 34, 1149-1152.

4 THE USE OF RPAS IN SUPPORT OF THE ATMOSPHERIC RADIATION MEASUREMENT PROGRAM

In Section 3 we have discussed the complex nature of the various cloud and water vapor feedbacks and their significant effects on climate change. In view of the important role of clouds, a major goal of the Atmospheric Radiation Measurement program (ARM) is to improve the parameterization of clouds in GCMs. More accurate parameterization may increase the predictability of the atmosphere's response to changing composition and temperature. In this section we examine the utility of remotely piloted aircraft for carrying out the airborne measurements required as part of ARM.

As discussed in detail in Section 3, the effect of clouds on the radiation budget, and therefore on climate, depends on several parameters: (1) the environment above and below the cloud, including the distribution of aerosols, the temperature and humidity profiles, and the surface optical properties; (2) the macrophysical structure of the cloud, including horizontal and vertical extent, optical thickness, temperature, and variation of temperature and liquid water content within the cloud; and (3) the microphysical structure, including particle size, phase, shape, impurities, and optical properties, as well as the statistical distribution of these parameters within a given cloud. Several of these quantities can be observed using remote sensing from platforms based in space or from instruments at the surface of the earth. Some of these parameters, however, particularly in the upper troposphere, can only be determined by airborne observations. Furthermore, these parameters must be correlated with measurements of upward and downward radiation flux

divergence at all altitudes, which again can only be carried out reliably by airborne observations. The radiation measurements are also needed for validating the predictions of the cloud models.

Small remotely piloted aircraft appear to be the only potentially affordable aircraft system which would meet these requirements of continuous measurements above an ARM site over a complete diurnal cycle at the altitudes necessary. Therefore RPAs constitute critically important platforms to consider for meeting the stated goals of ARM.

4.1 Small RPA Instrument Packages for ARM Measurements

In Table 4-1, we present a minimal set of instruments that could be carried aboard an RPA and which would meet the basic requirements of the ARM program outlined above. The entire package would weigh about 70 kg, light enough for the smallest RPAs under consideration.

The remote sensing instruments have been proposed by the combined DOE Labs (Vitko, 1991), who achieve the small size and weight by taking advantage of some of the newer technologies to be discussed in Section 7. The broadband radiometer measures the upward and downward radiative flux, and would be similar in function to the ERB satellite instrument and to its planned successor, CERES. The imaging spectrometer serves much the same purpose as the so-called AVHRR satellite instrument; that is, it would identify cloud amount, type, and thickness by measuring the relative transmission and reflection in a number of bands. The bands proposed by

Table 4-1. Minimal RPA Instrument Package for ARM

Measurement	Instrument	Wt. (kg)
	<u>Remote Sensing</u>	
Short wave, IR-flux divergence	Broadband Radiometer 0.2 – 5 μm , 5 – 50 μm	20
Cloud and surface properties	Imaging Spectrometer	12
Cloud morphology	Camera	2
Thin cirrus detection, profiling	Mini-lidar	5
	<u>In situ Sampling</u>	
2D ice crystal images	Shadow Photo (PMS 2DP)	7
Drops & crystals	Scatterometer (PMS FSSP)	7
Total H ₂ O	Lyman α photofragmentation	8
	Data Storage and Processing	10
	Package Weight	71 kg

the DOE Labs for their instrument (which they call MPIR for multispectral-pushbroom-imaging-radiometer) are shown in Figure 4-1.

The *in-situ* sampling instruments already exist and have been used aboard manned aircraft. Of these, the Particle Measurement System instruments should perform better in RPAs because RPAs move at a slower speed (80 m/s at altitude is reasonable for designs we have seen), which allows more time to image each particle and should yield resolution well below the current limit of about 100 μm particle size.

This minimal instrument package would help resolve the key issues we have discussed in Sections 3.3 and 3.4. By making observations of radiance and flux in the IR and visible, RPAs equipped with this package would provide for the first time an understanding of the radiance fluxes at the top of the troposphere, as opposed to the top of the atmosphere. Combining these observations with satellite-based observations at the top of the atmosphere will allow determination of the relationship between these two net fluxes and will help establish the role of stratospheric climate forcing. Direct measurement of the cloud forcing from RPAs has the potential of eliminating the difficulties.

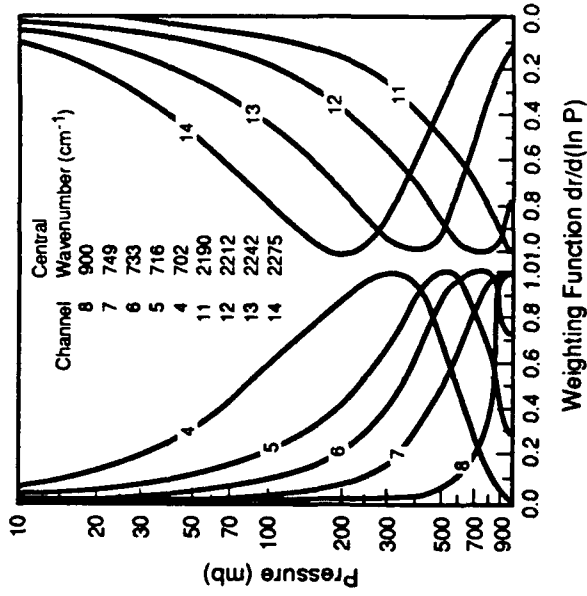
The combination of water vapor observation with the flux measurements will enable researchers to determine the role of water vapor in the column flux divergence. Observations between, above, and below clouds will help establish the role of the environmental parameters in determining the radiative flux and the difference in radiation between clear sky and overcast conditions.

Observations of CCN and cloud droplet or ice particle concentration and

Mission: MPIR (Multispectral Pushbroom Imaging Radiometer)

MPIR bands for transmission and cloud properties

- Phase, Particle Size - .75 μ , 1.6 μ , 2.21 μ
- Height - 4.464 μ , 4.525 μ
- Coverage - .665 μ (in & Crosstrack)
- Temperature - 10.8 μ , 12.0 μ
- Emissivity - 10.8 μ
- Optical Depth - .75 μ
- Aerosols - .665 μ , .91 μ
- Surface Albedo - .75 μ
- Water Vapor - 1.139 μ (in & Crosstrack)



Wielicki & Coakley, 1981

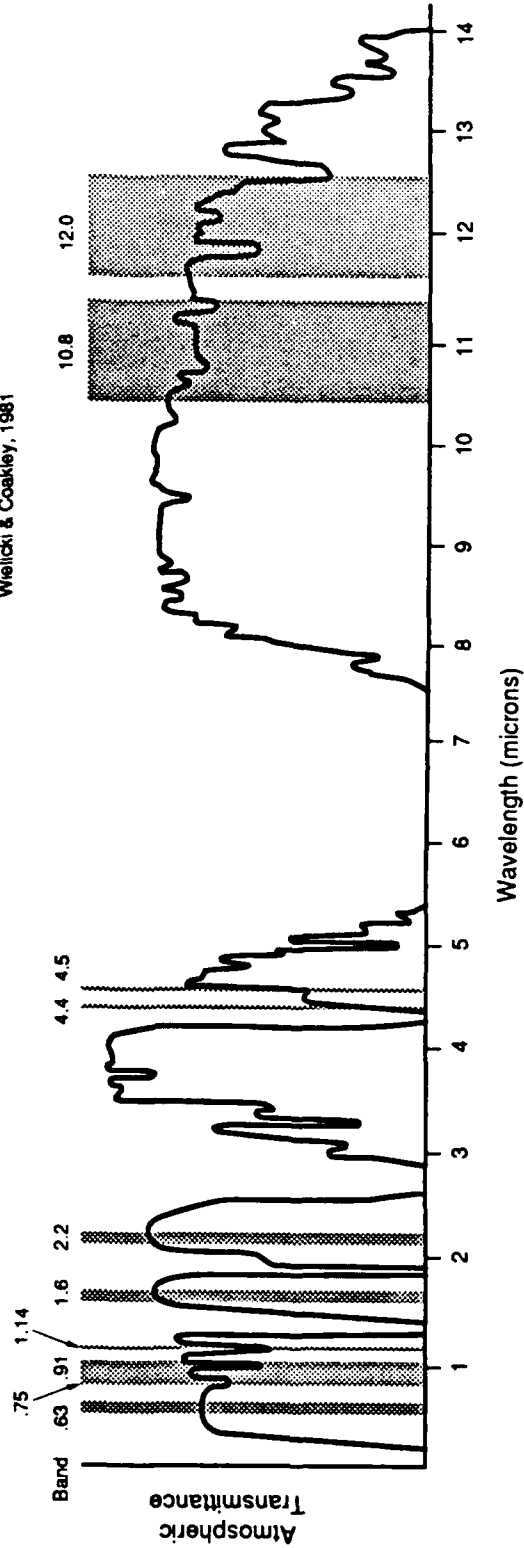


Figure 4-1. Transmission Bands for Imaging Spectrometer (Vitko, 1991)

size distribution will contribute to the description of the cloud microphysics, especially important for cirrus during both day and night.

Anderson (see Langford et al., 1990) has proposed a more complete suite of instruments than the above minimal set, adding UV detection and a greater variety of particle measurements (though without a lidar), which totals 105 kg and should be compatible with present small RPA designs. This instrument package is described in Table 4-2.

The biggest uncertainty associated with the instrumentation in Tables 4-1 and 4-2 is in developing new radiation instruments that are compact, lightweight, stable, and well-calibrated. As just one example, the CERES radiometer now being designed for satellites, with a proven calibration heritage, weighs 80 kg. By contrast, the broadband radiometer in Table 4-1 is projected to weigh only 20 kg. It is extremely important to begin serious design and development of such proposed small instruments to verify their feasibility as soon as possible. In this regard, it is noteworthy that similar instruments, of similar size and weight, would be necessary for the radiometric measurements proposed with small satellites in Sections 9 and 11, so there is an extra incentive for their development.

4.2 RPA Platform Requirements

The instrument payloads proposed above, which meet ARM requirements, weigh about 110 kg or less. Langford et al. (1990) suggest that a prudent design requirement would be to allow growth to 150 kg. This payload is small compared to the carrying capacity of manned aircraft such

Table 4-2. Integrated ARM Instrument Array (Proposed by J.G. Anderson, Harvard University)

Objective	Instrument Designation
IR Radiance IR Radiance Difference (Upwelling/Downwelling) IR Radiance Directionality IR Radiance Divergence	Dual Channel Interferometer Sounder Spectral Resolution: 1cm ⁻¹ Spectral Range: 600-2800 cm ⁻¹ Weight: 20 kg Instrument Description: Bias between upwelling/downwelling channel removed by 180° rotation, dual black body in-flight calibration
IR Broadband Flux IR Broadband Flux Difference IR Broadband Flux Divergence	Pyrogeometer Spectral Range: 3-50μ Weight Upwelling Channel: 2 kg Instrument Description: Bias between upwelling/downwelling removed by 180° rotation Subunits Commercially Available: EKO MS-200
Visible Radiance, Radiance Directionality, and Radiance Divergence	Dual Channel Ebert 1/4 meter Spectrometer with diode array detection Spectral Range: 300-700 nm Spectral Resolution: 1.5 nm Weight: 10 kg Instrument Description: Fiber optic coupled upward/ downward radiance directionality observing heads, 180° rotation to eliminate offset.

Table 4-2. (Continued)

Objective	Instrument Designation
Visible Flux, Flux Difference (Upwelling/Downwelling) Flux Divergence	Dual Channel (Upwelling/Downwelling) Pyranometer Spectral range: 0.3-3 μ Weight: 1 kg per channel Instrument description: Detector heads available commercially: K & Z CM 11
UV Radiance, Radiance Difference (Upwelling/Downwelling) Radiance Directionality Radiance Divergence	Dual Channel Ebert 1/4 Meter Spectrometer with Diode Array Detection Spectral Range: 250-400 nm Spectral Resolution: 1 nm Weight: 10 kg Instrument Description: Fiber optic coupled upward/ downward radiance directionality observing heads, 180° rotation to eliminate offset
UV Flux, Flux Difference (Upwelling/Downwelling) Flux Divergence	Dual Channel Fiber optic coupled UV integrating radiometer Spectral Range: 250-400 nm Weight: 2 kg
H ₂ O Vapor Cloud Liquid Water H ₂ O Ice	Lyman- α Fast Flow Fragment Fluorescence: $\text{H}_2\text{O} + h\nu \rightarrow \text{OH}^\bullet + \text{H}$ $\downarrow 309 \text{ nm}$ OH with simultaneous Lyman- α absorption heated inlet for ice and liquid phase Weight: 8 kg
Ozone	In situ UV Absorption Weight: 8 kg
CO ₂	In situ IR Absorption Weight: 8 kg
CCN Aerosols 0.1-3 μ	PMS ASASP-X Modified for unmanned aircraft Weight: 7kg

Table 4-2. (Concluded)

Objective	Instrument Designation
Cloud drop and large aerosol concentration and size distribution 2–50 μ size	PMS FSSP Modified for unmanned aircraft Weight: 7 kg
Two-dimensional images of ice crystals	PMS-2DP Modified for unmanned aircraft Weight: 8 kg
Pressure, Temperature and Relative Humidity	Weight: 1 kg
Data Systems, Instrument Control, Telemetry, Data Storage	386-based, space-qualified flight systems developed for ER-2 and unmanned aircraft Weight: 10 kg
	Total Weight: 105 kg

as the ER2. (See Section 4.3 for more detailed comparisons with manned aircraft.)

In order to carry out the required observations outlined above, the platform would have to reach altitudes at which cirrus clouds are abundant. At middle latitudes, the minimum altitude requirement is about 11 kilometers (km), or 36,000 feet. At lower latitudes, the tropopause is higher and altitudes of 18 km need to be reached. Ultimately, it would be desirable, in order to cross-calibrate satellite and RPA observations, to reach altitudes comparable to the top of the atmosphere, or about 24 km.

A major issue is the development of a small, doubly turbocharged engine suitable for the large range of pressure differentials associated with operation up to the desired altitudes of 15-20 km, or alternatively an engine with an on-board oxidizer. Obtaining designs and evaluation of performance of such engines should be an early priority in the RPA program.

The platform should be able to maintain altitude for at least a diurnal cycle in order to meet the ARM requirements. In addition, it should be capable of conducting nighttime observations, since information on nighttime cirrus is sparse and this data would be of great importance to analysis of the changes in radiation balance resulting from increases in greenhouse gases. The platform must also avoid severe weather, which means that an additional six to ten hours of endurance at altitude would be desirable so that severe storms can move over the landing site.

In order to calibrate observations and provide near-simultaneous measurements at altitudes above and below clouds, it would be desirable to have two platforms in the air at the same time. The experimental protocol sug-

gested by Langford et al. (1990) is based on simultaneous observation from two RPAs.

Moreover, the aircraft should exert minimum influence on the local environment. The airframe should permit easy observations both looking up and looking down in order to capture the downwelling and upwelling radiation. The microphysical instruments require clear flow into the inputs so that observations of particles are minimally influenced by the aircraft. In the Langford et al. (1990) design the instruments would be mounted in the nose of the aircraft, with a propeller mounted in the tail. If the aircraft is to operate in the troposphere, it must be capable of withstanding moderate turbulent conditions; extreme turbulence can be avoided by flying above convective storms.

We summarize here some additional requirements and issues. For measuring small particles, we have already mentioned the advantages of the slow speed (80 m/s) at altitude of the RPA designs we have seen. The location of the RPA should be known to better than 100 meters, and the relative location of 2 RPAs making radiation divergence measurements should be controlled to the same accuracy, both of which are now straightforward with a simple GPS receiver. The radiometers should be pointed with a readout accuracy of 10^{-2} radians; new miniature fiber-optic gyros are better than 10^{-4} rad/hour. It may not be necessary to actually stabilize the orientation of the radiometers to the readout accuracy, but if it should be, then using flotation or gimbals, with actuators to maintain alignment of the instruments, is a known and proven technology to this level of precision.

4.3 Manned Aircraft vs. Existing and Proposed RPAs

In Table 4-3 we show some selected flight-proven RPAs and some that are in planning and development, together with some current manned research aircraft for comparison.

A number of manned aircraft have been used or proposed for atmospheric research. The ER2 and WB-57F (the latter owned by the Los Alamos National Laboratory and not presently in operation) are manned aircraft with endurance limitations of six to ten hours. They carry a payload much heavier than the 150 kilograms required to meet ARM goals. Because of their size, and their manned operations, the overall cost of using these aircraft, about \$4000/hr, appears to be much higher than the estimated cost associated with the use of RPAs for a complete ARM mission.

We also considered small manned aircraft, such as the Beechcraft Bonanza as shown in Table 4-4, but its altitude and endurance are much lower than required for ARM.

Several of the unmanned vehicles in Table 4-3 have been suggested specifically for use in support of the ARM mission. The Condor vehicle, built by Boeing, meets the altitude and duration requirements, but its capability of lifting far greater weights than those needed for ARM makes it much too expensive to use in support of CART sites. The Amber RPA, built by Leading Systems, presents an interesting possibility for early experimentation. The Amber vehicles are limited in ceiling to 8.5 km, and thus cannot carry out the full ARM mission. However, these vehicles could be used in order to test out instrumentation and develop operational procedures. Fur-

Table 4-3. Existing and Proposed Research Aircraft

Type	Payload	Wing Span	Ceiling	Duration
Flight Proven:				
Amber I	150 kg	30 ft.	8 km	38 hrs
Condor	450-800 kg	200 ft.	20 km	58 hrs
In Planning and Development:				
Perseus A	50 kg	60 ft.	25 km	1 hr @ 25 km
Perseus B	150 kg	60 ft.	18 km	59 hrs @ 15 km
Gnat 750-93L	150 kg	60 ft.	18 km	75 hrs @ 13 km
Manned Aircraft for Comparison:				
Saberliner	≈ 400 kg		13 km	≈ 8 hrs @ 11 km
ER-2	1200 kg		21 km	10 hrs

Table 4-4. RPAs vs. Light Aircraft

RPAs	Light Aircraft
<p>Advantages:</p> <ol style="list-style-type: none"> 1. Long duration 2. High altitude 3. Dangerous missions 4. Flight line precision and repeatability 	<p>Advantages:</p> <ol style="list-style-type: none"> 1. Low cost 2. Easy availability 3. Relatively fewer FAA restrictions 4. Pilot judgment regarding observations of opportunity
<p>Disadvantages:</p> <ol style="list-style-type: none"> 1. Higher cost 2. FAA restrictions limit when and where one can fly 	<p>Disadvantages:</p> <ol style="list-style-type: none"> 1. Lower ceiling 2. Short duration 3. Pilot safety, e.g. shouldn't fly into bad weather
<p>Example: AMBER I carries 150 kg to 8 km with a duration of 38 hours</p>	<p>Example: Beech F-33A Bonanza carries 180 kg to 6 km with a duration of 5.5 hrs.</p>

Furthermore, they could meet many of the objectives associated with the CART site devoted to the study of marine stratus.

Langford et al. (1990) propose the use of Perseus-B as the appropriate platform for the ARM mission. The Perseus design is a high-wing monoplane with a single pusher propeller mounted in the tail. The wingspan is 17.9 meters (m) with a wing area of 60 m². The empty weight of the proposed airframe is 254 kg, while the gross takeoff weight is 695 kg. The Perseus design was first proposed (now called Perseus-A) for a series of stratospheric ozone missions (see our discussion in Section 6), which require higher altitudes than those needed for the ARM mission. Perseus-A might prove useful for initial high altitude tests of ARM-related capabilities. Perseus-B is a modified design tailored to meet ARM requirements. The altitude-duration-payload profile is shown in Figure 4-2. In terms of associated ground equipment, Perseus-B would need an airstrip with a runway of at least 2,000 feet, together with hangar, ground control, and support facilities.

Of equal interest to ARM would be the Gnat 750-93L, which has been proposed as a follow-on to the successful Amber aircraft. The Gnat 750-93L would be similar in size and performance to the proposed Perseus B.

The conclusion that the cost of small RPAs will be significantly less than that of a manned aircraft depends sensitively on assumptions with respect to the loss rate. The Langford et al. analysis, using information on commercial and military aircraft as well as on operations of balloons, establishes a loss rate goal of one operational loss per 500 flight operations. Given the newness of the technology, and the lack of operational experience, this seems like an extremely ambitious goal.

Profile for Planned Perseus B:

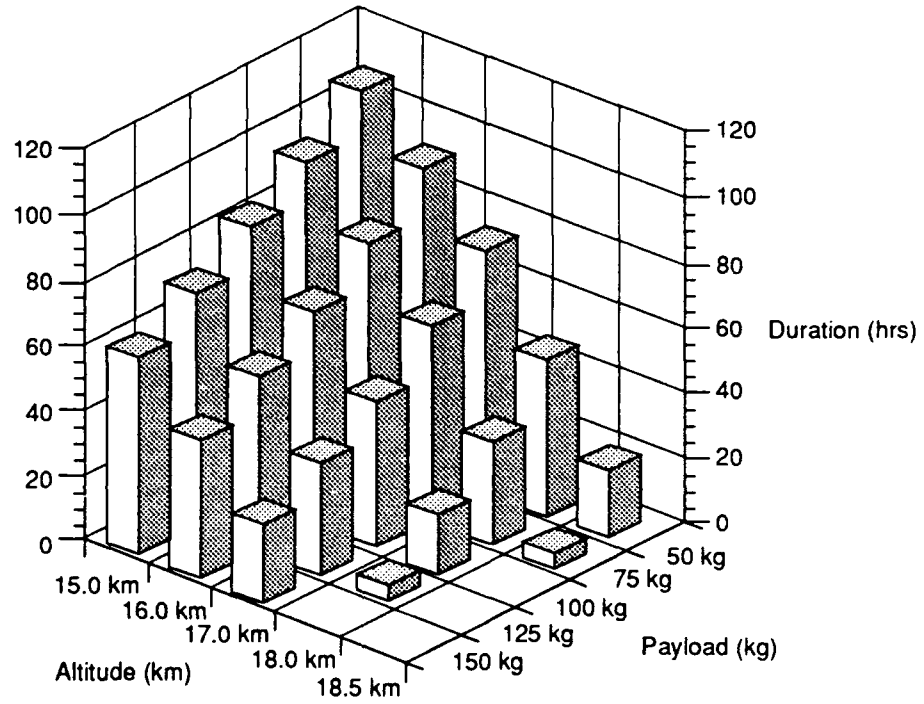


Figure 4-2. RPA Altitude - Payload - Duration (Langford, 1990)

Langford et al. (1990) have estimated the overall cost of a Perseus B system for a 5 year ARM deployment at a single site to range from \$20 M for a loss rate of 1 in 500 to \$25 M for a loss rate of 1 in 200 missions. To this must be added such extra developmental costs as the high altitude engine and the scientific instruments, plus the cost of instrument loss due to crashes, and the extra costs if 2 RPAs are to be used for simultaneous measurements.

4.4 FAA Requirements

A principal concern with respect to any RPA is compliance with Federal Aviation Administration (FAA) requirements. At present, all airspace above 18,000 feet is controlled by the FAA Air Route Traffic Control Centers. Experience with RPAs outside of government-controlled airspace is limited. The few test flights that have occurred within public airspace have all required manned aircraft as chase escorts for RPA flights above 3,000 feet.

Langford et al. (1990) are confident that procedures can be negotiated with local and regional FAA authorities so that an RPA could be operated in controlled airspace. This optimism is based on procedures developed and used over 20 years by the National Scientific Balloon Facility in Palestine, Texas. In the ARM scenario, the RPA would be equipped with a number of safety features.

- Command and control of the aircraft would be exercised over dual redundant radio frequencies.
- The aircraft would carry a Mode-C transponder, which emits a coded signal identifying the aircraft and its altitude when interrogated by an

FAA air surveillance radar or by another aircraft. The use of Mode-C will allow the operation of the TCAS collision avoidance system now being deployed by the FAA.

- The aircraft will also carry an in-flight destruction system that could be activated by a ground command or by internal logic within the aircraft flight control computer.
- All takeoffs and landings would be made at uncontrolled fields, where a Notice to Airmen clearly distinguishes the field as an unmanned aircraft operation closed to all but emergency traffic.

While the arguments for the operation of an RPA in controlled airspace appear convincing, we are concerned that the FAA may not permit operation, particularly over the Southern Plains ARM site, which is directly along the routes of transcontinental aircraft. In the case of balloon observations, a tracking aircraft escort is required when the balloon is not in direct contact with the Palestine ground site and when it is below 70,000 feet. The FAA would probably impose a similar requirement on any RPA not in direct contact with its control facility. This would limit aerial coverage over a CART site, but not seriously. In the Langford et al. proposal, an escort plane would be used during early operations, but not in routine operations.

4.5 Conclusions Regarding RPAs in ARM

If ARM is to meet its goals, it is extremely important to have aerial observations giving the microphysical characterization of cirrus clouds and of the environment below and above clouds, as well as providing vertical

profiles of radiation and the radiative balance at the top of the troposphere. While ground-based and satellite-based remote observations provide significant data, they cannot replace airborne, local observations. Because of the long endurance required to obtain observations over diurnal cycles, an unmanned aircraft would appear to be the preferred platform.

We have two principal concerns with respect to RPAs. First, there is an uncertainty as to whether or not RPAs can be operated in a manner consistent with FAA requirements. This issue should be settled early, before long-term commitments are made to purchase a number of RPAs. A second concern relates to the cost of RPAs in competition with manned aircraft. While a strong case can be made that the cost will be significantly less, there remain uncertainties about the cost and delivery schedule of a reliable high altitude, doubly turbocharged engine which has to be developed and tested, and about the costs related to the loss rate. There is no way to estimate the loss rate securely without operational experience. In addition, we emphasize once more that a lightweight, coordinated instrument package must be developed with sufficient lead time.

We understand that six Amber aircraft are potentially available for use in support of the first ARM site in the Southern Plains. While the Amber aircraft cannot meet all the requirements of a full ARM mission, it can provide valuable operating experience which undoubtedly would shed light on ways to meet FAA requirements, and perhaps even provide data with respect to the loss rate, although the capability of RPAs to ride out storms reaching above the 8 km Amber ceiling would, of course, still remain untested.

The Langford et al. proposal is technically extremely ambitious. It requires the combined development of an entirely new integrated instrument

package, and establishes design criteria for the airframe and engine of a platform that has never been flown. Against the risks posed by this untried technology are placed the potential advantages of a low-cost RPA. Since ARM is planned as a 10-year program, with occupation of five sites, it would seem that the early exploratory steps toward development of an RPA capability are warranted at this time.

4.6 Data Management

Including RPAs (and possibly small satellites) in the ARM program will raise new issues with respect to data management. Together, these sources would yield large amounts of data that must be processed, stored, and distributed in the most effective manner. In the case of RPAs, the additional volume of data is modest, since each of 16 channels will be transmitting data at a maximum 4800 baud rate. However, no attention has yet been paid to how this data will be incorporated into the CART site data management system and the overall ARM archive. The Langford et al. (1990) proposal does not discuss data, other than the requirements for communications between the RPA and the ground control center.

The ARM data management system design is based on the requirements for the ground-based instruments at the CART site. The architecture also provides for external data sources. It is not clear whether the RPA and small satellite data would be regarded as external data sources or as part of the CART instrument package. In the ARM data architecture, the observations from the CART instruments flow into the data whole system, which, in turn, prepares data for the archive. In view of the close connection between the ob-

servations to be secured through RPAs, and possibly through satellites, with the ground-based instrumentation, it is imperative that the data obtained by these remote platforms be integrated with the data secured by the CART instruments. As in many previous satellite projects, attention in the current RPA and small satellite activities of DOE has focused on platforms and instruments rather than on the associated data management requirements. If the overall system is to succeed, considerations of data management must proceed hand-in-hand with instrument and platform development.

To the extent that the small satellite missions discussed in later sections of this report are coupled to ARM, they will have a major effect on ARM data flow. While the requirements for data management for RPAs are relatively modest, those of a small satellite could swamp the proposed ARM data management system. Candidate instrument packages for small satellites, though not as completely developed as those for RPAs, indicate that the total data flow will be measured in terms of a few terabytes per year. This volume of data will be equal to or larger than the amount of data secured at the CART site.

The requirements for small satellite data differ from those for the RPA in another respect. While we would expect the data for the RPAs to be managed at the site at which the RPAs operate, small satellite data will undoubtedly be applicable to observational programs at the various sites as well as elsewhere. Thus, that data could be handled at a central facility or distributed among the various ARM sites. This issue remains to be addressed.

Because the RPA and small satellite activities are still in their early stages, it is important that the data management requirements be established at the same time the instruments are designed. In particular, as these

activities develop into actual programs, incorporating RPA data into the first site would seem to be a priority matter. At present, the software to be used at the first site is based on the NCAR-developed ZEB. An examination of whether or not the ZEB software is appropriate for the RPA mission is warranted.

4.7 A Role for Balloon Flights: Instrument Testing and Development

In Section 4.1 we discussed a number of light weight instruments needed for making ARM-related radiation measurements aboard RPAs. The proposed instruments have not yet been built or tested, and the very complex software that will be required to reduce and analyze the data does not exist at this time. Similar remarks apply to the development and use of small satellite instrumentation, which is discussed later in this report.

We suggest that the DOE and the various National Laboratories consider a high altitude balloon program to gain near term experience with instruments for RPAs and/or small satellites under realistic flight conditions. There are many precedents illustrating the value of balloon tests, a particularly relevant example being the on-going development of RPA instruments for studying ozone depletion in the stratosphere. The first balloon flight could take place within 12 to 18 months after a program is initiated. A full program would cost of the order of a few hundred thousand dollars (instead of a few hundred million dollars for a satellite) and participation in one of several possible existing balloon programs would cost even less. Such early flights of prototype versions of each of the proposed ARM RPA and satellite

instruments would give the designers and the community confidence in the performance of the instruments and the adequacy of the software under realistic environmental conditions. Almost always instrumental deficiencies and artifacts are detected in such quick turnaround low-cost programs before major resources are committed (for example, to a satellite program). Certainly this has been the experience of a very wide segment of the scientific community. Of perhaps even greater importance is the opportunity that such flights would provide for the testing of all of the software that will be required for the RPA and satellite programs.

We of course recognize that balloon flights probably cannot be controlled so that the observations are made over the ground-based ARM sites, and that they are restricted to certain seasons of the year and to certain geographical locations. In spite of these limitations, participation in such a balloon program would allow the instrument designers and builders to detect possible defects in their instruments, to evaluate environmental and instrumental background effects under actual flight conditions, and (perhaps most importantly) to obtain actual data on the atmosphere that could be used to test the data reduction and analysis software. We have been told that in the ERBE program, full data-reduction software to bring level zero data to top-of-the-atmosphere fluxes did not reach its finished form until four years after launch. Obviously, it would be far better for the ultimate scientific users of the data to have an early opportunity to evaluate the quality and utility of the final products of the observations. Their early inputs to the instrument designers and builders, based on actual flight data, would greatly strengthen the entire program, and would ensure that the program has been optimized to achieve the greatest scientific returns in a timely fashion.

High altitude balloons that will carry a 400 kilogram instrument¹ to an altitude of 40 kilometers for periods of several hours to several days are presently available at low cost (compared to the cost of aircraft or satellites). Also it should be noted that the US regularly flies such balloons on globe circling missions that can be used to obtain relevant atmospheric data from a large sample of sites.

¹The total "suspended weight" that a 29 Million Cubic Foot Balloon can carry to an altitude of 40 kilometers is about 1200 kilograms. Typically the instrument accounts for one third of the total "suspended weight." The remainder consists of batteries, thermal control systems, pointing devices, etc.

REFERENCES FOR SECTION 4

1. Langford, J., J. Anderson, and J. Wyss (1990) Unmanned Science Research Aircraft for the Atmospheric Radiation Measurement Program: A Feasibility Study, Battelle Northwest Laboratories. Contract 126351-A-R2.
2. Vitko, J., R. Abbink, T. Axelrod, C.A. Boye, I. Lewis, and P. Weber (1991), Presentation to JASON Summer Study, June 1991, La Jolla, CA.

5 INFLUENCING CLOUD ALBEDO FOR PROCESS DIAGNOSTICS

5.1 Introduction

An unclouded earth would reflect back into space about 0.15 of the sunlight incident upon it. However, because the extensive cloud layers (mainly cirrus and stratus) which typically cover half the earth's surface reflect nearly half (usually 0.25-0.65) of the sunlight incident upon them, the earth's albedo is about 0.3. These clouds also absorb almost all of the IR flowing up from the earth below them and reradiate IR to space from their (usually) cooler tops. In the equatorial zone the increased reflection of sunlight wherever such cloud cover exists is nearly balanced by the diminished IR radiated back into space by them. In other regions these two effects remain comparable but the cloud caused visual albedo increase exceeds the IR reduction. Because these clouds are so black to relevant IR, the IR emission from the cloud tops is not sensitive to most details of cloud microphysics such as droplet size or number density. This is not the case, however, for cloud optical albedo. When a thin cloud's column liquid water content ($W \lesssim 10^2 \text{g m}^{-2}$) is contained in droplets of radius (r) greater than several tenths of a μm , the cloud's optical albedo is proportional to W/r . Clouds rarely have a water content W approaching 10^4g m^{-2} , that needed for a typical cloud's visual albedo to exceed 0.9. Only then is the cloud albedo no longer sensitive to changes in details of the cloud's internal microstructure.

Present climate models suggest that an increase in total earth albedo by 10^{-2} (with no other changes in the earth's atmosphere) would result in a decrease in mean surface temperature of 2.6°C , about $2/3$ the increase in surface temperature expected from doubling CO_2 in such a model atmosphere (Anderson et al. 1990). Clearly, then, understanding and predicting changes in r , W , and fractional cloud cover, all of which vary greatly with time and location, are of crucial importance to understanding present climate and to fashioning reliable GCM's for climate change predictions.

The main approach to improving knowledge of cloud structure and formation has been based upon detailed measurements of clouds as they exist and change naturally. However, it may also be useful to consider deliberate controlled, anthropogenically introduced cloud changes which emphasize changing cloud albedo (by altering r for example) rather than inducing rain; the latter has, in the past, motivated most cloud seeding experiments. If successful, such manipulation could have several consequences. From "small" area (e.g. $30 \text{ km} \times 30 \text{ km}$) experiments, may come a better understanding of cloud processes and, ultimately, the cloud process parameterizations needed for GCM's. (Controlled cloud albedo changes over large areas [$\gg 10^4 \text{ km} \times 10^3 \text{ km}$] might even test improved GCM predictive reliability.)

5.2 Cloud Albedo

In the geometrical optics regime of drop radius $r \gtrsim r_o \equiv 4\lambda \sim 0.3\mu\text{m}$ the backscattering cross section (i.e. scattering into the back hemisphere) of a water droplet is approximately given by

$$\sigma_b \sim \pi r^2 \left(\frac{n-1}{n+1} \right)^2 \quad (5-1)$$

with n the liquid water index of refraction. In the single backscatter approximation cloud albedo (a) is then

$$a \sim 10^{-1}W/r, \quad (5 - 2)$$

for W in g m^{-2} and r in μm . Equation (5-2) is adequate only for thin clouds with $a \ll 1$, but quite generally cloud albedo is a function of the single variable W/r . More extensive calculations give the results of Figure 5-1 and Figure 5-2.

In the wave optics regime $r \ll r_o$, where Rayleigh scattering describes single droplet reflection, the σ_b of Equation (5-1) is reduced by a factor $(r/\lambda)^4$. In the single backscatter approximation cloud albedo for fixed W then has the dependence on droplet radius sketched in Figure 5-3. Because typical cloud droplets have $r \sim 10\mu\text{m} \gg r_o$, cloud albedo for visible light would generally be increased by dividing W into a larger number of smaller droplets. Only if the droplet effective radius is lowered below r_o could cloud albedo be decreased by doing this.

We turn now to some elementary considerations about relationships between water soluble cloud condensation nuclei and cloud droplet size.

5.3 Seeding Droplet Growth

To initiate the growth of small cloud droplets, nuclei are needed to mitigate the effect of water surface tension (σ) in increasing the equilibrium vapor pressure (p_v) around them. This fractional vapor pressure increase is

$$\frac{\Delta p_v}{p_v} = \frac{2\sigma\mu}{rRT\rho} \quad (5 - 3)$$

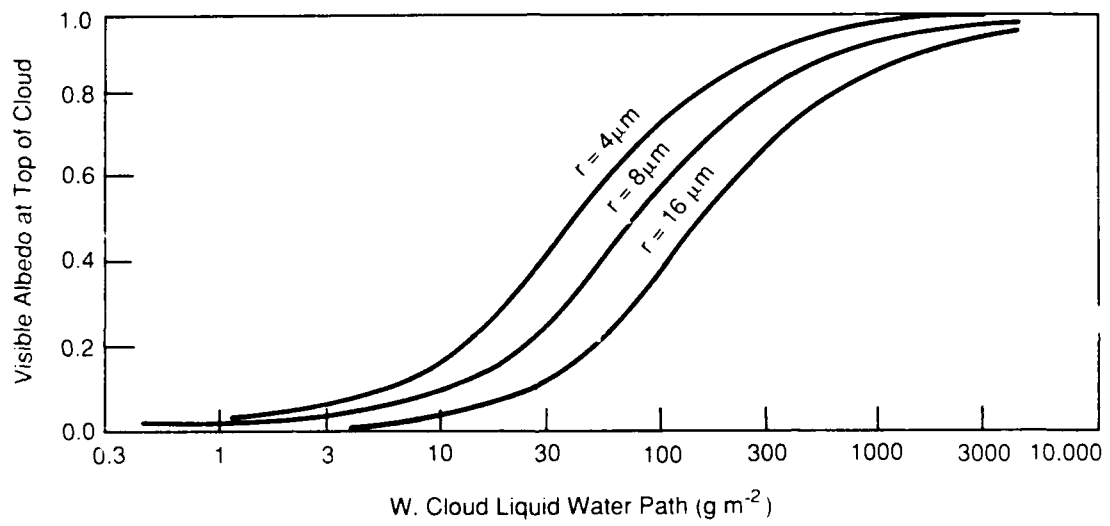


Figure 5-1. Cloud albedo as a function of W and r.

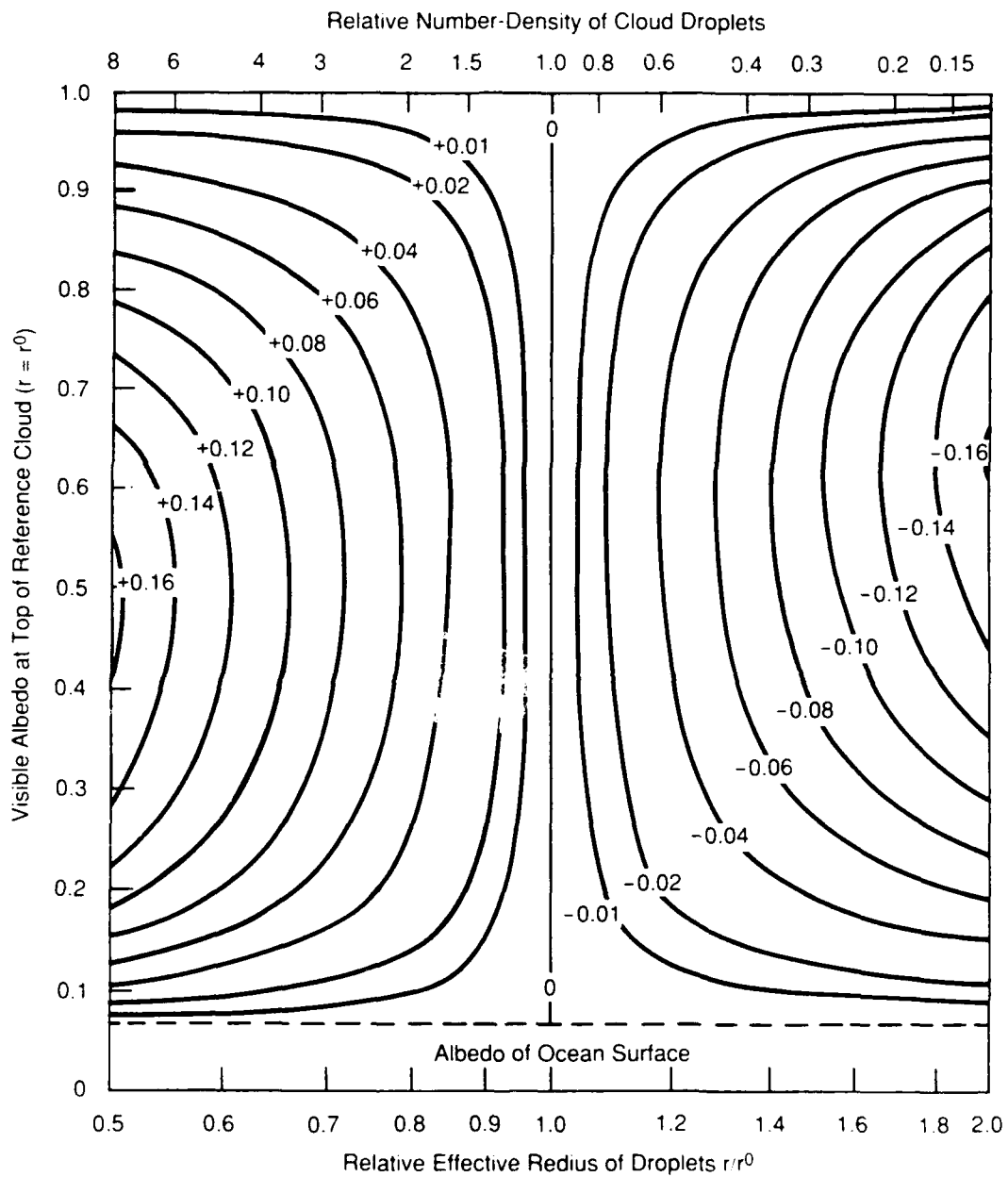


Figure 5-2. Change in albedo for clouds over ocean as droplet radius (r) changes.

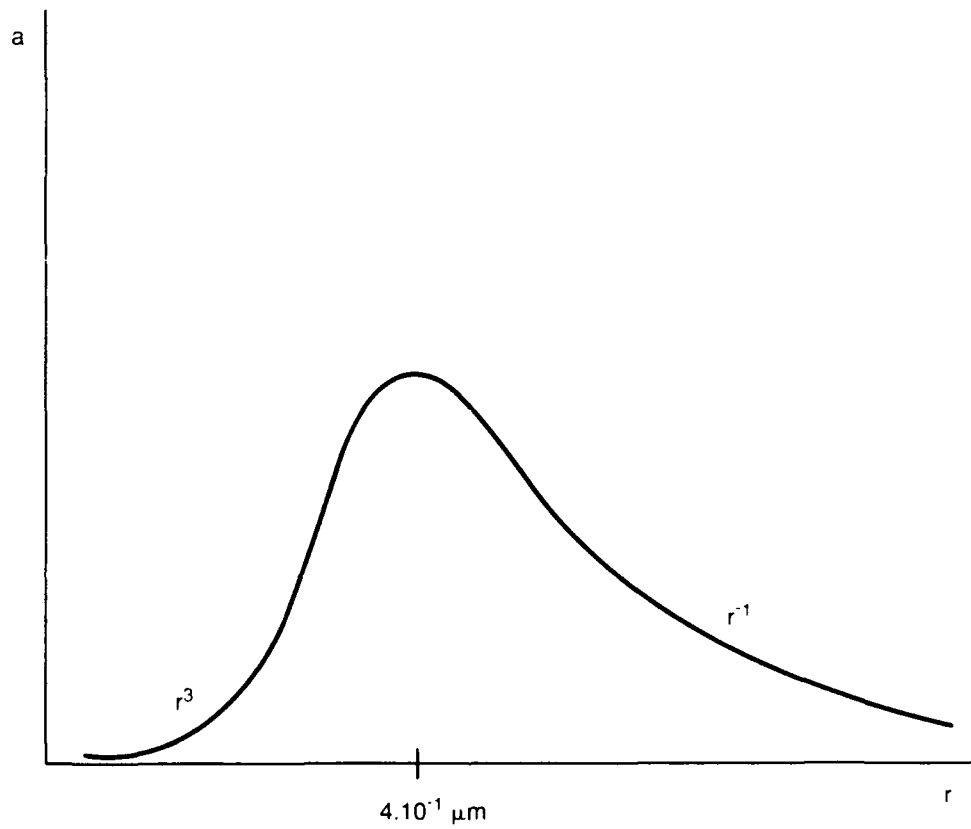


Figure 5-3. Albedo (a) of a thin cloud as a function of droplet radius r when water content W is fixed.

with $\mu = 18$ the molecular weight of water, ρ its density, R the gas constant and T the temperature.

A contribution to Δp_v of opposite sign is made by water soluble salts or acids (e.g. H_2SO_4 or NaCl) in the droplet which act to reduce that pressure (Raoult's Law). The fractional vapor pressure reduction for various solutes dissolved in liquid water is given below in Table 5-1.

Table 5-1
Fractional vapor pressure reduction - $\Delta p_v/p_v$ (in hundredths)
as a function of solute mol fraction (also in hundredths)

Mol Fraction of Solute (10^{-2})	0.9	1.8	3.6
H_2SO_4	1.7	3.5	8.3
NaCl	1.6	3.3	6.9
LiOH	2.1	4.9	10.3
NH_4NO_3	1.7	2.9	5.5
$(\text{HH}_4)\text{SO}_4$	1.5	3.2	6.2

To a reasonably good approximation

$$\frac{\Delta p_v}{p_v} \sim -2 \times \text{solute mol fraction.} \quad (5 - 4)$$

After a droplet forms around a water soluble nucleus, droplet growth by vapor absorption from a surrounding (super)saturated atmosphere will reduce the initial solute mol fraction. For a fixed number (N) of dissolved solute molecules $\Delta p_v/p_v$ depends upon droplet radius r as sketched in Figure 5-4.

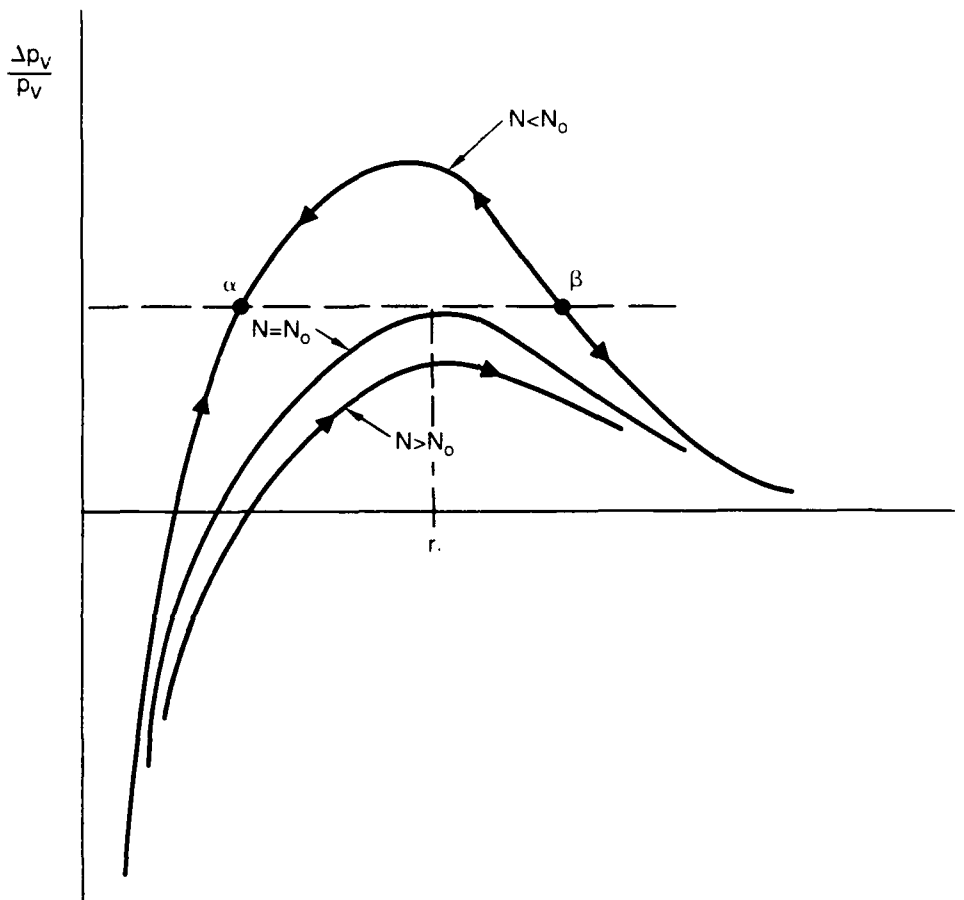


Figure 5-4. Equilibrium vapor pressure above a water droplet of radius r containing N dissolved solute molecules. For fixed external $\frac{\Delta p_v}{p_v}$, a droplet may grow indefinitely ($N > N_0$), grow or shrink to the point α ($N < N_0$) or grow indefinitely if $r > r_0$.

The droplet radius for maximum $\Delta p_v/p_v$ is

$$r_1 = \left(\frac{9 NRT}{4\pi N_A \sigma} \right)^{1/2} \sim 2N^{1/2} \cdot 10^{-8} \text{ cm}, \quad (5-5)$$

with N_A Avagadro's number.

The maximum $\Delta p_v/p_v$ is

$$\begin{aligned} \left(\frac{\Delta p_v}{p_v} \right)_{\max} &= \frac{4(4\pi)^{1/2} \mu}{9\rho} \left(\frac{\sigma}{RT} \right)^{3/2} \left(\frac{N_A}{N} \right)^{1/2} \\ &\sim 3N^{-1/2} \end{aligned} \quad (5-6)$$

From Equations (5-3), (5-4) and Figure 5-4 we conclude the following. In water vapor whose vapor pressure is supersaturated by a fraction $\Delta p_v/p_v$ there exists a critical number (N_o) of water soluble molecules which determines droplet growth. When $N < N_o$ a tiny droplet ($r < r_1$) cannot grow to reach the radius r_1 of Equation (5-3).

$$N_o \sim 9 \left(\frac{p_v}{\Delta p_v} \right)^2 \quad (5-7)$$

$$r_1 = r(N_o) \sim 6 \left(\frac{p}{\Delta p_v} \right) \cdot 10^{-8} \text{ cm}. \quad (5-8)$$

When $N > N_o$ tiny droplet growth is not limited. Typical clouds of interest here have $\Delta p_v/p_v \sim 10^{-3}$ and thus critical solute seed nuclei numbers $N_o \sim 10^7$ and $r_1 \sim 0.6 \mu\text{m}$, but there is great variation (even within a single cloud) as indicated in Figure 5-5. A dry aerosol consisting exclusively of N_o solute molecules would have a "droplet" radius

$$\hat{r}_{\min} \sim 6 \cdot 10^{-8} \left(\frac{p_v}{\Delta p_v} \right)^{2/3} \text{ cm}, \quad (5-9)$$

and thus a volume of order 10^{-3} that of the critical droplet it nucleates.

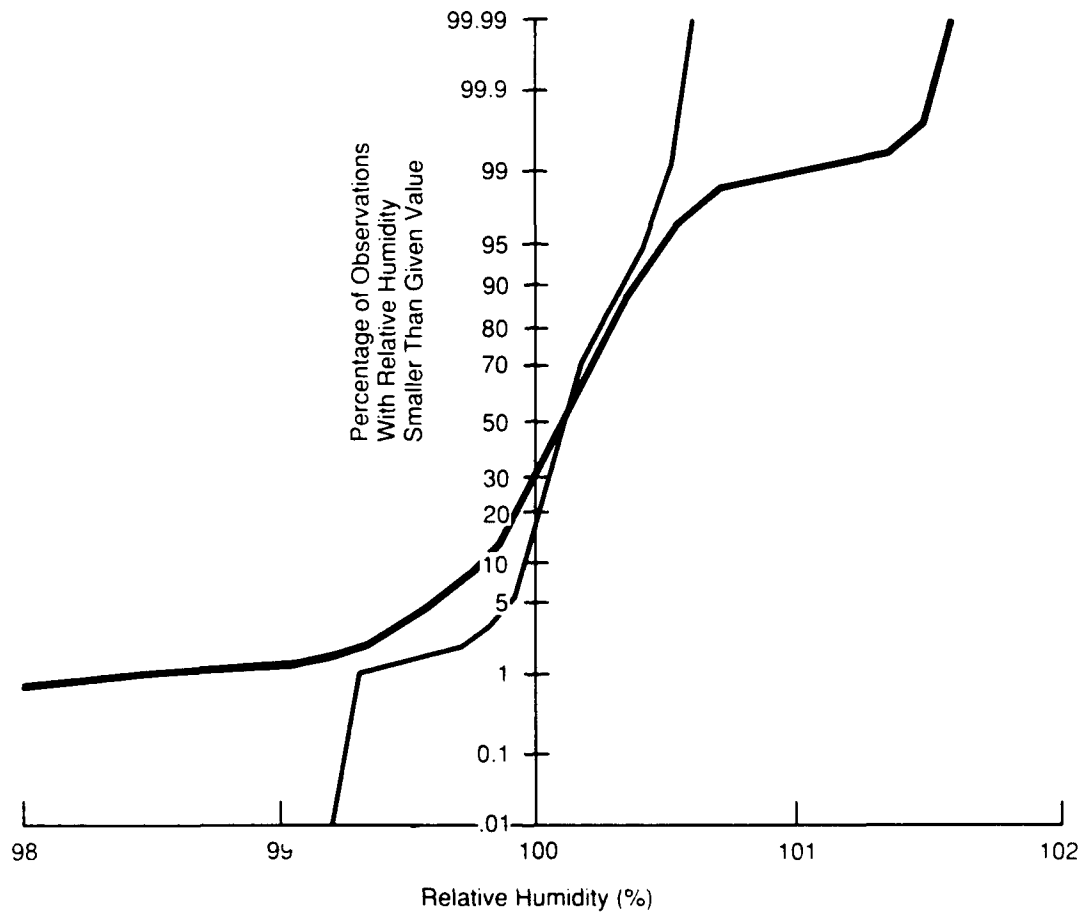


Figure 5-5. Percentage of observations with relative humidity less than a given value for all samples (heavy line) and for samples taken within 300 m of cloud base (thin line) (Pruppacher, 1981).

Once beyond the critical size, droplets can continue to grow by absorbing water vapor, so long as the ambient medium remains supersaturated. Eventually, surface tension and solvent effects become unimportant. Growth is then governed by diffusion of water vapor molecules toward the droplet. Because the heat of vaporization of water is large, heat conduction also plays a role. Suppose that the supersaturation $\Delta p_v/p_v$ is constant in time and small in magnitude. The droplet radius $r(t)$ at time t , r_0 being the radius at earlier time $t = 0$, is then given by

$$r(t) = \sqrt{r_0^2 + A \frac{\Delta p_v}{p_v} t},$$

$$\frac{1}{A} = \frac{\rho_L}{2} \left\{ L^2 M / K R T^2 + R T / p_v D \mu \right\}.$$

Here ρ_L is the density of liquid water, L the heat of vaporization, μ the molecular weight; R is the gas constant, D the coefficient of diffusion of H_2O in air, K the thermal conductivity of the ambient medium, T the ambient temperature, $p_v(T)$ the equilibrium vapor pressure of water. For a numerical example, take the case $\Delta p_v/p_v = 10^{-3}$, $T = 273^\circ K$. The time required for a droplet to grow to a radius $r(t) = 50\mu$, starting from a much smaller radius, is about 7 hours!

5.4 Observed Cloud Condensation Nuclei

Supersaturation excesses in marine stratiform clouds are in the range

$$\frac{\Delta p_v}{p_v} \sim (1 - 5) \cdot 10^{-3}. \quad (5 - 10)$$

According to Anderson, Wolfe, and Warren (1990) the minimum size cloud condensation nuclei (CCN) needed to support droplet growth have diameters in the range $0.14 - 0.05 \mu m$, in agreement with the estimate of Equation

(5-9). Figure 5-6 gives their summary of observed sizes of marine aerosol CCN's. The largest number of nuclei have $N \ll N_o$ and do not grow significantly. Their radius distribution peaks below $r \sim 2 \cdot 10^{-2} \mu\text{m}$ where the light scattering cross section is far into the Rayleigh regime and several orders of magnitude below that of Equation (5-1). These nuclei and the tiny water droplets they stabilize make an unimportant contribution to cloud albedo (as indicated in Figure 5-3). The "accumulation mode" nuclei have $N > N_o$. They can grow by continuing to absorb water vapor as shown at the end of the last subsection. Over most of the sea surface the number density of cloud droplets is similar to that of the accumulation mode nuclei, suggesting that the number of such CCN's limits that of the cloud droplets (and may, perhaps, also play an important role in determining W and/or fractional cloud cover).

A persuasive case has been made that the droplets in the very extensive marine stratus cloud layers are nucleated and allowed to grow because of the sulfuric acid contained within them (cf. Anderson et al., 1990, and references therein). The source of most of this sulphate appears to be microbiota in the upper ocean layers which produce dimethyl sulfide, $(\text{CH}_3)_2\text{S}$. These molecules must, however, be oxidized in the droplets or in the atmosphere before enough can be dissolved in a tiny droplet (as $\text{SO}_4^- + 2\text{H}^+ \cdot \text{H}_2\text{O}$) to give $N > N_o$. The formation rate of CCN accumulation mode nuclei could be limited either by the production rate and outflow from the sea surface of $(\text{CH}_3)_2\text{S}$ or by the availability of sufficient oxidant to convert the initial reduced sulfur to the droplet soluble sulfate.

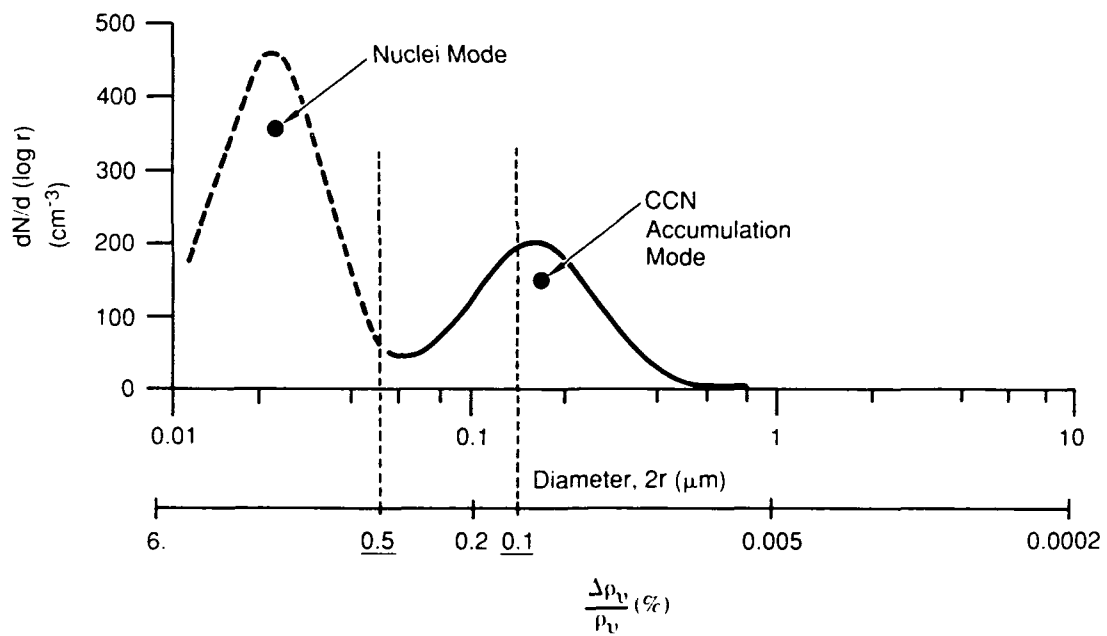


Figure 5-6. Marine Aerosol Number Distribution. Sources: Anderson et al. (1990), Warren (1991).

5.5 Sea Surface Sulfur Emission and Oxidants

We consider next how much additional sulfur might be needed to change CCN abundance, droplet size, W , or cloud cover fraction enough to cause significant alterations in the albedo from clouds.

Estimates for sulfur emission into the earth's atmosphere are given in Table 5-2. The putative sulfur source of CCN's for marine (stratiform) clouds

Table 5-2
Sulfur emission rates

Sulfur Source	Total Emission Rate (10^{12} g yr ⁻¹)
(CH ₃) ₂ S from ocean biota	15 - 30
total natural emission (mostly reduced S)	80
anthropogenic	80

has an average sea surface emission rate of about 10^{-3} tonnes km⁻² week⁻¹. It is not yet clear whether CCN sulfate formation is limited by this emission rate or by the availability of oxidants to make droplet sulfuric acid. This needed sulfur oxidation could be accomplished by photochemically produced H₂O₂ or O₃ already dissolved in droplet water or in homogeneous gas reactions with HO_x, H₂O₂, or O₃ in the atmosphere. A similar question is relevant for the oxidation of anthropogenic SO₂ emission to sulfuric acid in acid rainfall downwind of fossil fuel burning power plants. In that case there is evidence that in many regions, at least in winter, sulfuric acid in rain is oxidant limited (e.g., JASON 1985). Over the oceans far from sources of indus-

trial and transportation smog, tropospheric oxidant abundances are greatly diminished but so is the level of injected anthropogenic atmospheric sulfur. Until the question of the balance between them in making sulphate CCN's is resolved, it is difficult to draw compelling conclusions from the presence or absence of observed correlations between cloud properties and established SO₂ sources (Wigley 1989). There does appear, however, to be some evidence that anthropogenically emitted sulfur can increase CCN abundance and cloud albedo by increasing the number and decreasing the radius of cloud droplets. Increased albedo is seen in satellite pictures of oceanic stratocumulus clouds above ship engine exhaust emissions (Coakley et al., 1990, Radley et al., 1989, Conover 1966, Scorer, 1987) although these changes may be determined also by just heat deposition (e.g., Porch 1990). Similarly, clouds which pick up more CCN's when passing over urban pollution in Southern California do appear to have a raised albedo (Landsberg 1981).

5.6 Cloud Process Experiments

Very large perturbations (~ 100%) in near sea surface sulfur emission could be maintained over a 30 km × 30 km area by controlled sulfur emission of about one tonne per week. Such an emissions program might be useful in studying various critical cloud process questions. Those particularly relevant to understanding how to affect cloud cover albedo in a deliberate way include the following.

- (a) Is CCN production over the oceans oxidant or sulfur limited?
- (b) If the former, can CNN radii be reduced and cloud albedo increased by injecting already oxidized H₂SO₄ or (NH₃)₂SO₄ aerosols?

Could nitric oxide injection be used to increase local oxidation rates?

- (c) Would clouds with reduced droplet size drizzle less and survive longer? Would cloud cover be increased?
- (d) What is the optimum injected nuclear particle size for increasing total cloud albedo? Can controlled anthropogenic cloud nucleating particles be produced and distributed abundantly in such sizes?
- (e) If CCN creation over the oceans is not oxidant limited what is the consequence of large controlled SO₂ injection? Are more CCN's and smaller droplets a consequence or would the CCN number remain about the same but their size (N) become larger?
- (f) What are the relative advantages for changing albedo of controlled particle sulfate and gaseous SO₂ emission? What kind of controlled "seeding" is best adopted for affecting the product of cloud cover and reflectivity?

Questions such as these would seem best explored from ARM sites with associated RPA's.

(If enough progress can be made on such questions it might become appropriate to consider a possible cloud albedo alteration experiment over a very much larger area and to compare observed consequences with those predicted by various GCM's. The altered cloud region should be very much larger than the GCM grid scale. However, to double sulfur emission even in a 10³ km × 10⁴ km area may require an additional injection of about 10⁴ tonnes/week for the required period of time.)

Volcanoes can result in enormous quantities of sulphate settling down through the atmosphere very far from the volcano itself. These sulphate particles may be a very significant addition to the usual natural abundance of sulphate CCN. Monitoring changes in CCN abundances and sizes after volcanoes may support unique opportunities to test cloud albedo modelling and its consequences for GCM's over large areas.

If the microphysics needed for knowing how to affect cloud albedo were to be understood and GCM's could predict with some confidence consequences of albedo changes in selected areas, it may someday become possible to consider using controlled cloud albedo increases to counter CO₂ greenhouse warming in those regions where such warming would be most harmful. Important world-wide mitigation of CO₂ greenhouse warming might take an increase of order .01 in the earth's albedo. Half of this albedo is cloud cover reflection and an increase of order 10% would be needed from the product of cloud albedo and cloud cover fraction. From Figure 5-2 a droplet radius change $\Delta r/r \sim -10^{-1}$ and a droplet number fractional increase $-3\Delta r/r \sim +0.3$ might be needed if this albedo increase was accomplished only by increasing single cloud albedo. A smaller fractional increase would be needed if the earth's albedo was changed by increasing cloud cover. Therefore controlled CCN seeding rates of order 10^{-1} that of the natural one over the oceans may give an important earth surface cooling. This would correspond to a controlled anthropogenic input of almost 10^5 tonnes/week (roughly consistent with other estimates (NAS 1991, Albrecht 1989)). According to Slingo (1990) a 15-20% increase is needed in low cloud cover, 20-25% in W , and 15-20% in $\Delta r/r$ to balance the warming from doubled CO₂. If sulphate CCN production over the sea surface is mainly oxidant limited, at least 10 GW of UV light would be needed to produce the oxidant

photochemically *in-situ*.

However, more detailed information and understanding about gas/particulate/oxidant injection recipes and consequences, CCN and droplet lifetimes, etc., and especially how these affect albedo are needed urgently before one can have much confidence even in such rough estimates.

REFERENCES FOR SECTION 5

1. Albrecht, B. (1989) Science **245**, 1227.
2. Anderson, T. Wolfe, G. and Warren S. (1990) "Biological Sulfur, Clouds, and Climate" to be published in Encyclopedia of Earth System Science.
3. Coakley, J., Bernstein, R., and Durkee, P. (1990) Science **237**, 1020 (and references therein).
4. Conover, J. (1966) Journal of Atmospheric Sciences **23**, 778.
5. JASON Report JSR-83-301 (1985): "Acid Deposition".
6. Landsberg, H. (1981) The Urban Climate (Academic Press, New York).
7. Mitigation Panel Report of NAS Committee on Policy Implications of Greenhouse Warming (in press, 1991).
8. Porch, W., Kao, C-Y., and Kelley, R. (1990) Atmospheric Environment **24A**, 1051.
9. Pruppacher, H. (1981) Clouds, Their Formation, Optical Properties and Effects p.95 P. Hobbs and A. Deepak eds (Academic Press, New York).
10. Radke, L., Coakley, J., and King, M. (1989) Science **246**, 1146.
11. Scorer, R. (1987) Atmospheric Environment **21**, 1417.
12. Slingo, A. (1990) Nature **343**, 49.
13. Warren, S. (1991) JASON Briefing.
14. Wigley, T. (1989) Nature **339**.

6 OZONE DEPLETION

The possible formation of an Arctic ozone hole similar to the well-established Antarctic hole is an environmental disaster waiting to happen. For a detailed discussion of the evidence, see Brune et al. (1991). There is an urgent need for better and more extensive observations of the processes occurring in the polar stratosphere, so that the danger of a major loss of ozone can be accurately assessed. This section sketches the present state of knowledge and discusses what could be done to obtain more knowledge quickly.

6.1 Present Situation in the Arctic

The region we are concerned with is the "Polar Vortex", a part of the arctic air-mass that does not mix strongly with the remainder of the atmosphere during the winter months. It is useful to have in mind the quantities of material contained in the ozone layer, which extends roughly from 15 Km to 25 Km altitude, within the $2 \cdot 10^7$ Km² area of the polar vortex. The layer contains about:

$2 \cdot 10^{13}$	tons of air,
$4 \cdot 10^7$	tons of ozone (O ₃),
10^4	tons of chlorine oxide (ClO),
$2 \cdot 10^5$	tons of nitrogen oxides (mostly HNO ₃),
200	tons of bromine oxide (BrO).

When exposed to sunlight in the Arctic spring, ClO dissociates reversibly to atomic chlorine and becomes an exceedingly efficient catalyst for

the destruction of ozone. Each day the ClO destroys about 100 times its own weight of ozone. The BrO destroys ozone even more efficiently. Acting in conjunction with ClO, BrO destroys about 1000 times its weight of ozone each day.

If the ClO and BrO should remain in the ozone layer for 50 days after the winter ends and sunshine returns, more than half of the ozone in the layer would be gone. That is roughly what happens each spring in the Antarctic ozone hole. Fortunately, in the Arctic ozone layer, the nitrogen oxides convert ClO and BrO into chlorine and bromine nitrates (Cl NO_3 and Br NO_3) which do not destroy ozone. The reason why this protective action does not work in the Antarctic is that the nitrogen oxides and HNO_3 are adsorbed onto the ice particles of stratospheric clouds which form during the winter. Antarctic winter temperatures are low enough (below -80°C) so that stratospheric clouds persist and remove a large fraction of nitrogen oxides from the air.

The situation in the Arctic is delicate, because the winter stratospheric temperatures are just at the threshold for forming clouds. Stratospheric clouds are formed, but are not persistent enough to remove nitrogen oxides extensively. However, the margin of safety is small. The threshold for forming stratospheric clouds is sharp. If the Arctic winter stratosphere were only a few degrees colder, the destruction of ozone might easily become as bad in the Arctic as it is in the Antarctic. And the quantity of chlorine in the stratosphere is increasing from year to year as a result of the continuing influx of chlorofluorocarbon molecules from the troposphere.

To make a bad situation worse, the temperature of the Arctic winter stratosphere is probably decreasing from year to year as a result of the in-

crease of greenhouse gases, particularly carbon dioxide (CO₂) and methane (CH₄), in the atmosphere. The greenhouse gases produce a larger and more predictable effect in cooling the stratosphere than they do in warming the surface of the earth. The cooling of the stratosphere is a direct and calculable result of the efficiency of the greenhouse molecules in radiating energy away into space. It is possible that within a few years the increase of CO₂ and CH₄ will be pushing the Arctic winter temperatures low enough, so that stratospheric clouds will become persistent and the depletion of ozone will become as severe as it is in the Antarctic.

If these possibilities turn out to be real, the political consequences will be important. The effect of CO₂ emissions in destroying northern-hemisphere ozone may be more visible and more frightening than the effects of CO₂ on climate. It is therefore important, for political as well as for scientific reasons, to obtain reliable information about the physics and chemistry of the Arctic stratosphere. There is a strong case for investigating the Arctic stratosphere with higher priority than the other components of the global climate system.

6.2 Obtaining better information

Almost all the detailed information that we possess about the Arctic stratosphere was obtained by a few flights of ER-2 aircraft in the Arctic Airborne Stratospheric Experiment (AASE) in 1989. The ER-2 is the only aircraft now operational that is capable of flying far enough and high enough to make *in-situ* measurements of the crucial chemical processes occurring in the polar stratosphere. Unfortunately, manned aircraft flights are not well suited to regular monitoring of the stratosphere. The flights are expensive

and the aircraft are not regularly available. Observations with manned aircraft give us only a few glimpses, sporadically distributed in space and time, of complicated processes extending over large areas. To understand the processes well enough to make reliable predictions, we need observations that sample the whole area systematically at least once a month, and, during the critical period of ozone destruction in the spring, at least once a week. Observations are needed of the concentrations of all relevant chemical species, aerosols and cloud particles, together with radiation fluxes, horizontal and vertical wind-speeds, and temperature. Because of the sensitivity of cloud-formation to temperature, accurate measurements of local temperatures are particularly important.

Since observations by manned aircraft are inadequate, new observation platforms are needed. Two new types of platform could become available during the next few years if their deployment were given high priority. The new platforms are high-altitude Remotely Piloted Aircraft (RPA) and Small Satellites.

For information about RPA, see the report by Anderson and Langford (1991). Existing RPAs do not fly high enough to reach the ozone layer with useful payloads. Several new types of RPA are under development with greatly improved ceiling and endurance. Designers of the new generation of RPA claim that they will be able to fly with a 400-pound payload at altitudes of 15 to 20 Km for 36 to 60 hours. If these performance figures can be achieved, the RPA will give us a view of the ozone layer far more complete and coherent than the view provided by manned aircraft. The development and deployment of RPAs will not be cheap, but their ability to fly for several days at a variety of altitudes allows them to patrol the polar vortex in a fashion that no manned aircraft can match.

The job of patrolling the polar vortex may be conveniently combined with the job of local atmospheric monitoring that is included in the Atmospheric Radiation Measurement (ARM) Program already initiated by DOE. The ARM program is planning to establish a base for local monitoring on the North Slope of Alaska. The ARM base, under present funding limitations, will have only ground-based instruments. To be fully effective, the base should also include RPAs, together with the infrastructure of logistics and maintenance crews required to keep RPAs in year-round operation. The same infrastructure would be ideally suited to support a fleet of RPAs dedicated to monitoring the Arctic ozone layer. It would not be necessary to use the same RPAs for the local and the long-range missions. Probably the bulk of the local missions would be flown by RPAs smaller and cheaper than those required for the ozone layer. Even if the RPAs themselves are not shared, the sharing of a common infrastructure would greatly increase the cost-effectiveness of both programs. And the two programs would also benefit by sharing scientific instruments and data-handling facilities.

In addition to RPAs, the monitoring of Arctic ozone requires satellites to provide rapid coverage of wide areas. For the same reason, the ARM program hopes to include one or more ARM Satellites to supplement the local ARM measurements with global satellite data. Again, the same satellites could serve as adjuncts to ARM and to the ozone-monitoring program. The major problem with satellite observation is the length of time required to build and launch satellites and their payloads. The Arctic ozone problem is urgent and requires monitoring as soon as possible. To wait for the deployment of the big EOS satellites, now scheduled for 1998 or later, is not acceptable. It is therefore proposed that a new system of small satellites, capable of operating substantially sooner than EOS, be launched with instruments to survey the

Arctic ozone layer as well as the outgoing radiation and cloud-distribution data required for ARM.

The instruments to be carried on a small satellite for the purpose of ozone monitoring are partly the same as those required for ARM and partly different. Common to ozone-monitoring and ARM are infra-red spectrometers and imaging instruments for observing clouds. Unique to the ozone monitoring mission are active transmission measurements involving two satellites. A typical transmission measurement would have one satellite transmitting radio or laser radiation and another satellite receiving, with the orbits of the two satellites adjusted so that the transmission path grazes the limb of the Earth. Such measurements give accurate information about the distributions of density, temperature and chemistry in the stratosphere. They are uniquely sensitive indicators of the presence of optically thin polar stratospheric clouds, which are difficult to detect by other means.

Ordinary passive observations of the Earth's limb will give useful information about stratospheric clouds when the limb is in sunlight. But the stratospheric clouds that are crucial for the denitrification of the stratosphere and the consequent destruction of ozone are formed in the darkness of the polar winter. To study these crucial stratospheric clouds, transmission measurements using two satellites will probably be required.

In conclusion, we note new Arctic ER-2 observations in Winter 91/92 showed that the Arctic stratosphere was again near the threshold for creation of a "hole," though no hole actually appeared.

REFERENCES FOR SECTION 6

1. Anderson, J.G. and J.S. Langford, "Unmanned Aircraft: An Essential Component in Global Change Research," (Aurora Flight Sciences, Manassas, VA), 1991.
2. Brune, et al., "The Potential for Ozone Depletion in the Arctic Polar Stratosphere," *Science* **252**, 1260 (1991).

7 IR DETECTORS FOR RPAs AND SMALL SATELLITES

In Section 4 we discussed the possibility of using new developments in IR technology to make compact radiometers and imaging spectrometers for RPA measurements of radiation flux. In Sections 8-13 we will discuss similar possibilities for small satellites. In this section we review the different kinds of detectors and materials that have been developed in recent years and the ways in which they could be applied to radiation measurements from RPA or small satellite platforms.

7.1 Classes Of Imaging IR Detectors

HgCdTe -

The material is a random alloy of HgTe and CdTe whose bandgap can be adjusted by varying the Hg content. Photoelectrons are produced by absorption across the bandgap, and these detectors can be operated as photoconductors or photodiodes. Detectors made from HgCdTe have strong theoretical advantages, and are currently used in many military applications. However, the yield and reliability of these detectors has been limited by problems with the material and processing: HgCdTe is soft, unstable (the Hg tends to come out), inhomogeneous, and contains significant quantities of poorly characterized electrically-active defects. Surfaces are electrically active, and surface states are not well understood or controlled. These problems are particularly severe for large arrays with small pixels. Most current HgCdTe detectors are

linear arrays which are scanned to produce a two dimensional image. Two dimensional "staring" arrays are well along in development and are nearing application. The best examples of scanning HgCdTe arrays have excellent sensitivity and good performance, but are expensive.

Summary of Characteristics of Hg Cd Te

type - quantum detector - photoconductor, photodiode

wavelength response - below cutoff λ_c

wavelength cutoff - adjustable to $\lambda_c \approx 10\mu\text{m}$

temperature of operation - 80K for $\lambda_c \sim 10\mu\text{m}$ and 300 k background limited performance

sensitivity - excellent at best, can be much better than 300K background limit

array size - linear large (~ 400), two-dimensional moderate ($\sim 128 \times 128$)

array uniformity - moderate

long-term stability - variable

availability - now

Imaging Bolometers

Bolometers work by measuring the temperature increase associated with absorbed radiation. A scanned thermocouple bolometer was used for the ERBE satellite. Bolometers have the strong advantages for radiometric measurements that the wavelength response is determined by an absorbing coating which can be black over a wide range of wavelengths, they directly measure radiant power, and they can operate at room temperature. Uncooled imaging arrays have been developed in a classified program (HIDAD program - HI-Density Array Development), which was recently declassified (LOCUSP

program - Low Cost Uncooled Sensor Program), but remains restricted to US citizens. Bolometer arrays simply consist of many small bolometers fabricated using modern lithographic techniques on Si substrates. Two varieties are currently available: Honeywell makes resistive bolometers using temperature sensitive resistive films, and Texas Instruments makes capacitive bolometers using materials with temperature-sensitive electric polarizability, currently BaSrTiO₃. The sensitivity is limited by thermal fluctuations in the bolometer element determined by the thermal conductance to the substrate. Because bolometer arrays are based on Si technology, they can be made cheaply and reliably relative to newer material systems such as HgCdTe.

Summary of Characteristics of Imaging Bolometers

type - thermal detector

wavelength response - determined by absorptive coating over a wide range from visible to $> 25\mu\text{m}$

design wavelength cutoff - adjustable to $> 25\mu\text{m}$

temperature of operation - $\sim 300\text{K}$ for $\lambda_d \sim 10\mu\text{m}$, also cooled

sensitivity - low to moderate

array size - large (240×336)

array uniformity - good

long-term stability - good

availability - near future

PtSi and GeSi/Si Detectors

These devices work by internal photoemission of electrons over a barrier: a Schottky barrier between a thin metal Pt film in the case of PtSi, and a heterojunction in the case of GeSi/Si detectors. Both types have the

disadvantage of poor, wavelength-dependent quantum efficiency associated with internal photoemission. PtSi detectors have been around a long time, but are limited to MWIR applications wavelength $\sim (5 \mu\text{m})$; GeSi/Si detectors are new, grown using molecular beam epitaxy and have adjustable cutoff wavelength to $\lambda_c \sim 25 \mu\text{m}$. Both have the strong advantage that they have been integrated with an Si charge coupled device (CCD) readout. The demonstrated uniformity and yield (0.2% variation for a 400×400 pixel PtSi array with all pixels operating) are excellent.

Summary of Characteristics of PtSi and GeSi/Si Detectors

type - quantum detector, internal photoemission

wavelength response - slow roll-off in quantum efficiency to cutoff λ_c

wavelength cutoff (PtSi) - $\lambda_c \sim 5 \mu\text{m}$

wavelength cutoff (GeSi/Si) - adjustable to $\lambda_c \sim 25 \mu\text{m}$

temperature of operation - $\sim 80\text{K}$ for $\lambda_c \sim 5 \mu\text{m}$, $\sim 50 \text{K}$ for $\lambda_c \sim 10 \mu\text{m}$

sensitivity - wavelength dependent: moderate to low

array size - large (400×400 and above)

array uniformity - excellent

long-term stability - very good

availability - now (PtSi) and near future (GeSi/Si)

GaAs/AlGaAs Quantum Well Detectors -

These detectors are based on the ejection of electrons from quantum wells in GaAs/AlGaAs heterostructures. The wavelength sensitivity can be varied by adjusting the depth and width of the quantum well, and is peaked near the binding energy of electrons in the well. This class of detectors

has limited quantum efficiency and requires lower operating temperatures due to the short lifetime of photoexcited carriers. However, the material system is well characterized and is capable of producing custom materials using "bandgap engineering." The flexibility associated with bandgap profile design may allow one to overcome some apparent limitations.

Summary of Characteristics of GaAs/A/GaAs Quantum Well Detectors

type - quantum detector, photoconductor

wavelength response - adjustable peaked near design wavelength λ_d , from $\lambda_d \sim 5\mu\text{m}$ to $\lambda_d > 10\mu\text{m}$

wavelength cutoff - adjustable near design wavelength λ_d

temperature of operation - $\sim 50\text{K}$ for $\lambda_d \sim 10\mu\text{m}$

sensitivity - moderate

array size - moderate (128×128)

array uniformity - very good

long-term stability - very good

availability - near future

7.2 Applications Of Imaging IR Detectors For Radiation Measurements

For purposes of continuity, any new detector should probably be accompanied by an ERBE type bolometer, both to check the ERBE data and analysis, and to verify the calibration of the new sensor. It would be important to produce two measurements of radiant flux from space using different instruments, that agree closely. Even if the ERBE data and analysis are

internally consistent at the 1% level, it is not clear that they are actually accurate to 1%.

The primary disadvantages of arrays are questions concerning *uniformity* of the array, *long-term stability*, and *calibration*. For stable operation in radiometric applications, imaging bolometers are probably the best detectors, for reasons described below. Internal photoemission detectors are attractive for their excellent uniformity, but they have a soft cut-off at long wavelengths. It is questionable whether HgCdTe detectors have sufficient uniformity or stability for these applications, and quantum well detectors appear to be unsuitable due to their peaked wavelength response. Therefore, we will concentrate the following discussion on bolometer arrays. As described above, these are of two types at present: resistive bolometers and pyroelectric detectors.

Uniformity - The pixel-to-pixel uniformity of the array is determined by the uniformity of the absorptive coating and the resistive or ferroelectric film, by the processing techniques used to divide the film into pixels, and by the readout circuitry. Uniformity in the absorptive coating and films does not appear to be a serious problem, because these materials are typically deposited at once across the entire detector. Processing strongly influences uniformity. The sensitive area of each pixel is determined lithographically and is subject to dimensional errors. For bolometers, the response is also proportional to the thermal resistance to the substrate, which is determined by the fabrication process. The readout electronics also influences uniformity. In current designs, the pixels are read out by a small number of amplifiers whose inputs are scanned across the array using a switching matrix. Differences between the readout amplifiers can produce non-uniformity determined by the multiplex pattern.

Long-Term Stability - Because imaging bolometers are relatively new, we have little data on their long-term stability, and it is difficult to make accurate predictions. For this reason, it seems sensible to compare them with older approaches in tests conducted over a period of time. Nonetheless, there is reason to believe that the long-term stability of suitably designed bolometer arrays can be very good. Single bolometers have been used for many years for calibrated radiometric measurements (including the ERBE experiments), and we have good data on the stability of absorptive coatings. The new factors for bolometer arrays are the new techniques used to produce thermal resistance for small pixels, and (to some extent) the materials used to detect temperature rise. The thermal resistance in both approaches is determined primarily by geometry and by the thermal resistivity of the material, which could be fairly stable. However, the novel processing techniques used to fabricate bolometer arrays introduce interfaces in the thermal conduction path; the stability of these connections over time could be less certain. For applications with large signals, such as downward looking satellite measurements, sensitivity could be traded off for stability in the choice of materials and fabrication of arrays.

Calibration - To a large extent the problems of calibration are the same for single bolometers and bolometer arrays. These problems include the stability of the calibration source and the optics of the instrument. The obvious difference is that bolometer arrays contain a large number of elements, up to $\sim 10^5$. If the calibration time required were longer than for a single pixel in proportion to the number of pixels, arrays might be impractical. However, the readout electronics for bolometer arrays operate at fast rates (~ 1 MHz): current arrays are designed to readout at 30 frames per second. Calibration images can be recorded in comparable times. The actual calibration pro-

cedure will require several images in order to compensate for variations in zero level, nonlinearity, and absolute responsivity as well as appropriate on-board computation. Analogous techniques have been developed for HgCdTe detector arrays in order to remove fixed pattern noise caused by differences between pixels. The worst case for array calibration is that in which each element drifts independently, and must be separately calibrated. For the best case, all pixels drift together, and only one calibration is required. Because bolometer arrays are made from single sheets of sensor material, there is some hope that uniformity of calibration may be fairly good, as discussed above.

Two dimensional arrays could be used for a variety of purposes in satellite applications: *two-dimensional imaging*, measurements of the *angular distribution* of outgoing radiation, and *imaging spectroscopy*. Arrays also have the advantage of *redundancy*, which we discuss first.

Redundancy - Arrays naturally possess massive redundancy, which has a number of benefits, particularly when the array is calibrated. The continuity of an image or spectrum is an important internal check on the operation of the detector, which can easily identify bad pixels. If a number of elements fail, they can be removed from the array in the calibration procedure with no major impact on the performance of the array as a whole. Arrays can be operated with variable spatial or spectral resolution, by adding the outputs of nearby pixels under the control of an on-board processor. Finally, redundancy is important for the observation of unusual events, e.g., the eruption of a volcano: the availability of correspondingly unusual image or spectral data provides additional information and checks which could make the result believable, whereas the output of a single sensor would not be.

Two-Dimensional Imaging - Bolometer arrays can provide two-dimensional images of the radiant energy flux from the earth. They provide instantaneous images which do not need to be built up over a number of orbits as for a single scanned bolometer. The availability of images reduces uncertainty in the characterization of radiometric data, e.g., one should easily be able to tell whether the scene is cloudy or clear, and should speed up the analysis considerably. Instantaneous images are important for the study of time-dependent phenomena such as clouds and the diurnal cycle as well as unusual events.

Angular Distributions - One of the most important factors in the analysis of radiometric data for energy budgets is the angular distribution of outgoing radiation. These angular distributions change with the type of scene viewed, e.g., land under clear sky or clouds. Considerable uncertainty is associated with estimating the total flux from measurements made at large angles. A two dimensional array permits simultaneous imaging and measurements of the angular distribution of radiation along the path of the satellite. Array elements perpendicular to the direction of motion provide scanned images, while elements along the direction of motion provide a cut through the bi-directional angular distribution of the radiation from the same point as the satellite passes over. The other relevant angle is the direction of the sun. The angle between the sun's illumination and the satellite's path can be varied by appropriate selection of the orbit to obtain average information about both directions of the bi-directional angular distribution. For example, lateral imaging can be used to obtain the radiation from the same point on successive orbits. Multiple small satellites provide better coverage at proportionally higher cost.

Imaging Spectroscopy - Two-dimensional bolometer arrays can be used to perform imaging spectroscopy from a small satellite. The array direction

perpendicular to the satellite's path forms the image, while the elements along the path are used to record the spectrum formed by a dispersive element such as a grating or prism. This technique has been used for visible and infrared radiation; the availability of broad-band arrays make possible measurements over a wide range of wavelengths from $< 1\mu\text{m}$ to $> 25\mu\text{m}$. Infrared spectral information should prove very useful in detecting changes in radiation from the earth. If these are due to greenhouse gases, one expects the changes near certain wavelengths reducing uncertainty in the measurements. Another very important application for an imaging spectrometer of this type is as an adjunct to a broad-band bolometer to classify scene type; cloud cover, etc. We have discussed this application already in Section 4.1 (see especially Figure 4-1) in connection with RPAs, and will return to it again in connection with ERB measurements from small satellites in Sections 9.2, 10.2 and elsewhere.

8 POTENTIAL USES FOR SMALL SATELLITES IN THE STUDY OF GLOBAL CLIMATE

Small satellites have a variety of potential applications in the study of global climate change, both in the area of specific process studies and in the area of long-term monitoring. In this section we present a general survey of these applications. In Section 9 we discuss some specific candidate science missions for small satellites.

8.1 Process studies

Small satellites can be used to further our understanding of specific physical and chemical processes affecting global change. For this application, long satellite mission duration is not required. For some physical processes, a lot can be learned from as little as a few months of uninterrupted, high-quality data. In most cases a mission duration of three years would be adequate.

A. Process studies in support of DOE's ARM program.

DOE's ARM program seeks to study five specific geographical sites in considerable detail, to improve our understanding of atmospheric radiation processes and, in particular, of the role of cloud radiative forcing and feedbacks.

One can envision two generic types of satellite measurements in sup-

port of ARM. The first would involve global measurements of climate-related quantities (for example limb sounding measurements of stratospheric ozone, aerosol measurements, radiation balance measurements). Such satellite missions would in the course of their orbits measure these quantities directly over the ARM sites, but the main thrust would be to obtain a more quantitative grasp of macroscopic factors affecting climate.

The second type of ARM-related satellite measurement would be focused towards specific measurements to be made over ARM sites. Some of these measurements would be made simultaneously and in the same air column as ground-based and airborne measurements. They would then provide the capability to measure profiles of the air column piecewise (e.g. from the ground to an aircraft, from the aircraft to a satellite, and from the satellite to the ground). We have noted already in Section 4 the importance of adding extensive aircraft measurements to the ground-based ones in ARM. The addition of profiling instruments on satellites would be a significant further enhancement in the ability to characterize profiles of critical quantities such as water vapor or aerosol content. Furthermore, the instruments used in these simultaneous measurements would have to be carefully calibrated with respect to each other, and the satellite orbits would need to be chosen in the manner discussed in Section 10 with the specific goal of optimizing opportunities for overflying ARM sites.

Satellites would provide snapshot-like coverage of the extended ARM site. Aircraft can of course cover the extended ARM site too, but the elapsed time makes it necessary to include modeling of the dynamics to interpret the measurements.

In principle, a third type of ARM-related satellite measurement would

use ARM sites as the central points for studies of regional processes in the surrounding areas. This combination of space-based and ground-based instrumentation could provide an important new class of data for regional climate studies. However, this type of application needs considerable study before it should be endorsed as an explicit ARM science goal. The specific regional experiments to be done, types of data needed, required satellite orbits, and candidate data products need to be developed with an eye toward this new regional application.

Relatively inexpensive small satellite platforms, or individual ARM-oriented instruments on flights of opportunity, offer the only financially feasible way to obtain space-based measurements dedicated to the ARM program.

B. Satellites in support of other process studies and campaigns.

These could be similar in approach to the ARM-related satellites described above, but would be fielded in support of other global climate programs such as WOCE, GEWEX, TOGA-CORE, and their descendents. An early example of such an interaction is the fact that results from the TRMM satellite will be used in the design of GEWEX (Global Energy and Water Cycle Experiment) to be launched towards the end of the decade.

C. Satellites to pursue specific geophysical targets of opportunity.

If a flexible and relatively inexpensive small satellite platform were available for global change applications, a fruitful use would be to take advantage of time-urgent targets of opportunity. Examples would include flying an atmospheric aerosol measurements experiment immediately following a large volcanic explosion such as that on Mount Pinatubo last year, or flying an

ozone-mapping experiment if the Arctic ozone hole starts to evolve rapidly in future years.

8.2 Long-term Monitoring

A second general class of missions for small satellites is in the area of long-term monitoring of global change. In this case, long mission duration is critical (at least 5 years would probably be desirable for many applications). Continuity from one mission to the following one is also critical, as are well-tested calibration procedures and freedom from instrumental drift.

8.2.1 Precursors to EOS

Several long-term monitoring missions are potentially important in the years between the present and whenever EOS-A is launched, to avoid gaps in the quantitative climate record. These include the following:

- Missions to monitor "telltale signs" of climate change, so as to give "early warning" to policy makers. Specific missions will be discussed in Section 9.
- ERBE or CERES-type radiation budget experiments, to fill in gaps in the monitoring of radiation balance. There is currently no such satellite flying.
- Missions to develop new generations of detectors, long-term monitoring methods, and calibration techniques.
- Satellite measurements of upper tropospheric ozone, stratospheric water vapor, or aerosol profiles in a monitoring mode.

- Solar monitors (if NASA's plan to field them on satellites of opportunity is insufficient to guarantee that 2 solar monitors are always flying).

8.2.2 Adjuncts to EOS (satellites which could fly simultaneously with EOS)

After the first components of the Earth Observing System are launched, there are several other missions in which small satellites could make important contributions. These include:

- Constellations to give additional diurnal coverage for earth radiation budget experiments (flying simultaneously with EOS platforms). This issue will be discussed more fully in Section 10.
- Constellations or single satellites to measure supplementary quantities to those measured on EOS:
 1. Water vapor profiles; tropospheric water vapor.
 2. Rainfall measurements. Rainfall has even greater diurnal variation than radiation budget quantities, and it is therefore especially important to obtain global diurnal coverage. Instrumentation (such as satellite rain radars) for this mission would be developed based on knowledge gained from TRMM.
 3. Measurements of cloud heights via stereo imagery or cloud-height LIDAR (perhaps in formation with EOS).
 4. New diagnostics of thin cirrus (in formation with EOS).
 5. Ocean altimetry to provide monitoring continuity and fill in data gaps.

An important issue concerning the role of small satellites is the certification of a new generation of climate measuring instruments. The EOS platforms, together with their European and Japanese brethren, will provide a long time period in which well-calibrated and well-tested instruments are flying. However, the concepts for these EOS instruments will be more than twenty years old by the time the EOS mission comes to an end. If we are ever going to develop a new generation of instrumentation with greater capability than those on EOS, the time to establish the heritage of this new generation would be during the period when EOS is operational, so that the new instruments can be cross-calibrated against the better-proven experiments on EOS. Small satellites flying concurrently with the EOS platforms would provide an ideal vehicle for accomplishing this goal.

9 CANDIDATE SCIENCE MISSIONS FOR SMALL SATELLITES

9.1 Introduction

Among the suggestions for small satellite missions in support of the Global Change Research Program is a set of very small, very light satellites and instruments, suggested by members of the Brilliant Pebbles program. Such satellites have been dubbed "microsats" and "lightsats"; their instruments are proposed to have weights ranging from one-twentieth to one-hundredth of the weights of EOS instruments which perform roughly analogous functions. In principle the extremely small size of these instruments could permit deployment of quite a large constellation of "microsats", if the small weights are reflected in similarly small costs for the systems.

In a less extreme version, participants from DARPA and from the DOE laboratories have put forward proposals for satellite instruments that are somewhat larger and heavier, but still well below the weights of instruments contemplated for the EOS platforms.

We suggest that a useful procedure to follow in proposals for small satellites and microsats is the following one:

Decide on several specific candidate missions for small satellites, including possible microsats. Then ask, what size satellite and

how large a constellation are needed to do the job of each of these missions.

To us, a focus on candidate science missions makes much more sense than an approach which looks one by one at EOS instruments, and then tries to duplicate their individual functions with "microsat" or "lightsat" technology. An integral approach based on the geophysical knowledge needed to understand a specific global change issue seems to us to be more fruitful. Below we will suggest several such "issue specific" science missions which seem to us to be useful candidates for further development.

In addition, it is important to note that there are a few specific EOS instruments which are in some sense in difficulty, either because the desired technology is not yet mature, or because of technical problems, or because they have been dropped from the newly reconfigured EOS program. Small satellites could very well play a useful role in fielding scaled-down, simpler versions of some of these instruments. This latter possibility we discuss in Section 11.

9.2 Specific Proposed Missions

One class of science mission that is well suited to small satellites is measurements for which several satellite platforms are needed, in order to accumulate acceptable statistics on quantities subject to large temporal variations. Missions to monitor the earth's radiation budget and missions to measure global rainfall are in this category, and are included here.

1. Earth Radiation Budget Mission.

Global radiation budget measurements require at least three satellites, if adequate statistics on monthly regional means are to be obtained. The instrument package can be designed to weigh one to two hundred kilograms or less, thus qualifying for the "small satellite" designation. Because one needs to measure monthly averages to 1% accuracy in order to detect the expected signal from increased atmospheric CO₂ concentrations, radiation budget satellites require great attention to calibration and stability issues. For this reason, we recommend for the near term that ERBE or CERES type instruments be considered for the broadband radiometry, due to their well-established heritage and well-understood calibration.

These radiation measuring instruments must be accompanied by an instrument to classify scene types using some sort of cloud measurements. There seems to us to be room for considerable innovation in the design of this second instrument. The MODIS experiment on EOS is designed to perform many more functions than the simpler imaging spectrometer needed for only the radiation budget function, and MODIS is consequently much heavier than such an instrument needs to be. The MPIR instrument proposed by Vitko et al. (1991) is much closer to the weight and performance that would be appropriate for this job. The similarity in requirements with RPA instruments has already been stressed in Section 4. Along with the radiation measurements and the cloud imager, there is the possibility of including other functions on the radiation budget satellites, although at the cost of increased weight and power requirements. Hansen has proposed (Hansen et al. 1991) a limb-scanning spectrometer (SAGE III), a solar photopolarimeter (EOSP) for aerosol and cloud characteristics, and a thermal Michaelson interferome-

ter for cloud properties. (In Hansen's case this last instrument plays the role of the cloud imager mentioned above.)

Our own preference would be to put the limb measurements on a separate small satellite mission (described below), since they do not have the same simultaneity and congruence requirements that the nadir-looking instruments have. Attractive options for instruments to accompany the radiation budget experiment include a capability for determining cloud-top height (for example via stereo images or a small cloud-top LIDAR).

The decision concerning which accompanying instruments make sense should be made based on flying the minimum number (and weight) of instruments that can do a good job on the specific science mission. This decision is closely coupled (via the total mission cost) with the decision on how many satellites must fly simultaneously in order to obtain the desirable level of statistical accuracy. Sampling analyses are absolutely critical to the issue of determining how much orbital coverage is needed. The sampling analyses are not merely straightforward applications of conventional statistical methods; they must include an analysis of the actual algorithms used to unfold the net radiation budget from the raw data, using statistical models of the bi-directional radiance function and taking into account the determination of the scene type. We recommend that members of the ERBE science team be asked to help develop and critique sampling analyses for any radiation-monitoring small-satellite mission.

2) Limb-Scanning Mission: Stratosphere, Mesosphere, and Upper Troposphere.

This mission would include several instruments that make limb-scanning

measurements of the stratosphere, mesosphere, and upper troposphere. Candidates are SAGE type grating spectrometers for temperature profiles, aerosols, and measurements of molecules such as O₃, H₂O, NO₂, and NO₃ down to the cloud tops, a lighter equivalent of the HIRDLS scanning radiometer, a lighter equivalent of the SWIRLS stratospheric wind sounder, or (if technically possible) a lightweight microwave limb sounder.

3) Global Precipitation Mission.

Knowledge of global precipitation trends is critical to assessing changes in the hydrological cycle. Yet global rainfall is not known at present to within a factor of two. Satellite-based rain radars and passive microwave sounders will be tested on an aircraft platform (ARMAR) beginning in 1992, on the TRMM satellite mission to be launched in 1997, and later on the two JEOS platforms. These new instruments are designed to reduce the variances of the rain-rate measurements from the present 30%-50% to perhaps the 10% level. Together with the increased geographical coverage possible from a modest constellation of satellites, these new instruments offer the possibility for the first time of doing meaningful global monitoring of rainfall and precipitation patterns. Careful ground-truth experiments will be crucial to the success of TRMM.

Rainfall is known to be very variable both spatially and temporally. In the spatial dimension, even ground-based rain-gauge measurements do not converge particularly well, and there have been suggestions that spatial rainfall patterns are fractal. In the temporal dimension, tropical rainfall statistics have variances that are just as large as the mean. As a result, it will be difficult for one satellite to accumulate enough independent data points to lower the uncertainty of even monthly averaged regional rainfall

rates. Sampling analyses based on the TRMM data will be needed in order to decide on how large a constellation is required to do a meaningful job of monitoring changes in the global rainfall and precipitation rates.

REFERENCES FOR SECTION 9

1. Hansen, J., W. Rossow, and I. Fung (1990), "The Missing Data on Global Climate Change", *Issues in Science and Technology* **VII**, pages 62-69.
2. Vitko, J., R. Abbink, T. Axelrod, C.A. Boye, I. Lewis, and P. Weber (1991), Presentation to JASON summer study, June 1991, La Jolla, CA.

1 ISSUES IN THE CHOICE OF ORBITAL COVERAGE FOR SMALL SATELLITES

1.1 Flexible Space-Time Coverage

A number of remote sensing satellites are in sun-synchronous orbits. Such orbits have significant advantages in that a given location on Earth can always be observed at the same local time of day, i.e., during daylight hours for visible and reflective IR sensors. Landsats have used such orbits and plans are for EOS-A platforms do the same. While there are significant advantages to sun-synchronous orbits, they can provide only one type of observation in terms of space-time coverage. *Frequent coverage of a set of small regional sites at varying times of day is not possible with a sun-synchronous orbit.* Satellites in other orbits can provide a wide variety of coverage. Because of their low cost it may be efficient to use small satellites in a variety of orbits to provide "tailor-made" space-time coverage for a specific application. Below we discuss some characteristics of sun-synchronous orbits and the flexibility available from other orbits, in particular low-inclination, low-altitude, near-circular orbits.

Sun-Synchronous Orbits: A number of earth sensing satellites, such as Nimbus, Landsat & some meteorological satellites (ITOS, NOAA, TIROS, etc.), are deployed in sun-synchronous orbits. That is, the satellite orbital plane remains nearly fixed with respect to the sun. These orbits are usually near-circular at altitudes of 500-1500 km and have retrograde inclinations

near 90°. For example, Landsats 1 and 2 had perigees of 900 km, apogees of 907 km and inclinations of 99 degrees. This orbit allows global coverage between 81° N and 81° S latitude once every 18 days. Further, a sun-synchronous orbit is designed such that the satellite observes a given location at the same local times (one day and one night). The advantages of such orbits are well known:

1. Near global coverage
2. Observation of a given location at constant local time
3. Nearly constant solar cell illumination, i.e., no extended periods of reduced solar cell power (eclipse periods).

However, sun-synchronous orbits place significant constraints on space-time coverage of a given site. For example, coverage at a given site is infrequent and diurnal variations can not be studied. Further, high inclination orbits, such as for Landsat, are usually at relatively high altitudes, i.e., ~ 900 km. There can be substantial advantages in terms of sensor cost and capability by operating at lower altitude (~ 500 km).

More specifically, a sun-synchronous orbit is constrained by the need to have the orbit's nodal precession rate match the Earth's average rotation rate around the sun of 0.9856 degrees per day. Setting rotation rate equal to the nodal precession rate $\dot{\Omega}_{J_2}$ we have an approximate equation showing the constraints placed on the semi-major axis of the orbit (a), the eccentricity of the orbit (e) and the inclination of the orbit (i), namely

$$0.9856 \approx \dot{\Omega}_{J_2} \approx -2.06474 \times 10^{14} \times a^{-7/2} \times \cos(i) \times (1 - e^2)^{-2}.$$

(see Wertz and Larson (1991), Chapters 6 and 7), where a is in km, i is in deg and $\dot{\Omega}$ is in deg/day. Thus for a sun synchronous orbit with $e = 0.0$ the ratio $[\cos (i)/a^{7/2}]$ must remain constant. The point here is that requiring sun synchronism places a very strong constraint on possible orbits and hence the space-time coverage that can be accomplished.

Flexibility of Non-Sun-Synchronous Orbits: Satellite applications that do not require global coverage, but rather need frequent observation of a small number of sites are generally not well served by sun synchronous orbits. For example, sites such as those proposed for the Atmospheric Radiation Measurement (ARM) program would be best served by frequent observations at varying local times of day. An example of such an orbit, covering tropical sites, is shown in Figure 10-1. This orbit can cover all the sites along the subsatellite track once per day and, where ascending and descending passes cross, twice each day. Further, this coverage varies through local time with coverage about 1/2 hour earlier each day. The result over two months of observation would be satellite data over a given site or group of sites once or twice a day with observations at every 1/2 hour through the local day and night. Since the ascending and descending passes could be spaced by many hours, there would usually be one daylight and one night pass per day. For example, the orbit of Figure 10-1 provides twice daily coverage of Chiapas state in Mexico (with side looking sensors). The descending pass follows the ascending pass by 6 hours and 40 minutes with both passes occurring about 28 minutes earlier from one day to the next (Medsat, 1991).

Conclusions: Major earth remote sensing satellites, such as Landsat and SPOT, as well as the proposed EOS platforms use sun synchronous orbits to obtain near global coverage with observations at the same local time for a given location. Small satellites in other orbits, such as shown in Figure 10-1,

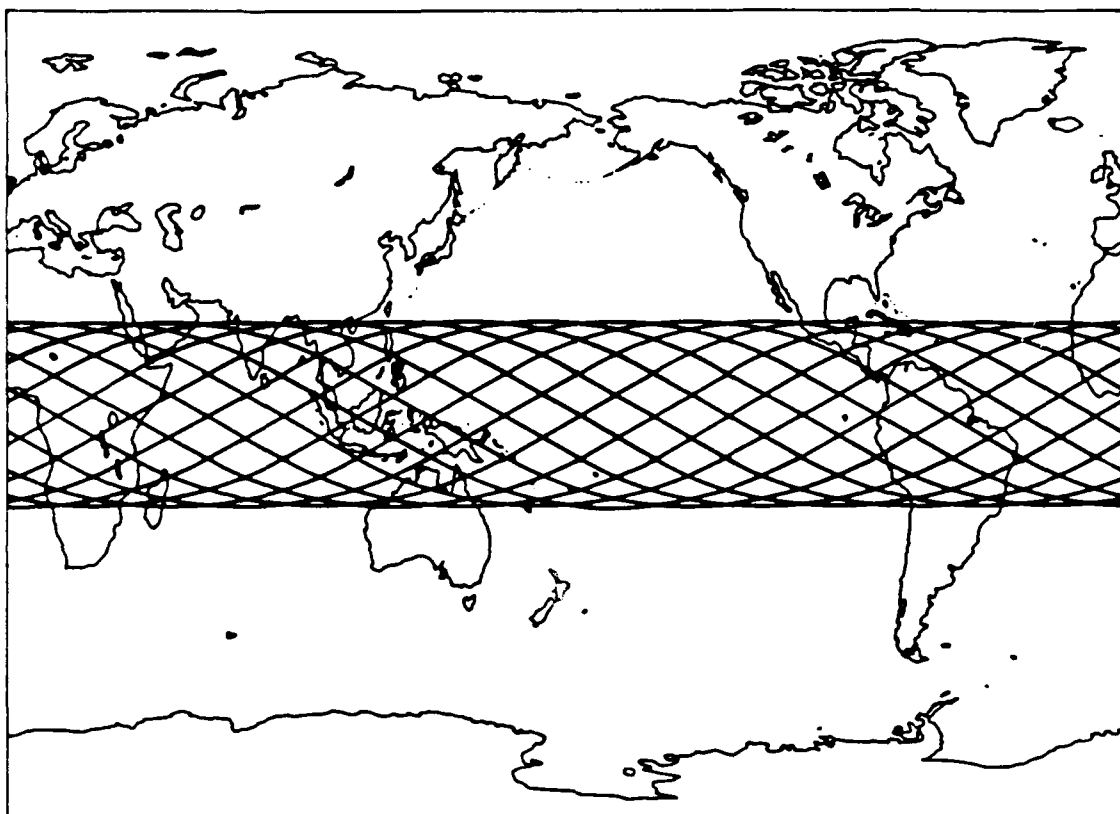


Figure 10-1. Subsatellite ground track for a low altitude, small satellite orbit covering the tropics. At each orbit crossing point twice-daily coverage is provided with observation times occurring about 1/2 hour earlier each day. Orbit altitude = 477km, with circular geometry, inclination = 21° . After Medsat (1991).

offer space-time coverage which is complementary to sun-synchronous orbits in the following ways:

1. Satellites in orbits such as Figure 10-1 would give frequent coverage (once or twice a day) of a set of small regional sites. This is in contrast to the once every 18 day frequency of a Landsat orbit with nearly global coverage.
2. Satellites in orbits such as Figure 10-1 would allow coverage over a range of local times of day, e.g., to study diurnal variations. sun-synchronous orbits yield observations at fixed local times of day.
3. Satellites in orbits such as Figure 10-1 can allow observations from lower altitudes (~ 500 km) with advantages in sensor resolution, power and cost. sun-synchronous orbits are usually higher (~ 900 km) and thus require larger optics and antennas for the same surface resolution.
4. Small satellites in orbits such as Figure 10-1 can provide cost-effective coverage of a number of small regional sites (such as ARM sites) in a manner complementary to sun-synchronous satellites such as Landsat, SPOT and the planned EOS platforms.

10.2 Implications of Diurnal Variability

10.2.1 The Context of Diurnal Variability

Several of the important processes affecting measurements of global climate change are subject to significant diurnal variations. Phenomena such as earth radiation, cloud cover, precipitation, and winds are known to vary over periods of minutes or tens of minutes. In addition, these processes are highly localized geographically, and the pattern of diurnal variability that is "typical" of one geographical location will not in general be the same as at a different location.

Any single climate satellite is not able to sample the full diurnal cycle over a significant fraction of the earth's surface. The choice of sun-synchronous orbits for the EOS platforms makes the diurnal sampling of these satellites less comprehensive than for an inclined orbit, since each sun-synchronous satellite passes over a specific place on earth at the same local time each day. Thus while an inclined-orbit satellite can build up diurnal information on a particular geographical area using data from many satellite passes, a sun-synchronous satellite must rely either on interpolation or on other satellites to develop an adequate model of diurnal statistics.

The quantitative effect of this diurnal and geographical variability on the assessment of global climate depends on its statistical properties. If the variations with time of day can be averaged out by taking many observations and focusing only on the monthly or seasonal means of climatic quantities,

then the existence of diurnal variation leads to an rms error that will decrease as the number of observations increases.

In the case of radiative energy balance it appears that diurnal variations also lead to a bias in the monthly and seasonally averaged climate quantities. Less is known about the statistics of precipitation or winds, since these have not been monitored from satellites in the past. But it is known that precipitation is even more variable than the radiation budget. In the tropics, where two-thirds of all global precipitation is concentrated, the standard deviation of the monthly rainfall is comparable to its mean value (Simpson et al, 1988). It is likely that biases will appear in precipitation data as well as in radiation budget data, due to the correlation of the diurnal variation pattern with geographical location.

If satellite orbits are such that there is not full diurnal coverage, the accuracy of the measurements of climatic quantities will be limited by the rms sampling error due to diurnal variability. This additional rms error will place a limit on the accuracy attainable with a given set of satellite orbits, regardless of the inherent accuracy of the individual measurement instruments.

In the case of global energy budget measurements, one of the objectives of the global climate change program is to detect a change in the regional monthly mean radiative energy balance of about 1% of the incident flux. It is therefore crucial to design a set of satellite orbits with enough diurnal sampling that the rms sampling errors due to diurnal effects will be well less than 1%, or at least will not be the dominant source of error in the

determination of regional monthly mean quantities. It is not clear to us that certain alternative satellite concepts, such as Hansen's 2-satellite CLIMSAT, actually meet this test.

In the case of global rainfall measurements, the natural statistical variations in the data are much larger, and the precision of satellite rain radar measurement techniques is poorly known. Furthermore, comparison of satellite measurements to "ground truth" is difficult, since ground-based techniques such as rain gauges also show significant inherent variability. In the past, rain rate measurements have been stated to be accurate to 30% - 50%. The TRMM mission, currently scheduled for launch in 1997, will help to improve this accuracy to the 10% level, and will couple analysis of rain radar data with data from a co-located passive microwave radiometer and a visible/infra-red radiometer. After TRMM, the two JEOS platforms (scheduled for launch in 1998 and 2000) are scheduled to carry dual precipitation radars.

10.2.2 An Important Role For Small Satellites

In this context, an important role emerges for small inexpensive satellites, if the latter can be proliferated in orbits giving more complete diurnal sampling. The specific costs and benefits of developing small special-purpose satellites to obtain better diurnal data will depend on the physical process being measured, and on the precision and number of satellites needed. For processes where diurnal sampling is not the largest contributor to the error budget, the added costs of obtaining diurnally complete data may outweigh the benefits. However, in the cases of earth radiation budget and of precipitation, available data suggest that the opposite is true.

A. Earth Radiation Budget Measurements

The radiation budget is determined from combined observations of the outgoing longwave radiation, and the absorbed solar shortwave radiation. Both show significant geography-dependent diurnal variability.

1. Diurnal variability of longwave radiation

Outgoing longwave radiation was measured by the ERBE satellite experiments over broadband channels, and can also be estimated from narrow-band channels on several meteorological satellites (see e.g., Barkstrom 1990, Session 5). Some geographical areas such as cloud-free deserts show regular patterns of diurnal variation, as shown in Figure 10-2. For these locations, the diurnal variations observed on a given day will come quite close to the monthly mean diurnal variation. However, regions where clouds play a larger role show much larger variances in their diurnal variation patterns, as illustrated in Figure 10-2. For such regions, use of the monthly mean diurnal variation to interpolate between observations from a sun-synchronous satellite would lead to significant sampling errors in the overall radiation budget statistics.

2. Diurnal variability of shortwave radiation

A similar picture prevails for shortwave radiation, whose diurnal variability is dominated by the varying cloud albedos under different local weather conditions. Sampling errors due to diurnal variation of shortwave radiation tend to be somewhat larger than those for longwave radiation.

Harrison et al. (1983) used data from the GOES satellites to perform sampling analyses of regional monthly mean reflected radiation measure-

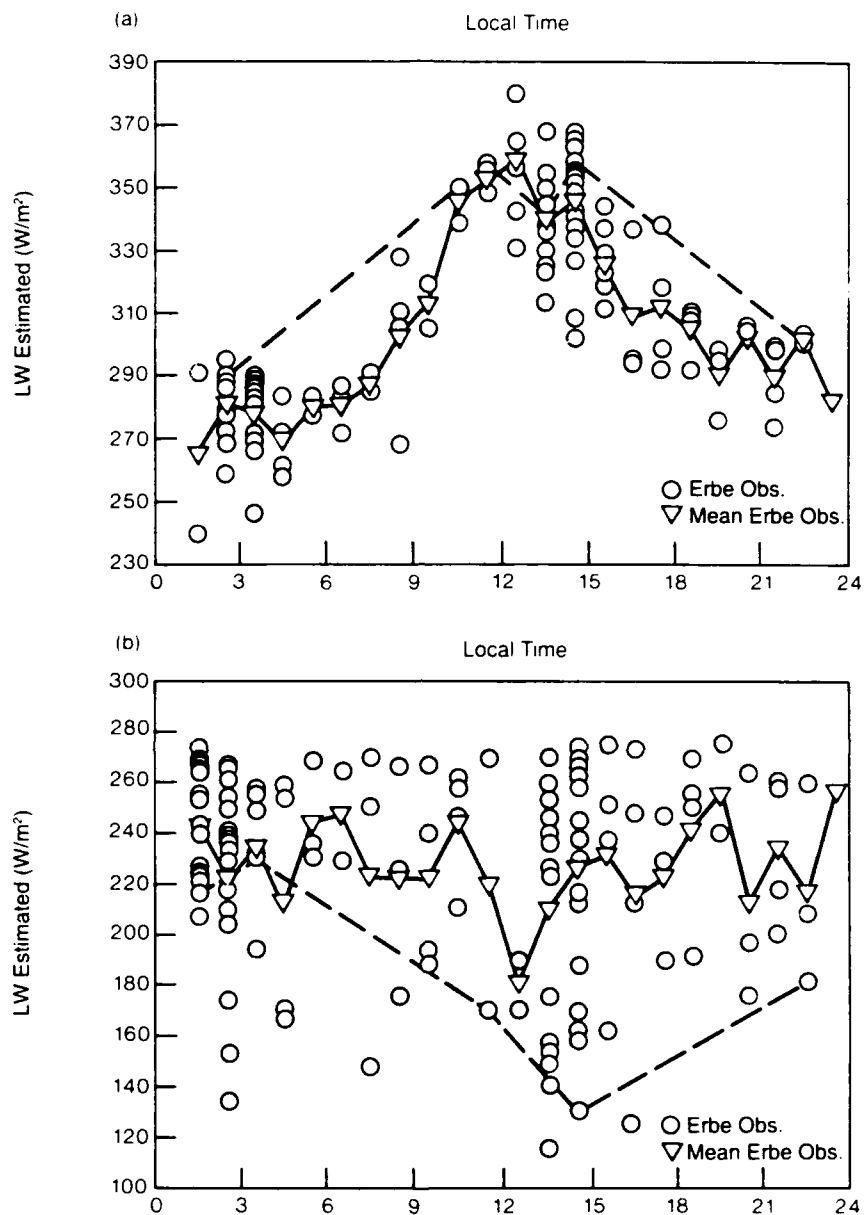


Figure 10-2. ERBE observations (open circles) of outgoing longwave radiation for the month of July 1985. Filled triangles show the mean for each hour. Dashed line shows evolution during one specific day of the month. a) Observations of the desert region at $20^{\circ}N$, $40^{\circ}E$, which was mostly cloud-free. For this case of cloud-free desert, the variation during one day followed the mean variation quite closely. b) Observations of the tropical Atlantic region at $(10^{\circ}N, 25^{\circ}W)$. Dashed line shows one specific day of the month which had deep convection in the afternoon. In this example the variance is very large, and a typical day's variation does not in general have the same shape as the mean. Source: Kandel et al. (1990).

ments. They considered the rms sampling errors from constellations of one, two, or three satellites. Some typical results are shown in Figure 10-3. Only with three satellites, at least one of which is in an inclined orbit, do the sampling errors for monthly mean data fall significantly below 4 watts per square meter for the Southern Hemisphere.

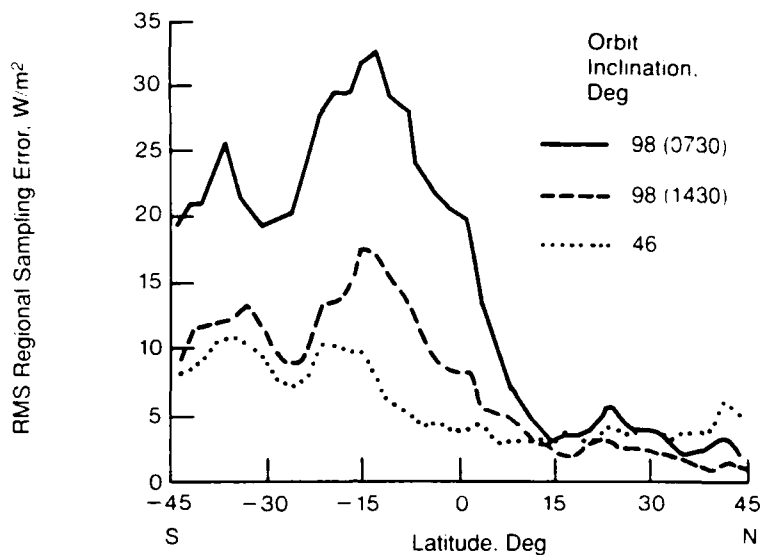
3. Sampling error budget for net radiation

Similar analyses are in progress using more recent ERBE data, to project the rms sampling errors associated with the CERES instrument. The trends projected for the net radiation fluxes are similar to those shown in Figure 10-3. In general one needs at least three satellites to get the sampling error of net regional monthly mean fluxes close to 1 watt per square meter, as would be needed to detect the net flux change projected from expected CO₂ increases.

These analyses indicate that CERES should fly on at least three satellites at the same time, in order to obtain good sampling statistics. Assuming three CERES satellites (for example EOS-A and EPOP in sun-synchronous polar orbits, and either TRMM or JEOS 55° in an inclined orbit), sampling errors in the monthly regional average are projected to be considerably smaller for CERES than they were for the ERBE experiment. This is due to the fact that CERES has two scanners (ERBE had only one), and to CERES' improved resolution in latitude and longitude (1° instead of 2.5°).

Table 10-1 shows an illustrative example of this type of sampling analysis, courtesy of Bruce Wielicki (Wielicki 1991). While we caution that the details of Table 10-1 are still in preliminary form and may be subject to some changes, the overall trends of the sampling analysis are clear. Instantaneous

(a) One Satellite



(b) Two and Three Satellites

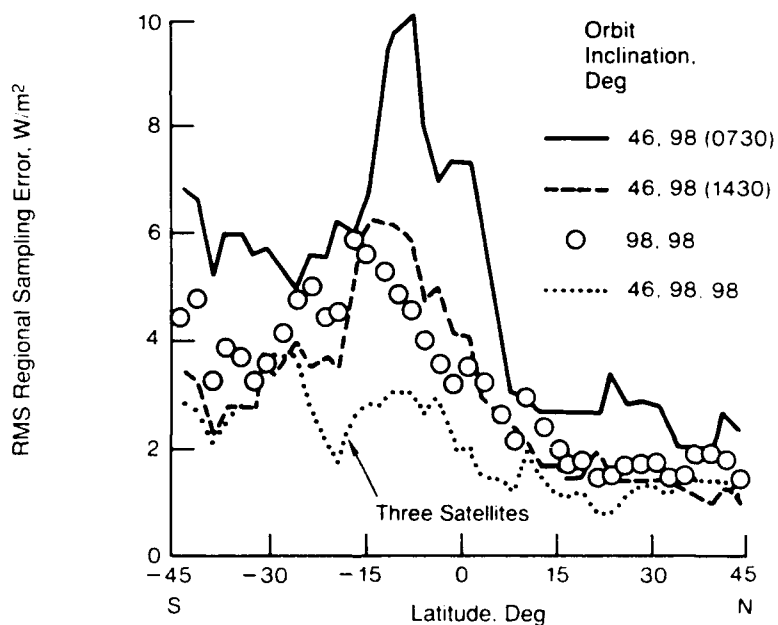


Figure 10-3. Zonal regional reflected radiation errors based on sampling analyses of GOES cloud data for November 1978. a) Errors expected for one satellite, at three possible inclinations (given in the legend). RMS regional sampling errors for one satellite are in the range of 10 to 30 watts per square meter for the Southern Hemisphere. b) Errors expected for two or three satellite constellations, at inclinations shown in the legend. For three satellites, the rms regional sampling errors are in the range 2 to 4 watts per square meter for the Southern Hemisphere. Source: Harrison et al. (1983).

Table 10-1. Shortwave and longwave top-of-the-atmosphere error budgets projected for ERBE and CERES, assuming that CERES is flown on three satellites as described in the text. While detailed numbers represent preliminary calculations and are subject to revision, the overall trends are expected to be robust.
Source: Wielicki (1991).

Errors given in units of Wm^{-2}

	Monthly Average Regional 5yr trend $S_o = 348 \text{ Wm}^{-2}$		Monthly Average Regional 1 std dev $S_o = 348 \text{ Wm}^{-2}$		Instantaneous pixel 1 std dev $S_o = 1000 \text{ Wm}^{-2}$	
	ERBE	CERES	ERBE	CERES	ERBE	CERES
SW Radiation						
Calibration	2.0	1.0	2.1	1.0	6.0	3.0
Angle Sampling	0.0	0.0	3.3	1.1	37.5	12.5
Time Sampling	0.0	0.0	2.6	1.0	0.0	0.0
Space Sampling	0.3	0.3	0.3	0.3	0.0	0.0
Total SW Error	2.0	1.1	4.7	1.8	38.0	12.9
LW Radiation						
Calibration	2.4	1.2	2.4	1.2	2.4	1.2
Angle Sampling	0.0	0.0	1.6	0.5	12.5	4.2
Time Sampling	0.0	0.0	0.9	0.7	0.0	0.0
Space Sampling	0.2	0.2	0.2	0.2	0.0	0.0
Total LW Error	2.4	1.2	3.0	1.5	12.7	4.3
Net Radiation						
Calibration	3.1	1.6	3.2	1.6	6.5	3.2
Angle Sampling	0.0	0.0	3.7	1.2	39.5	13.2
Time Sampling	0.0	0.0	2.8	1.2	0.0	0.0
Space Sampling	0.4	0.4	0.4	0.4	0.0	0.0
Total Net	3.1	1.6	5.6	2.4	40.1	13.6
Science Requirement	2 to 5	< 1	10	2 to 5	None	10

pixel results have about a three times smaller standard deviation for the CERES constellation than for ERBE. Likewise, monthly averages have a two to three times smaller variance for CERES than for ERBE.

4. Potential implications for Hansen's proposed CLIMSAT

These sampling studies have interesting implications for Hansen's proposal to fly a two-satellite "CLIMSAT" constellation for the mission of global climate monitoring (Hansen et al., 1990). To our knowledge, Hansen has not yet completed the type of sampling analysis shown in Figure 10-3 and Table 10-1, for the instruments proposed in his system. But because Hansen's satellite can sample clouds at night only in a narrow swath (via a Michelson interferometer), because his CERES has only one scanner, and because his constellation is proposed to have two rather than three satellites, we estimate that his radiation-budget sampling errors will be significantly worse than those shown in Table 10-1 for CERES.

This raises the question of how meaningful Hansen's radiation-budget "monitoring" will be. It seems possible that Hansen's satellites will be able to obtain zonal averages over 4 or 5 years that will have error budgets in the desired range of less than one watt per square meter. However, for the equally urgent questions of unravelling cloud-radiation feedbacks and obtaining meaningful regional averages, it seems unlikely that Hansen's proposed constellation will be adequate.

These issues underline the urgency of performing a full sampling analysis of Hansen's proposed satellite constellation. It would be a shame to field a "climate monitoring" satellite if it turns out to have such large sampling errors that its capabilities to quantitatively monitor climate change are

limited.

5. A role for small satellites

The sampling analysis for CERES shown in Table 10-1 is based on the assumption that there are three CERES instruments flying at the same time. The proposed configuration is EOS and EPOP in polar, sun-synchronous orbits, and either TRMM in a 35° inclined orbit or JEOS in a 55° inclined orbit.

EOS A and EPOP are currently scheduled for launch in 1997-1998, TRMM in 1997, and JEOS 55° in 2000. However, there is at present real uncertainty in the actual scheduling of these platforms, and the probability of three of these required CERES platforms flying at the same time is not nearly as high as we would like. In particular, it seems reasonably likely that the three-year TRMM mission may be over well before EOS A is actually launched, thus leaving the inclined-orbit satellite missing. While other platforms such as Space Station Freedom are sometimes mentioned as backups, this option seems to us to be even more uncertain than EOS A.

In addition, there is at present no earth radiation budget experiment flying, and none is scheduled except for two French SCARABE instruments in polar orbit in 1992. Because of the lack of a SCARABE in an inclined orbit, it seems likely that this experiment too will lack adequate diurnal coverage to achieve small sampling errors.

Given the fundamental importance of earth radiation budget measurements to global change, we recommend that a constellation of at least three small satellites be dedicated to the earth radiation budget mission. At present

our view is that the best instrumentation for these satellites would be at least CERES (with two scanners), and a cloud imaging spectrometer (to be determined). The cloud imager is an area where advanced instrumentation designs could fruitfully be used.

B. Precipitation Measurements

In spite of the central importance of precipitation to the world economy and global climate change, less is known about global rainfall sampling statistics than about earth radiation budget statistics. Satellite measurements of rainfall appear to be the only way to achieve true global coverage. Yet the first rain radar will not fly until the Tropical Rainfall Measurement Mission (TRMM) in 1997. The motivation for studying the tropical region first is that two thirds of all precipitation falls in the tropics. The goal of the TRMM mission will be to reduce the uncertainties in rain rate measurements from the present values of 30% - 50%, down to the 10% level.

Simpson (1988) states that "the quantitative distribution [of precipitation] over the tropical oceans is uncertain to a multiplicative factor of two or three." Adequate spatial and temporal coverage is critical for the understanding of changes in global rainfall patterns, since even in "normal" years rainfall has high inherent variability. For example, monthly tropical rainfall data typically have a variance roughly equal to the mean. In other words, in a "typical" month the rainfall in a particular tropical location is likely to be either twice the mean (floods) or near zero (drought). The average annual rainfall rarely occurs (Simpson et al., 1988).

Under these conditions, it is likely that effective monitoring of changes in global rainfall patterns will require even more than the three satellites needed

to monitor the earth radiation budget. While reliable sampling analyses must await the arrival of data from TRMM, we anticipate that an eventual rainfall monitoring mission will be ideal for a constellation of modest-size satellites. Current estimates for the TRMM rain radar are that it will weigh around 300 kg, with an average power consumption of about 200 watts. While this is not a "microsat" or perhaps even a "lightsat", it is not a very large satellite either. With further development work it is likely that the weight of the rain radar can be decreased for future follow-on missions. The TRMM mission will help to clarify whether the rain radar will have to be accompanied by passive microwave and visible/ir instruments, thus increasing the mission weight further, or whether the radar itself will suffice for global rainfall monitoring. In either case, the importance of water as an economic resource will make it crucial to develop over the next decade the capability to effectively monitor precipitation and rainfall on a global basis.

At present the evidence suggests that rainfall measurements based on infrared data alone will be considerably less accurate than the desired 10% level which is the goal for TRMM. However, the infrared and visible instruments on TRMM will allow the accuracy of various infrared techniques to be compared directly with rain-radar results, and a more quantitative assessment of the potential for infrared-based global rainfall measurements (as suggested by Ledebuhr 1991) will then be possible.

Given the high importance of precipitation for the global economy, it is important to examine technologies for an advanced, lightweight rain radar suitable for deployment on an eventual constellation of satellites to monitor global precipitation. The number of required satellites, and the exact nature of the accompanying instruments, would be determined later in the decade using results from the TRMM mission.

REFERENCES FOR SECTION 10

1. Barkstrom, B. (1990) editor, "Long-Term Monitoring of the Earth's Radiation Budget", Proc. S.P.I.E. volume 1299.
2. Hansen, J., W. Rossow, and I. Fung (1990), "The Missing Data on Global Climate Change", Issues in Science and Technology VII, 62.
3. Harrison, E.F., P. Minnis, and G.G. Gibson (1983), "Orbital and cloud cover sampling analyses for multisatellite Earth radiation budget experiments", J. Spacecraft and Rockets 20, 491.
4. Kandel, R.S., F. Cheruy, and J.Ph. Duvel (1990), "Determination of outgoing longwave radiation and its diurnal variation using ERBE and Meteosat observations", in Barkstrom (1990), page 243.
5. Ledebuhr, A. (1991), presentation to JASON summer study, La Jolla, CA.
6. Medsat, "Project Medsat: The Design of a Remote Sensing Platform for Malaria Research and Control," Aerospace Engineering and Atmospheric, Oceanic and Space Science Departments, College of Engineering, University of Michigan, Ann Arbor MI 48109-2143 (1991).
7. Simpson, J., R.F. Adler, and G.R. North (1988), Bull. Amer. Met. Soc. 69, 278.
8. Wertz, J. R. and W. J. Larson (eds.), Space Mission Analysis and Design, Space Tech. Lib., Kluwer, Dordrecht (1991).
9. Wielicki, B. (1991), viewgraph from presentation to EOS-A Engineering Review Committee, La Jolla, CA, July 1991.

11 SMALL SATELLITE INSTRUMENTS TO ADDRESS PROBLEMS FACING PRESENT EOS-CLASS EXPERIMENTS

Some of the instruments proposed for EOS are currently facing technical or funding difficulties. In the process of addressing these problems, it seems to us to be fruitful to ask whether there are advantages to be gained from splitting up the scientific functions of these large instruments into smaller experiments that would have the possibility of being flown sooner.

We discuss below some of the EOS instruments which have been mentioned to us as having various implementation problems. We present these options as examples of a class of experiment where innovative technology from the defense community may be of help in the future in broadening the design options for global change missions.

11.1 Solid-state Lasers for LIDARS and Laser Rangers

The Geosciences Laser Ranging System (GLRS) originally proposed for EOS B consists of a solid-state Nd:YAG laser running at 40 pulses per second, which is doubled and tripled in frequency. As designed, the laser's average output power is between 10 and 15 watts. The GLRS has several distinct applications: laser ranging for geodynamical measurements of crustal motions, ice-sheet altimetry and motion, along-track cloud and aerosol distributions and vertical profiles, and cloud and aerosol backscatter cross sections. The current design calls for one laser to accomplish all of these applications.

As specified, the laser hardware requirements for GLRS are quite challenging. However, laser requirements for individual LIDARs to accomplish the mission goals one by one are in many instances less stressing. For example, a cloud-height LIDAR can be much less powerful than a laser-ranging laser. Similarly, the ice-sheet altimetry mission requirements are less stressing than for the laser ranging mission.

The technology of diode-pumped solid-state lasers is one in which DARPA, DOE, and the Brilliant Pebbles program have made substantial progress in recent years (Dube, 1991). For example, diode-pumped infrared and blue-green lasers with tens of watts of average power are now realistic hardware options. It seems to us that these developments could be of considerable assistance to accomplishing the missions for which GLRS was proposed. In our opinion, it would be timely to convene a study to assess which GLRS mission requirements could be met by a smaller laser system, and which (if any) of the developments from the DOD and DOE community would be most useful in fielding such a system on a satellite. The field of compact solid-state lasers is one in which there is good potential for technology transfer from the DOD and DOE community.

The possibility of a DOD lidar mission is discussed further in Section 12.

11.2 Synthetic Aperture Radars (SARs)

The international community is planning to launch four synthetic aperture radars between 1991 and 1998. These will fly on ERS-1 and 2, JERS-1, and Radarsat. Although these SARs have a variety of operating param-

eters to address different geophysical and biological process, all are single frequency, single polarization instruments.

By contrast, the proposed EOS SAR was planned to operate at three frequencies and four polarizations. It therefore has the potential to have much better discrimination, for example for forests and other vegetation types. Since a SAR with these new capabilities has not yet been flown in a satellite, the quantitative benefits of multi-polarization and multi-frequency operation are not yet explored. Small satellite missions can be designed to begin such an exploration in a timely fashion. For example, tropical forest cutting will greatly impact the environment in the next decade and we currently have no comprehensive way of monitoring this process from space. (Optical observations are hindered by clouds, and radar observations with ERS-1, etc. have only limited coverage).

In the evolution of synthetic aperture radar as a remote sensing tool, it has become evident that the use of multiple data channels is the next likely route of advance. This can be accomplished by either multiple frequency operation or the use of multiple polarizations at a single frequency, or both. The analogies at optical wavelengths are the multi-spectral scanner or thematic mapper types of instruments. However, a fully polarimetric SAR (e.g., horizontal and vertical polarization plus relative phase) operating at several frequencies is big and expensive, e.g., the proposed EOS SAR (1,100 kg. instrument with ≈ 5 kW average battery power). In terms of exploring the utility of multiple SAR data channels, a small satellite with limited capability makes sense. As we shall see, the simplest option is a single frequency SAR with full polarimetric capability.

A number of SAR applications are well recognized, for example vege-

tation observations (tropical rain forests), hydrological cycle variables (soil moisture, flooded terrain, snow cover, etc.), sea ice coverage and characteristics, and air-sea interaction parameters. Most of these applications are based primarily on single frequency, single polarization data sets. Recent research suggests that in many cases multiple frequency and/or multiple polarization data would make the interpretation of observations more accurate and reliable. For example, multiple frequency observations of sea ice readily distinguish between first year and multi-year ice without absolute calibration. As with Landsat multi-spectral data, ratios between data channels are used to good effect without absolute calibration.

Probably the simplest implementation of a multiple-data-channel SAR is the use of a single frequency with fully polarimetric data collection. An example of such a design for a small (340 kg), Pegasus launched satellite is given by the MEDSAT design team (1991). This instrument is an L-band (23 cm) SAR with full polarimetric capability and a 4-look ground resolution of 75 m (similar to Landsat MSS). The instrument, including the antenna, has a mass of 70 kg and a DC power draw of 860 W. It is designed to collect a 50 x 250 km SAR image every other orbit with the ability to store four SAR images (as well as 4 x 4-band visible/IR images) on board before downlinking the data. The SAR uses a variety of techniques, including burst-mode to conserve power and make a small satellite deployment possible.

Power and mass are the primary constraints. Multiple polarization (as opposed to multiple frequency) was chosen as the lowest mass and power method of obtaining multiple data channels. The multiple polarization mode is obtained by pairs of radiating patches on the microstrip antenna shown in Figure 11-1 below. Multiple frequency mode would require an additional set of transmit/receive modules and other items as well as a second set of

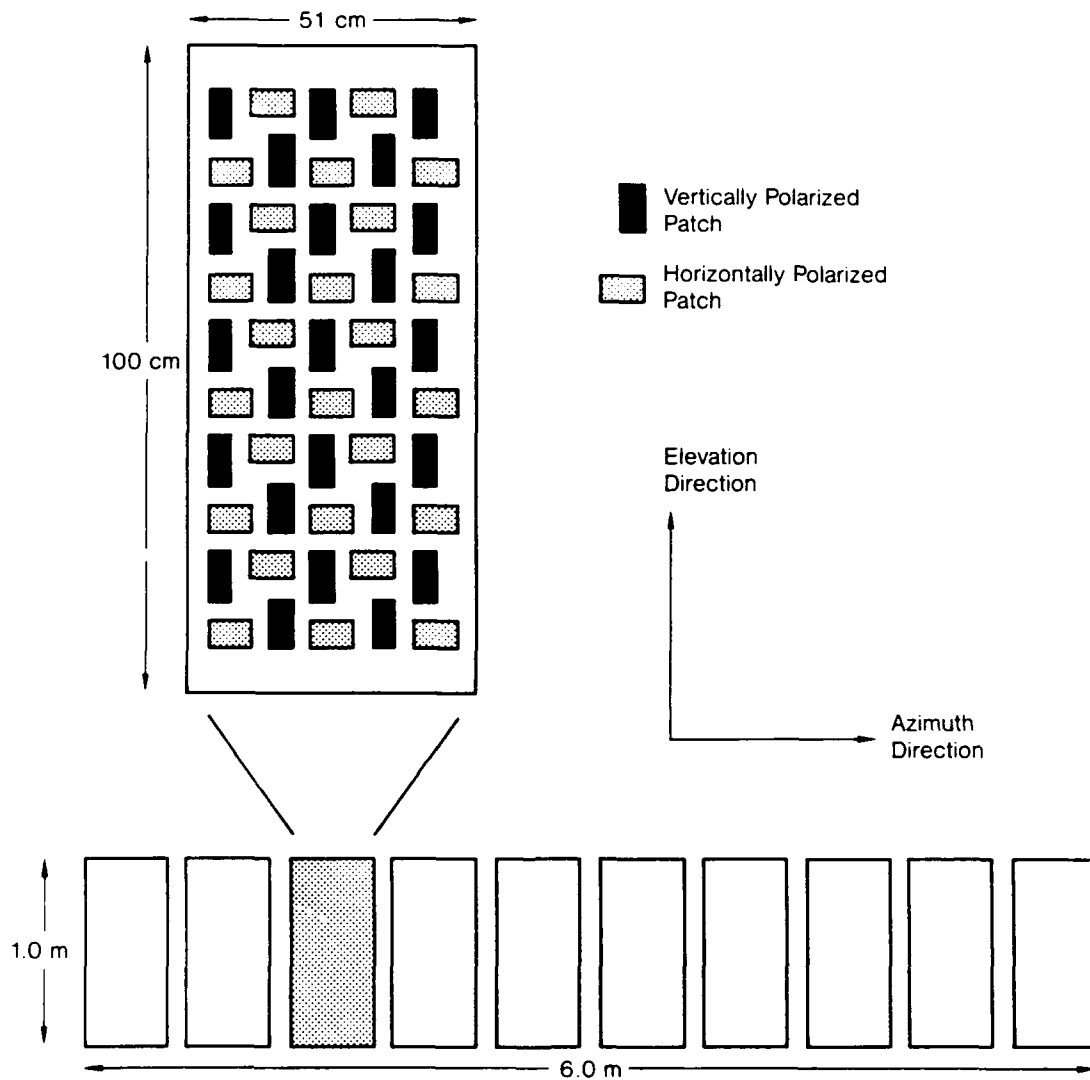


Figure 11-1. a) Multiple polarization SAR antenna for a small satellite SAR. Source: Medsat Design Team (1991).

radiating patches. The main power considerations are the peak discharge rate allowed and the time needed to recharge batteries after periods without sunlight. As a SAR image is improved, i.e., contains more and higher resolution pixels, the power required is increased. Hence, some hard choices must be made in order to keep power consumption low. For example, resolution and swath area must be carefully selected.

We conclude that a small satellite SAR is possible and can explore the utility of multiple SAR information channels. Multiple polarization SAR is less costly to implement in terms of mass and power than multiple frequencies. It is suggested that initially, a small number of sites be covered frequently with significant ground truth, rather than attempting global coverage.

Preliminary design work by TRW and others has resulted in innovative concepts for small SARs, as has the Medsat project (1991). This is a fruitful area for further research.

11.3 A High Resolution Imaging Spectrometer (HIRIS)

The HIRIS instrument originally scheduled for EOS A-2, is to be a high spectral and spatial resolution imaging spectrometer. It has a 30 meter pixel size for imaging, and a spatial swath that is 24 km across. It also has 10 nm spectral sampling resolution, covering the wavelength range from 0.4 microns to 2.45 microns in 192 spectral bands. HIRIS is projected to weigh many hundreds of kilograms, and to consume several hundred watts of power.

HIRIS scientific missions are very varied. They include the study of

biological processes such as vegetation, chlorophyll concentration, leaf properties, and biomass distributions over land, and of chlorophyll concentration, absorption, and backscatter coefficients over ocean. In addition, it would be able to address several cloud characteristics as well as aerosol optical depth, precipitable water, and column density of ozone.

DARPA (Demitry, 1991) and the Brilliant Pebbles program (Ledebuhr, 1991) have both proposed lighter weight imaging spectrometers that would have some, but not all, of the functionality of HIRIS in a package suitable for a small satellite. Figure 11-2 illustrates a candidate design from the Brilliant Pebbles program, to make the point that with a system that is physically small, one has the possibility of gaining increased functionality by having two or three such instruments on a spacecraft, each with somewhat different design parameters.

In general we think that imaging spectrometers are a promising small-satellite application. The spectrometers proposed by both DARPA and the Brilliant Pebbles program are in very preliminary stages of development. They should be regarded as illustrative of the range of smaller instruments that could take on some of HIRIS's functionality on a small satellite. Now that these two concepts have been proposed, it is important for their proposers (as well as potential proposers of alternative implementations) to interact much more strongly with the global change community before fixing on a specific set of capabilities, size, and weight for the instruments.

HIRIS was designed to address a wide variety of scientific missions, not all of which can be addressed from a smaller platform. Hence there needs to be an evaluation of which of the HIRIS missions have the highest priority in the national global change research program, so that the candidates for

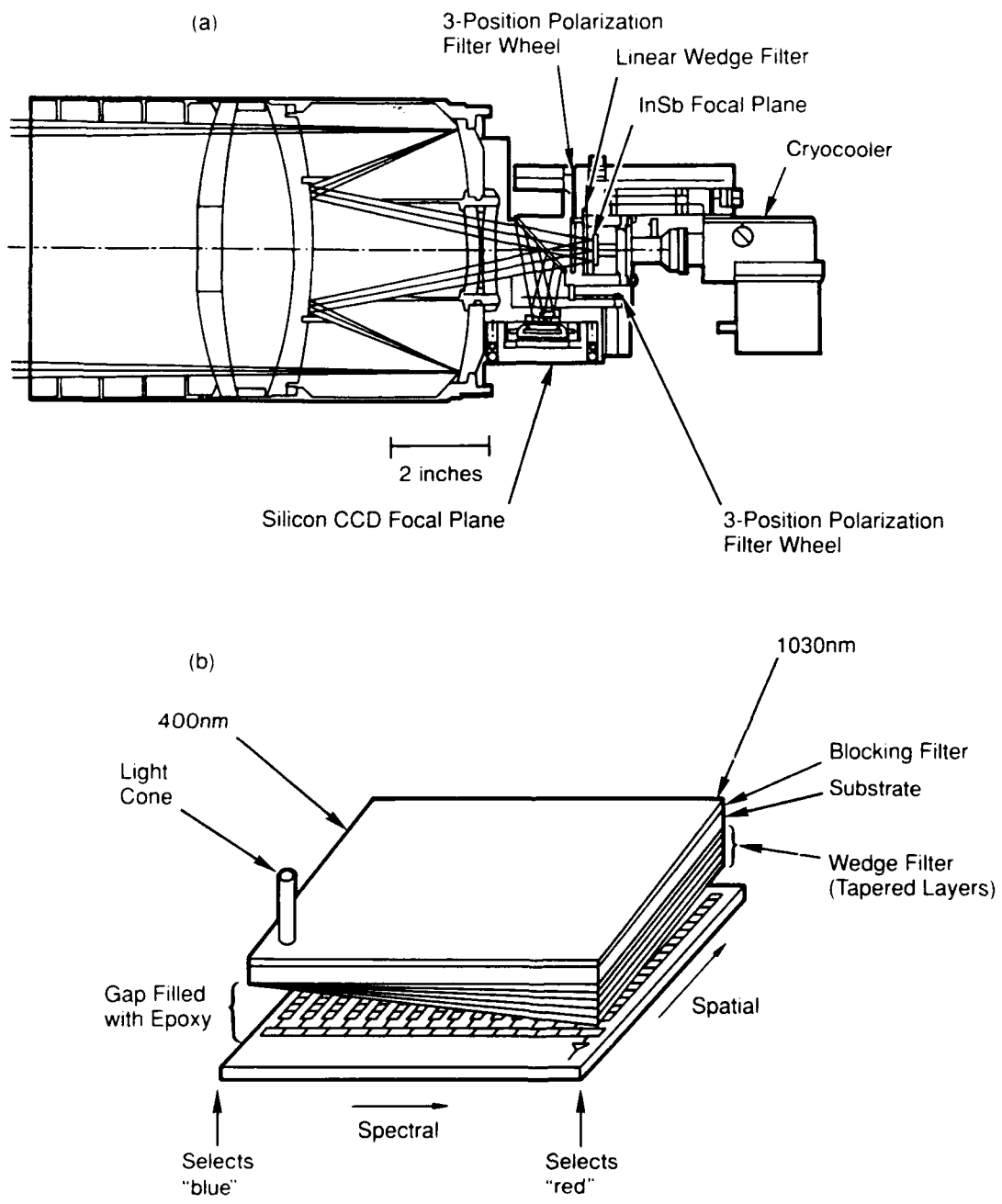


Figure 11-2. a) Conceptual optical design for linear wedge spectrometer. b) Wedge filter concept. Source: Ledebuhr (1991).

small-satellite imaging spectrometer implementations can focus on the most important HIRIS science goals. There also needs to be a dialogue on the issue of whether such an imaging spectrometer needs to fly in formation with EOS instruments in order to provide congruent or simultaneous data, what kind of global and orbital coverage is required for each of the missions of the spectrometer, and what levels of calibration and instrument lifetime are optimum for each of the most important missions.

REFERENCES FOR SECTION 11

1. Demitry, L. (1991), presentation to DOE EOS-A Engineering Review Committee, July 1991, La Jolla, CA.
2. Dube, G. (1991), editor, "Solid State Lasers", Proceedings S.P.I.E. **1223**.
3. Ledebuhr, A. (1991), presentation to JASON summer study, June 1991, La Jolla, CA.
4. Medsat Design Team (1991), "Project MEDSAT", Aerospace Engineering and Atmospheric, Oceanic, and Space Science Departments, The University of Michigan, Ann Arbor, MI.

12 SOME POSSIBILITIES FOR JOINT SURVEILLANCE/GLOBAL CHANGE SMALL SATELLITES

In the summer of 1991, DARPA requested JASON to "define specific payload requirements for a joint Small Sat demonstration which simultaneously satisfies global climate remote sensing and tactical surveillance needs", using multi-spectral sensor technologies. At the same time, DARPA carried out its own concept study in this area, a study of which we were unaware until our own work was finished. Here we will present two concepts devised by JASON, and then we will briefly compare them to the DARPA concept.

There are some good reasons for investigating a joint tactical surveillance/global change satellite, but there are also some inherent mismatches in sensor requirements which cannot be glossed over. In general, tactical surveillance calls for good spatial resolution and modest spectral resolution (usually a few IR bands), while it is usually the other way around for global change research. It would not be very interesting to build a satellite which simply consisted of two sets of instruments, one specialized for surveillance and the other for global change, so we try to do better than that.

Perhaps the best reason for a joint-mission satellite is the transfer of technology between DOD and the global-change research community. DARPA can offer its Small Sat bus and lightweight support hardware, and it will be very useful to both sides for DOD and the global change community to combine in the design of advanced lightweight sensors.

The two JASON concepts concern a satellite with visible and IR sensors,

capable of either high spatial or high spectral resolution; and a dual-purpose lidar satellite, capable of running at low duty cycle and high power or vice versa. The lidar satellite would be a variant of the ONR LASERSCAT proposal to DARPA. Before giving details, we discuss the contrast between surveillance and global change sensor-performance requirements.

12.1 Surveillance vs Global Change

Consider first passive visible and IR surveillance. Table 12-1 gives some nominal spatial resolutions as they might be associated with certain surveillance functions of interest to DOD, as carried out from satellites in low-earth orbit (nominal altitude 400-500 km). The finest resolution of 1 m in the visible ($0.5 \mu\text{m}$) calls for an optics aperture of ≥ 30 cm, which of course corresponds to 10 m resolution in the MWIR at $5 \mu\text{m}$. The main aperture should have a scan capability and a capability to lock onto a given point.

Table 12-2 gives a corresponding set of resolution and other requirements for a global-change satellite using visible and IR sensors. Together, these tables indicate that surveillance requires only a few spectral bands and a much finer spatial resolution than global change, while global change requires coarser spatial resolution and high spectral resolution in numerous IR bands.

Table 12-1: Visible and IR Surveillance Resolution Needs

High resolution:

1-5 m visible
5-10 m MWIR (3-5 μm) — several bands

Used for clutter rejection; target identification; cueing

Medium resolution:

5-25 m visible
25-50 m IR

Used for tracking known targets: ships, trains, trucks, missile launchers, aircraft; for wide-area search

Low resolution:

25 m – 1 km visible
50 m – 1 km IR

Early missile-launch warning; missile tracking for launch point, impact point prediction, handover to interceptor; ship wakes

Table 12-2: Visible and IR Global-Change Needs

Broad-band radiometry: for radiation budget, albedo

Measure total radiation 0.5-4 μm , 4-50 μm
Few pixels—some angular diversity
Each pixel calibrated to $< 1\%$
Spatial resolution 1-20 km

Imaging IR spectrometry: for cloud scenes; surface temperatures;
H₂O column content and profiles

Measure radiation in numerous bands between 0.5-15 μm
High spectral resolution ($\Delta\lambda/\lambda \sim 10^{-2} - 10^{-3}$) in multiple bands
Spatial resolution 0.25-1 km for cloud scenes;
to > 100 km for other missions
Imaging: cross-track scan or scanning FPA

Visible imaging: for cloud scenes; albedo; aerosol opacity

Several visible bands
Spatial resolution 0.25-2 km

12.2 Visible/IR Satellite

This satellite, in its global change role, is fundamentally a cloud and radiation dynamics satellite of a type discussed earlier, with broad-band radiometry and imaging IR spectrometry to meet the needs laid out in Table 12-2.

It will also have a visible camera, presumably a CCD FPA, and optics of the size necessary for the surveillance missions of Table 12-1. As we have already said, this means an aperture of 30 cm or so. The main optics would be used with a variety of secondary optics to direct light to the CCD FPA or to the IR sensors described below. Both the visible and the IR instruments must be capable of dealing with the different requirements for surveillance and global change given in Tables 12-1 and 12-2.

To meet these disparate needs we suggest, for the IR sensors, an imaging FPA array of the type discussed in Section 7, currently under development by the Army (see Figure 12-1). These are arrays of thin-film bolometers some $50\ \mu\text{m}$ on a side, made of vanadium oxide or alternatively barium strontium titanate. They have been constructed in sizes up to 240×340 , and the yield seems good enough to allow bigger arrays if needed. The detectivity of one pixel corresponds to a noise-equivalent ΔT of $\sim 0.1^\circ\text{K}$, at a TV frame rate of 30 Hz.

This array is to be used in two modes. The first is as a high-resolution IR imager for surveillance purposes, viewing a narrow FOV through a telescope whose primary mirror has ≥ 30 cm diameter. A few spectral bands could be selected with simple filters, if need be. The second mode, for global

$$\text{Responsivity} = \frac{\text{Pixel Current} \cdot \text{TCR} \cdot \text{IR absorption}}{\text{Thermal conductance}}$$

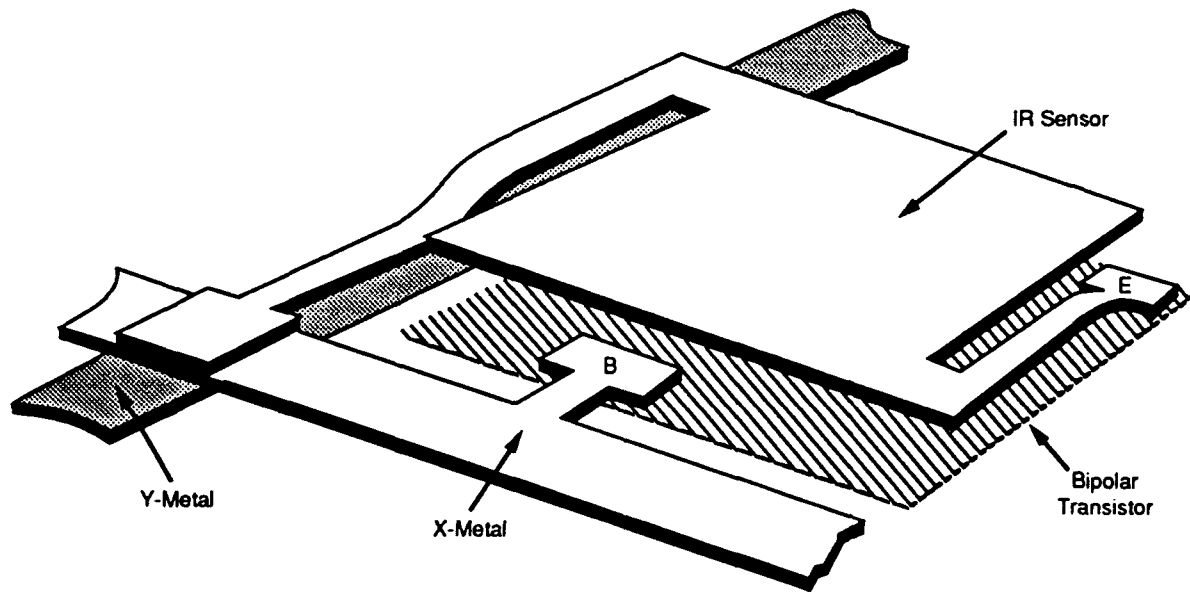


Figure 12-1. LOCUSP FPA Pixel Design

change research, treats large subportions of the array, perhaps the entire array, as single pixels by electronically adding the outputs of a large number of individual detectors. If the FPA has N detectors, and is used as a single pixel, the detectivity will be increased by a factor of $N^{1/2}$, allowing for high signal-to-noise ratios and precision for the global change mission. Rather than forming an image at high (\sim meters) resolution, one simply adds all the photons arriving on the FPA at the same time, which amounts to forming a pixel footprint $N^{1/2}$ times as large which will be in the range of hundreds of meters. This footprint can be further enlarged by shortening the focal length.

This second, few-pixel mode is to be used with some sort of spectral dispersing element, such as a circular variable filter, the closely-related linear wedge filter, or a grating spectrometer for the highest needed resolution. The *few-pixel mode should offer no more calibration problems than any other few-pixel system*, like the NASA radiometer called CERES, and can perform the radiometric mission called for in Table 12-2.

The IR FPA can also be used with every detector corresponding to a single pixel, or at most a few detectors grouped together, using a secondary mirror appropriate to the resolution of ~ 250 m called for in Table 12-2 for the imaging IR spectrometer. Note that this resolution is well-matched to the along-track blurring of some 200 m produced by the satellite motion of 7 km/sec, when the frame rate is 30 Hz. To get higher resolution for surveillance would require a faster frame rate, which may not be easy because of the finite bolometer response time (governed by the detector heat capacitance and thermal conductance), or active pointing of the optics at a fixed point on earth.

It is not likely to be feasible, both for instrumental and data-handling reasons, to use the high spatial resolution modes at a high duty cycle or to cover any large swath. High spatial resolution data gathering for surveillance would be done only as tasked or cued by other sensors, possibly including the satellite's own sensors working at ≈ 1 km spatial resolution. The normal mode of satellite operation would be at a spatial resolution sized for the global change mission, and it would routinely gather radiation and cloud data, as well as surveillance data on missile launches, ship wakes, and the like. At any time it could be converted into the high spatial resolution mode for viewing selected spots.

The instruments described here should be readily compatible with the DARPA Small Sat bus, with a payload of ~ 150 kg and 600 W power.

12.3 Dual-Mode Lidar Satellite

In response to a DARPA request for Small Sat proposals, ONR has suggested a satellite-mounted laser scatterometer (LASERSCAT). It would perform various surveillance missions of the ocean surface, the details of which are classified.

Table 12-3 shows the operational system parameters suggested by ONR, which include an undoubled Nd:YAG laser at 10 J/pulse, 200 Hz PRF, and an efficiency of 0.12 (this high efficiency is due to diode-laser pumping). ONR has also suggested a set of parameters for a demonstration experiment, which differ primarily from those of Table 12-2 by having reduced laser power (1 J at 120 Hz PRF) and a 5 km swath width instead of 50 km.

Table 12-3.

System	
Orbit	Circular Sun-synchronous
Type	400 km
Altitude	7.67 km/sec
Velocity	Global (some possibly mobile)
Ground Station Locations	
Instrument Accommodation	
Option 1	
Launch Vehicle	Taurus (also known as SSLV)
Launch Location	Eastern Test Range
Payload Weight Limit	680 kg
Faring Dimensions	
Cylindrical Section	2.44 m long, 1.27 m diameter
Conical Section	2.64 m long, diameter tapered from 1.27 m to 0.14 m
Power	2 kW (ave.), 5 kW (peak)
Option 2	
Launch Vehicle	Enhanced Taurus (ALLV)
Launch Location	Eastern Test Range
Payload Weight Limit	1045 kg
Faring Dimensions	
Length	2.5 m
Diameter	2.0 m
Power	TBD
Instrument Duty Cycle	25% to 50% active (selectively)
Scan Pattern	
Type	Pushbroom/Whiskbroom
Footprint Size	1.34 km x 1.34 km
Swath Width	50 km
Center of Swath	Nadir
Resolution	
Diffraction-Limited	0.212 m
Optical System Limited	1.5 m
Fundamental Pixel Limited	10 m
Output Pixel Limited	30 m
Instrument	
Transmitter	
Laser	
Type and Wavelength	Nd YAG, 1.064 μ m
Configuration	Diode-pumped, Q-switched
Energy Per Pulse	10 J
Pulse Repetition Frequency	200 Hz
Pulse Duration	20 nsec
Wallplug Efficiency	0.12
Optical Train	
Scanner Aperture Diameter	0.4 mm
Overall Optical Efficiency	0.92
Field-of-View	3.35 mr
Cross-Track Field-of-Regard	125 mr
Receiver	
Optical Train	
Telescope	
Type	Modified Cassegrain
Aperture Diameter	2 m
Focal Distance	4.4 m
Optical Filter Spectral Width	50 to 100 A
Overall Optical Efficiency	0.58
Detector	
Type and Material	Intrinsic Silicon CCD (hybrid)
Mode and Configuration	256 x 256 Photovoltaic

ONR proposes to use conventional silicon CCD arrays as detectors, but they have rather low quantum efficiency (~ 0.3) at the fundamental Nd:YAG wavelength of $1.06 \mu\text{m}$. We believe that they could carry out their fundamental surveillance mission just as well by using a doubled-frequency laser, since the quantum efficiency at $0.53 \mu\text{m}$ is very high, compensating for the $\sim 50\%$ loss in energy that doubling requires. Moreover at $0.53 \mu\text{m}$ the laser light would penetrate deeply into the ocean, allowing for other missions to be carried out. Note that the wall-plug power needed to run the laser is about 16 kW, far greater than available from solar arrays on a small satellite. For this reason, the orbit-averaged duty cycle is low, around 5%, with batteries being used to store solar generated power when the lidar is not in use. In this aspect its operation is similar to that of the MedSat SAR described in Section 11.

Let us compare the parameters in Table 12-3 to those of the NASA lidar GLRS (Geoscience Laser Ranging System) proposed for flight on an EOS-B satellite early in the next century. The GLRS numbers are shown in Table 12-4. GLRS goals are to measure cloud structure and heights, ice sheet heights and other properties, aerosol properties, and even crustal motion and seismic strain using ground-based retroreflectors.

In every respect, GLRS parameters fall well below the maximum for LASERSCAT, so that it is possible to use the LASERSCAT laser for the purposes of GLRS, and at 100% duty cycle, simply by reducing the diode-laser pump power by a factor of 10 and adjusting the PRF.

As with the visible/IR satellite, we see that the global-science mission will be the normal mode of operation, with the surveillance mission carried out on a low duty cycle. Running the laser in GLRS mode constantly will have some, but not an important, impact on the surveillance duty cycle, since it consumes 440 W out of a satellite budget of 2 kW (see Table 13-2).

12.4 The DARPA Proposal

DARPA has independently proposed a visible/IR satellite, using dual-aperture imaging spectrometers as well as a separate radiometer in the CERES (or better, as far as weight goes, LARI) class. The IR part of the spectrometers would have large arrays (512×1024 , 2048) operating at 1-5 μm . DARPA suggests InSb, PtSi, or HgCdTe arrays. It is true that these detectors, in practical terms, are an order of magnitude or so less noisy than the passively-cooled bolometer FPAs discussed above, when the detectors are cooled to 77°K. But cooling places more demands on support hardware, including weight and reliability. Moreover, none of the above detector materials is presently suitable for large FPAs at wavelengths beyond 5 μm (HgCdTe can be used at longer wavelengths in principle, but this has proven to be fairly difficult and expensive in practice). And the most uniform and reliable material for large FPAs, PtSi, has a very poor quantum efficiency ($\approx 1\%$). It is questionable whether InSb or HgCdTe FPAs as large as called for can really be done.

The DARPA proposal also calls for dual apertures to meet the disparate spatial resolution requirements of surveillance and global change. The dual apertures would give the desired large spread in focal lengths, and would be

Table 12-4. GLRS Instrument Parameters

Laser:

Nd:YAG	at	106, 0.53, 0.35 μm
Pulse energy		0.12, 0.06, 0.04 J
PRF		40 Hz

Optics:

Two telescopes, apertures of 18 cm and 50 cm
Laser footprint 70
Pointable $\pm 50^\circ$ along and across track

Mass and power:

350 kg, 660 W (peak), 440 W (ave)

used with the IR imaging spectrometer. A separate small-aperture radiometer, of the CERES or LARI type, would be also carried.

We have not yet had the opportunity for detailed review of the DARPA joint-mission satellite proposal. But the general concept of a joint-mission satellite seems to us to be quite feasible, and we hope that some serious design studies can be made.

A PRE-1998 EARTH SYSTEM SCIENCE EXPERIMENTS CURRENTLY PLANNED FOR SATELLITES

We present tables that summarize the "earth system science" experiments to be flown on small, medium, large, and very large satellites/platforms between now and 1998. US, European, and Japanese satellites are included. The information is sorted in two different ways. The first (Tables A-1 and A-2) is by date of launch. The second sorting is by topic, and shows those satellites/instruments devoted to earth radiation budget measurements (Table A-3), atmospheric chemistry (Table A-4), and synthetic aperture radar (Table A-5). Table A-6 breaks out the currently scheduled "earth probes" relevant to climate studies. Table A-7 includes estimates of the masses of the platforms listed in Table A-1 (this excludes, for example, experiments flying in the shuttle payload bay).

Table A-1 includes the satellite/experiment, the country responsible, the orbital inclination, and a very brief description of the types of experiments. Note that the NOAA satellites (which include AVHRR), the GOES series, and DMSP are not included in this list; each of these series has a launch scheduled every couple of years.

As a matter of interest, Table A-2 shows the large platforms which are considered part of the "international earth observing system" as of summer of 1991 (EOS-A is only one of several).

The instruments listed in Table A-3 are those which will contribute to measurement of the earth's radiation budget. The ERBE instrument

Table A-1. "Earth System Science Experiments"

1991	ERS-1	Europe	Polar	(3 years)	Several instruments: scanning radiometer (cooled IR, 4-channel), passive μ wave (column H_2O), scatterometer, SAR (ocean dynamics, ice), altimeter
	UARS	US	57°	(3 years)	10 instruments: stratospheric chemistry (vertical profiles), upper atmosphere winds (Doppler), T profile, solar radiation (uv+total)
	METEOR-3	USSR	Polar		TOMS (ozone), radiometer (SCARAB), + ??
1992	ATLAS-1	Shuttle/Germany	57°	(days)	IR spectrometer (10-70 km), mm-wave sounder (T, P, H_2O vapor), solar spectrum
	JERS	Japan	Polar	(3 years)	SAR (L-band), high res. vis/IR imager
	LANDSAT-6	US			Enhanced thematic mapper (8 bands, 30 m res.)
	METEOR-4	USSR	Polar		Scanning radiometer (SCARAB) (4 channel) + ??
	TOPEX	France/US	66°	(5 years)	Altimeters (2), μ wave radiometer (H_2O vapor correction)
1993	ATLAS-2	Shuttle/Germany	57°	(days)	Same as ATLAS-1 (underfly UARS)
	SLR-1	Shuttle	57°	(days)	SAR (L, C, x-band), laser (LITE)
	SeaStar	US			Ocean color (8 channel, vis/near-ir)
	TOMS	US (Pegasus)			Ozone
1994	RADARSAT	Canada	Polar	(5 years)	SAR (C-band)
	ATLAS-3	Shuttle/Germany	57°	(days)	ATLAS-1, + cooled IR spectrometer (underfly UARS)
	SRL-2	Shuttle	57°	(days)	SAR (L, C, x-band)
	ERS-2	Europe	Polar	(3 years)	Same as ERS-1, + ozone, + improved scanning radiometer (adds 4 channels in visible)

Table A-1. (Concluded)

1995	ADEOS	Japan	Polar	(3 years)	~Instruments: scatterometer, TOMS (ozone) visible & IR imagers (3), trop. chemistry
	ATLAS-4	Shuttle	57°	(days)	Instruments not yet selected
1996	ATLAS-5	Shuttle	57°	(days)	Instruments not yet selected
	SRL-3	Shuttle	57°	(days)	SAR (L, C, x-band)
1997	TRMM	Japan/US	35°	(3 years)	Radiometer (CERES (1)), active & passive μ wave, medium res. vis/IR imager
	POEM-1	Europe	Polar	(3 years)	~15 instruments: radiometer (CERES (1)), vis/IR imagers (3), trop. and strat. chemistry, altimeter
	ATLAS-6	Shuttle	57°	(days)	Instruments not yet selected
	<TOMS>	US			<Proposed additional earth probe>
	Earth probe	US			Instrument not yet selected
1998	JEOS	Japan	Polar	(5 years)	~12 instruments: visible & IR imagers, active & passive μ wave, trop & strat. chemistry, altimeter, lidar
	Earth probe	US			Instrument not yet selected

Table A-2. Platforms ("EOS")

1995	ADEOS	Japan	Polar	(3 years)	~8 instruments: scatterometer, TOMS (ozone), visible & IR imagers (3), trop. chemistry
1997	POEM	Europe	Polar	(3 years)	~15 instruments: radiometer (CERES (1)), vis/IR imagers (3), trop. and strat. chemistry, altimeter
1998	JEOS	Japan	Polar	(5 years)	~12 instruments: visible & IR imagers, active & passive μ wave, trop. & strat. chemistry, altimeter, lidar
	EOS-A	US	Polar	(5 years)	~12 instruments
1999	EPOP-N1	Europe	Polar	(5 years)	~ 5 instruments (including SAR)
2000	EOS-SAR	US	Polar		SAR
	JEOS	Japan	55°	(5 years)	
2001	<EOS-B>	US	Polar	(5 years)	~12 instruments

Table A-3. Radiation Budget

1991	"Along track scanning radiometer" (ATSR)	ERS-1	4 IR channels, 2 views of same scene (nadir & 45°), no measurements in visible
1992	"Scanning radiometer for earth radiation budget" (SCARAB)	METEOR-2	French instrument, Soviet satellite. 2 broad channels (.2-4m, .2-50m), 2 narrow bands for scene identification. res. ~50 km. (onboard resolution suspect for this flight)
1993	SCARAB	METEOR-3	(Calibration problems may or may not be solved)
1994	"Advanced ATSR"	ERS-2	ERS-1 instrument, with visible channels added
1997	CERES (1)	TRMM	35° orbit; current plans: 1 scanner
<1997>	<CERES (1)>	POEM-1	Proposed polar orbit; 1 scanner
1998	CERES	EOS-A	Polar orbit; 2 scanners

stopped functioning last year; there are currently no instruments making radiation budget measurements. ERS-1, launched in July, 1991, carries an along-track, scanning radiometer (ATSR), which will collect data in 4 IR channels and from two viewing angles (nadir and 45°). Unfortunately, there are no measurements in the visible, so the shortwave component of solar radiation is not measured. The follow-on instrument, the "advanced ATSR", is planned to include shortwave measurements, and is scheduled to fly on ERS-2, in 1994.

The French instrument, SCARAB (scanning radiometer for earth radiation budget), is scheduled to fly on a Soviet satellite in 1992. It is a capable instrument, with two broad channels (.2 to 4 μ , and .2 to 50 μ), and two narrow bands for scene identification. Its resolution is approximately 50 km. The problem with this instrument is the onboard calibration. The Soviets were to supply the onboard calibration source, but apparently will not have it ready for flight. As a result, the instrument is being considered a "prototype", and will not gather useful radiation budget data. A second SCARAB is scheduled to fly on another Soviet Meteor spacecraft one year later. The onboard calibration problem may be solved for this 1993 flight.

The CERES instrument is considered the next generation ERBE. Information on this instrument is available in the EOS handbook. It consists of two broadband scanning radiometers (3 channels each), one cross-track, the other conically scanning. The first CERES is currently scheduled to fly in 1997 as part of the TRMM mission (in a 35° orbit); only one of the two scanners is scheduled for this flight. CERES has also been proposed for flight on the European polar platform, POEM-1, and the two-scanner configuration was proposed to be part of the EOS-A polar platform.

Table A-4 lists those instruments which will make ozone measurements during the next decade. All of these instruments except TOMS and the European "global ozone monitoring experiment" measure other upper atmospheric constituents as well.

TOMS is a small instrument (~ 25 kg) which measures the total ozone in a 50×50 km column by measuring the backscattered UV in 6 wavelength bands. It obtains a global map of the total ozone column every day. (It is the TOMS series which has been making the satellite ozone measurements for the last several years.) The series was in danger of being terminated in 1985, but since then the importance of ozone measurements has been recognized and TOMS instruments are now scheduled to fly approximately every two years, on a variety of platforms. The next TOMS will fly on a Soviet satellite (Meteor) in 1991. In 1993, a TOMS will be the only instrument on a small satellite launched by a Pegasus. In 1995, yet another TOMS will fly on a large Japanese platform.

The UARS satellite carries several instruments to measure the vertical profiles of ozone and other constituents of the upper atmosphere. Its instruments are obtaining vertical profiles with a typical resolution of 3 km. UARS includes a cryogenic limb spectrometer, which measures IR thermal emissions from 20 atmospheric altitudes simultaneously (from 10 to 60 km), in the wavelength range from 3.5 to 12μ ; a microwave limb sounder, which measures thermal emissions at wavelengths of a few millimeters; a stratospheric sounder that employs a filter radiometer and 8 detectors to measure IR emissions between 4.6 and 16.6μ ; and an instrument to measure the atmospheric absorption of solar radiation between 2.4 and 10.2μ . UARS was launched in the fall of 1991 into a 57° inclination orbit, and has a projected lifetime of 1.5 to 3 years.

Table A-4. Ozone Measurements

1991	CLAES ISAMS MLS HALOE TOMS	UARS UARS UARS UARS Meteor	(57°) (57°) (57°) (57°)	Limb spectrometer (cryogenic) (altitudes 10-60 km) "Improved stratospheric and mesospheric sounder" Limb sounder (microwave) (altitudes 5-85 km) Occultation experiment
1992	ATMOS MAS	ATLAS ATLAS	(57°)	Polar IR spectrometer (57°) Mm sounder (ozone from 20-80 km; ~4 km resolution)
1993	ATMOS MAS	ATLAS	(57°)	Same as above (57°)
1994	TOMS "Global ozone monitoring exp."	(Pegasus) ERS-2		Polar Polar orbit; no information on instrument
1995	ATMOS MAS CRISTA TOMS	ATLAS ADEOS ATLAS		Same as above (57°) Same as above (57°) Cryogenic IR spectrometer & telescope (vertical res. ~1 km)
1998	(No details of specific experiments)	JEOS		Polar; Japanese EOS platform studying "tropospheric and stratospheric chemistry"

About once a year, beginning in 1992, a group of instruments (collectively called ATLAS) will be carried in the Space Shuttle payload bay. The instruments will include an IR spectrometer (measuring atmospheric absorption of solar radiation) and a millimeter wave sounder (measuring thermal emissions). The absorption spectrometer is capable of measuring the vertical profile of ozone from 10-100 km with 2 km resolution; the sounder measures the profile from 20-90 km with 4 km resolution. In 1994 a cryogenic IR spectrometer and telescope will be added, which can measure vertical profiles with a resolution of 1 km. These instruments will fly in 57° inclination orbits, on missions lasting approximately 1 week.

The European platform ERS-2 will carry a "global ozone monitoring experiment" into polar orbit in 1994. We don't have information on this experiment at this time.

Table A-5 shows the several synthetic aperture radars scheduled to fly in the 1990's. Four non-US platforms will carry SARs. ERS-1 (1991), and its follow-on ERS-2 (1994), will carry C-band SARs in polar orbit, primarily to look at ocean dynamics and sea ice. They will have a resolution ("nominal high resolution") of about 30 m, fly in polar orbits, and should last 2-3 years. During the same period (1992 launch), the Japanese earth resources satellite (JERS) will carry an L-band SAR. It will also go into polar orbit, and will have similar capabilities. Unlike ERS, JERS-1 will include onboard data storage.

The Canadian RADARSAT, scheduled to launch in 1994, will carry a C-band SAR, again to look primarily at sea ice. Its SAR will have approximately the same resolution, but will have an adjustable look angle and swath

Table A-5. Synthetic Aperture Radars

1991	ERS-1	Polar	(3 years)	C-band (ocean dynamics, ice)
1992	JERS	Polar	(3 years)	L-band
1993	SRL-1 (shuttle)	57°	(days)	L, c, x-band
1994	RADARSAT	Polar	(5 years)	C-band
	SRL-2 (shuttle)	57°	(days)	L, c, x-band
	ERS-2	Polar	(3 years)	L-band
1996	SRL-3 (shuttle)	57°	(days)	L, c, x-band

Notes: SRL-1, 2, and 3 are shuttle-flown radars (follow-ons to SIR-A and SIR-B) and are precursors to the EOS SAR

width. It will also be able to record data on board, a capability which allows it almost global coverage.

Each SAR described above operates at a single frequency and a single polarization. All but RADARSAT also operate at a single look angle and with a specified swath width. The SAR scheduled to fly on the Space Shuttle will be able to operate at multiple frequencies and with HH or VV polarizations (both transmit and receive polarizations are selectable).

The US will be flying SARs on several Shuttle flights. These radars are follow-ons to the shuttle imaging radars (SIR-A, -B, flown in 1981 and 1984) and are supposed to be precursors to an eventual EOS SAR. The "Shuttle Radar Lab", as these flights are called, carries a SAR in the shuttle payload bay. The SAR will operate in L, C, and X-bands with a controllable cross-track look angle and selectable polarizations. Data can be stored onboard.

The Earth Probes, shown in Table A-6, are small instruments. An Earth Probe may fly alone on a small satellite, or it may fly "piggy-back" on a larger platform. The list of Earth Probes in Table A-6 is not complete, but includes those instruments which are directly associated with climate studies.

The TOMS satellite measures the total amount of ozone in a 50×50 km column, and is able to map the global ozone once a day. It measures the backscattered solar UV in 6 channels.

The SeaStar is an ocean color instrument which will measure radiance in eight visible/near-IR bands with 1 km resolution.

The NSCAT is a scatterometer which will provide surface wind speed and direction with high resolution over the oceans. It measures backscattered

Table A-6. "Earth Probes"

1991	TOMS	USSR/Meteor	Ozone measurements
1993	SeaStar	Pegasus	Ocean color (commercial flight; NASA buys data)
	TOMS	US/Pegasus	
1995	TOMS	Japan/ADEOS	Ozone
	NSCAT		Scatterometer
1997	TRMM	Japan/H-2	Precipitation
	TOMS		Proposed additional
	Earth Probe		Approved flight; instrument not yet selected

Note: Though some earth probes are flying as small satellites, several are riding "piggy-back" on larger, previously approved, platforms.

radiation (from more than one angle), which gives the surface radar cross-section as a function of angle, which is affected by wind speed and direction.

TRMM will measure the precipitation between latitudes 35° north and south. The mission includes three types of instruments related to precipitation measurements: a precipitation radar, passive microwave sensors (including a cross-track scanning, multichannel radiometer), and a modified AVHRR (to enable comparison of visible and IR measurements to previous instruments).

Table A-7 shows the approximate weights of the various platforms, and their launch vehicles. In some cases, the weight of the satellite was not known, so the payload weight or the instrument weight was listed instead.

Table A-7. Satellite Weights (and/or launch vehicles)

1991	ERS-1	2600 kg	Ariane 4
	UARS	~7500 kg	Shuttle
	Metero-3	<2500 kg>	<Proton?> (carries an "earth probe": TOMS (25 kg))
1992	JERS	<~2500 kg>	<H-1/2> (carries an "earth probe": NSCAT (237 kg))
	Metero-4	<2500 kg>	<Proton?>
	TOPEX	2650 kg	Ariane-4
1993	SeaStar	(instr. ~25 kg)	Pegasus
	TOMS	(instr. ~25 kg)	Pegasus
1994	RADARSAT	<~2500 kg>	(US ELV)
	ERS-2	~2600 kg	Ariane 4
1995	ADEOS	<~2500 kg>	H-2 (carries 2 "earth probes", TOMS, NSCAT)
1997	TRMM	~3200 kg	H-2 (TRMM = "earth probe", CERES added to platform)
	POEM-1	(instr. ~2400 kg)	Ariane 5 <satellite ~6000 kg>
	<TOMS>	(instr. ~25 kg)	Proposed. (LV or platform not chosen)
	Earth Probe	?	? (instrument not yet selected)
1998	JEOS	<~6000 kg>	(One of the IEOS platforms)
	Earth Probe	?	? (instrument not yet selected)

Notes: Weights in (..) are instrument weights, not satellite weights;
weights in <..> are estimates of satellite weights (based on type if instruments, or ELV)

B MULTIPLE SATELLITE PERFORMANCE FOR EOS MISSION: (Presentation Made by R.L. Garwin to the EOS Engineering Review Advisory Committee, La Jolla, CA, July 1991)

It would, of course, be desirable to have the ability to fly replacement or additional instruments for EOS, or to have a flight schedule that is not determined by the instrument that is latest in readiness to fly. So we look at the feasibility of flying two or more satellites in formation adequate to provide a basis for "congruence" and simultaneity of the line of observation, if so desired.

The problem is broken into two - having the two satellites sufficiently coincident in space and time, and pointing the line of the sight of one satellite sufficiently accurately in comparison with that of the other.

B.1 Coincidence in Space and Time

We assert that the two satellites can have identical observing positions (to ± 5 m) at the time each makes an observation.

We plan to fly the two satellites in trail at a spacing of 200 m, which means that at orbital speed of almost 8 km/s (really 6.7 km/s, but we continue to use 8) a satellite will arrive at the position of its predecessor in 26 ms. If the satellite orbits can be matched sufficiently closely, and if the pointing

of the line of sight can be done sufficiently accurately, then the line of sight at the sensor will be coincident ± 5 m, and the second observation will be delayed 26 ms from the first.

We intend to match the orbit essentially perfectly, and to provide sufficiently frequent bursts of propulsion to keep one satellite from moving from the desired relative position, despite a difference in drag. Nevertheless, the eastward rotation of the Earth means that for a line of sight directed toward nadir (approximately toward the center of the Earth), the point observed by the second satellite will be due West of the point observed by the first satellite by the ratio of Earth equatorial linear velocity to satellite linear velocity, multiplied by satellite spacing and the cosine of the latitude. In the example given (200 m satellite spacing), this amounts to 12 m of displacement at the Equator. This is being compensated by having the second satellite look slightly to its right in the ascending pass, and slightly to its left in the descending pass. The half-amplitude of this squint (12 m) is about 4 arc-seconds of angle.

How do we "station keep" to this accuracy?

To simplify this presentation we refer to three very useful papers, rather than deriving equations ourselves. So the presentation is heuristic, but we have no doubt that the conclusions are correct. We refer to (I) the joint report by NASA personnel and those of TRW comparing the results of their individual papers, (II) and (III).

In (II) we find that two spacecraft in the nominal EOS orbit at 705 km altitude and at solar maximum would have a separation that grows to 3.5 km in six days, if the "ballistic coefficient" of the two satellites differs by

40%. The ballistic coefficient is given by the ratio of mass to the product of frontal area and drag coefficient, and this whole parameter is often rendered as β . In (II) we also find that this growth would require a Δv correction of 7×10^{-3} m/s (really 14 mm/s) in six days.

In order to prevent initial position or velocity errors from resulting in such large displacements that grow secularly in time or oscillate with the orbital period, one might attempt to measure and to control the initial conditions extremely accurately. In fact, it is far better to measure what matters – namely the time dependence of the relative position of the two satellites, and to deduce from this behavior the corrections that must be made to the satellite velocity in order to achieve such accuracy in trail. Thus, we measure drift, not β or ΔR .

So if one wants to stabilize a separation of 200 m to an accuracy of a few m, it is necessary to measure that separation only to this accuracy, but to measure it over an orbital period to correct the oscillating components of displacement and over several orbital periods in order to correct for the difference in drag. Of course, it is certainly possible to match the drag of the two satellites before launch, and even to trim the drag on orbit, and there is little doubt that this could be done to 1% or even 0.1%. Nevertheless, we continue to assume in this example a ratio of β of 1.4:1. In any case there is even a small reduction of drag on the trailing satellite due to the wake of the leading satellite.

This “3.5 km” drift acquired in six days (Ref. II) grows like the square of time, since the higher-drag satellite will have an orbital altitude declining linearly with time and an orbital speed that increases linearly with time.

Since we want to reduce the maximum 3.5 km displacement to 10 m (in this example), we need to reduce it by a factor of 350. If velocity corrections were given not every six days but every 6/19 days, the desired goal would be achieved. Of course, the 7 mm/s velocity change (six days) would be reduced to something like 0.4 mm/s every eight hours. One could use cold gas for this purpose, and with a specific impulse of 100 s (exhaust speed of about 1 km/s), one would expend some 0.4 ppm of the spacecraft mass with each shot. For a 5-tonne spacecraft, this would amount to about 2 g of gas per shot (6 g per day) or some 2 kg/hr. A slightly lower specific impulse would make no significant difference. (These values are still negligible if doubled or if reduced by a factor 40 because satellite β s are matched to 1% accuracy.)

We assume that the reference satellite has a GPS receiver, while the other(s) is optical sensing and microwave ranging to the reference satellite. It is only necessary to determine the range to about 1 m out of 200 m, and to measure the angle between satellites to a corresponding accuracy of a few milliradian (mr). It is extremely important that one allow rocket pulses every few hours, and adaptive control, so that most of the correction can be applied on a schedule, and open loop.

For instance, any maneuver to adjust ground track should be done by the reference satellite and (to good accuracy) simultaneously by other satellites, according to the adaptively calibrated thruster performance.

As an aside, since EOS is very likely to communicate via TDRSS or some other similar relay satellite, it is interesting to note that the rf footprint of a relay satellite would cover two or more EOS birds in trail at 200 m spacing.

At this point, we believe that we have described a system that will work

to keep two satellites on the same orbital track to the required accuracy. The key to this performance is to measure what matters, and to be willing to give a set of thruster pulses every few hours.

B.2 Pointing

Now for pointing! It is not our purpose to set the requirements for the relative pointing accuracy for various instruments in the EOS suite. The reference satellite is required to direct its line of sight (LOS) to a certain accuracy. Some of the other sensors must then point “accurately” with respect to that reference LOS. There are several possibilities. First is the case of a single small pixel positioned with respect to a single large pixel from another instrument. Both (II) and (III) discuss the relative pointing accuracy and indicate that in this case it should be no more than 0.5 of the large pixel size. For a normal distribution of pointing error, this will be achieved 67% of the time if the “0.50” is taken as $1 = \delta$.

The second case consists of two pixels of comparable size, for which a similar result (0.25 of pixel size) holds for allowable pointing error.

The third case is two imaging sensors (“staring sensors”). In this case, there is the possibility of re-mapping the output images in order to do the positioning after the data are obtained, rather than in the sensor itself.

The fourth example is that of two push-broom sensors, in which one has a line of small pixels which is to be registered with a line of large pixels. Here, too, there is the possibility of re-mapping the resulting images.

In addition, one has to consider the question of hard-edge vs. soft-edge pixels. In fact, unless one is guaranteed that the entire scene within a large pixel is uniform, there is not a lot to be gained by knowing the absolute position of a (single) small pixel within the large pixel.

There are different cases, also, if the good overlap is required for registration of output images, or for calibration of the sensor, for which special, uniform areas could (and should) be chosen.

As one example (I) shows HIRIS with an instantaneous field of view (IFOV) of 30 m, while ASTER has an IFOV of 90 m. A required pointing accuracy of 30 m at 705 km corresponds to 2 arc-seconds standard deviation for 99% confidence in overlap or 7 arc-seconds for 67% confidence in overlap (I).

B.3 Pointing Accuracy and Stability

Now for some considerations of pointing accuracy and stability. A nominal (really very poor these days) navigation drift rate of 1 deg/hr corresponds to 1 arc-seconds in one second.

“Blind pointing” of an Earth-oriented satellite such as EOS would normally be done by determining satellite position continuously by GPS, determining the Earth position by a clock, and determining (and establishing) satellite orientation by star sensors.

On such a satellite, the star sensors could be body-mounted, so that stars pass the slits of these star sensors. The satellite would have a constant

angular rate set up by reaction shells or control-moment gyros (CMGs).

(At one micron wavelength, one could obtain a star image of 10 arc-seconds diameter by the use of a 3-cm diameter lens. For a 100-min orbit, the transit time of a star across this 10 arc-seconds image diameter or slit would be 50 ms. There is no difficulty in determining the center of such an image or passage to better than 1%.) In principle, such accuracies would allow independent pointing of two satellites with accuracy adequate to provide the requisite overlap confidence. In practice, however, there would be biases between the instrument mountings, which could, in fact, be determined by appropriate calibration in flight. Still, it would be better, if possible, to “measure what matters” and determine the pointing error between the two LOS by the data output.

For instance, one could remap the data by cross correlation, if, indeed, the data were obtained, as in the case either of steering sensors or push-broom sensors, or even in the case of a single pixel to be correlated with a push-broom sensor.

For calibration of a single pixel with a single pixel of another sensor, one can measure and then correct (the pointing) to the requisite accuracy. Consider a reference satellite (R) with a large single pixel tracking at nadir, followed at the desired 200 m by a “following” (F) satellite with a smaller pixel. Both pixels are moving over the ground at almost 8 km/s along the ground track.

For example, suppose there are two roads or natural features which make angles of +45 deg and -45 deg with the ground track. These should be not too far apart. As each sensor passes the ground features, there is a

transition from one sensor level to another at the beginning of each obstacle, and the center (in time) of this transition can be very accurately measured. One could, in fact, have this re-pointing pattern followed by a "calibration field" for which re-pointing would have been accomplished.

In Figure B-1, the first shows the trace of the R pixel and the F pixel (the broad dark track graph shifted by 26 ms in order to make the procedure clearer). This shows correct trail and correct cross-track positioning.

The second graph shows the F satellite correct in trail, but offset to the right. It intercepts the first obstacle later and the second obstacle earlier than it should, so that the spacing between transitions of the F satellite is less than normal. The third graph shows the F satellite ahead of the desired position in trail but in correct cross-track position. The interval between the transitions for F is the same as that between transitions for R, but the pattern is advanced in time. Such measurements can be made to 1% of the relevant pixel size, which is more than sufficiently accurate for acquiring re-pointing data.

Finally, one might consider active laser reference. In this approach, a solid-state laser in the reference satellite would illuminate a region on the ground, which is to be the center of the pixel of the following satellite. When such measurements are to be taken, 10-cm diameter optics on each satellite would require a laser of about 5 W power when it is operating, for an integration time of one second.

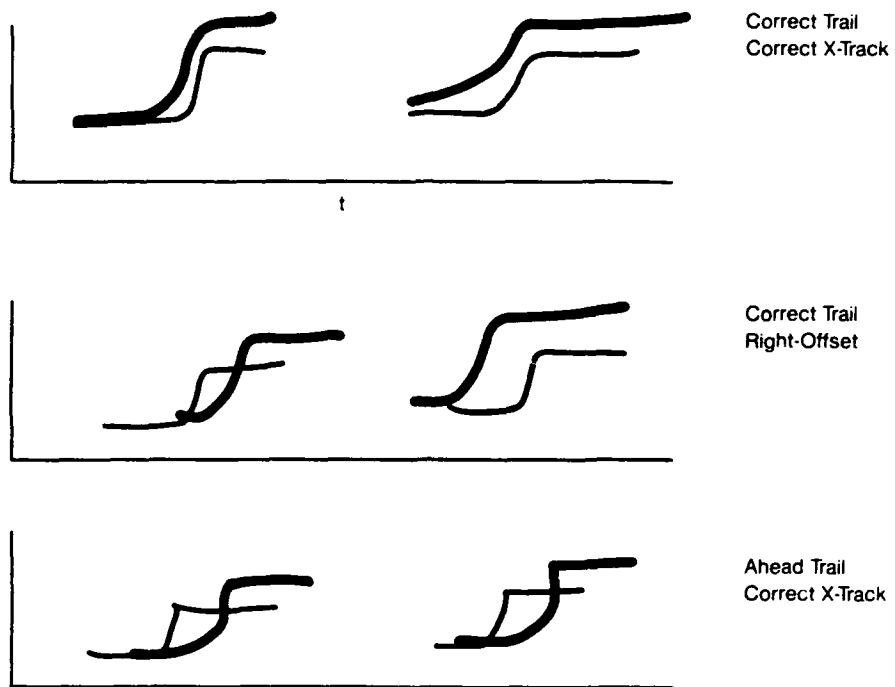


Figure B-1. Acquiring re-pointing data.

REFERENCES FOR APPENDIX B

1. 07/03/91 Memo C.J. Scolese to Mark Pine re "Comparison of the TRW paper and the AAS/AIAA Paper," with 5-page enclosure signed by TRW authors and NASA authors. ("I" in the text.)
2. 1991 "Coordinated Measurements for Earth Observations," by C.D. Graves, P. Gottlieb, A. Rosen (TRW), (25 pp. plus 5 Tables and 6 Figures). ("II" in the text.)
3. 02/11/91 "Field of View Location and Formation Flying for Polar Orbiting Missions," by C. Scolese, D. Folta, F. Bordi, Paper AAS-170. ("III" in the text.)

DISTRIBUTION LIST

CMDR & Program Executive Officer
US Army/CSSD-ZA
Strategic Defense Command
PO Box 15280
Arlington, VA 22215-0150

Mr John Bachkosky
Deputy DDR&E
The Pentagon, Room 3E114
Washington, DC 20301

Dr Joseph Ball
Central Intelligence Agency
Washington, DC 20505

Dr Peter M Banks
3485 Narrow Gauge Way
Ann Arbor, MI 48105

Dr Arthur E Bisson
DAWSD (OASN/RD&A)
The Pentagon, Room 5C675
Washington, DC 20350-1000

Dr Albert Brandenstein
Chief Scientist
Office of Nat'l Drug Control Policy
Executive Office of the President
Washington, DC 20500

Mr Edward Brown
Assistant Director
DARPA/NMRO
3701 North Fairfax Drive
Arlington, VA 22203-1714

Dr H Lee Buchanan, I I I
Director
DARPA/DSO
3701 North Fairfax Drive
Arlington, VA 22203-1714

Dr Curtis G Callan, Jr
Physics Department
PO Box 708
Princeton University
Princeton, NJ 08544

Chief, Library Branch [2]
AD-234.2, FORS
U S Department of Energy
Washington, DC 20585

Dr Ferdinand N Cirillo Jr
Central Intelligence Agency
Washington, DC 20505

Brig Gen Stephen P Condon
Deputy Assistant Secretary
Management Policy &
Program Integration
The Pentagon, Room 4E969
Washington, DC 20330-1000

Ambassador Henry F Cooper
Director/SDIO-D
The Pentagon, Room 1E1081
Washington, DC 20301-7100

Dr John M Cornwall
Department of Physics
Univ of California/Los Angeles
Los Angeles, CA 90024

D A R P A Library
3701 North Fairfax Drive
Arlington, VA 22209-2308

DTIC [2]
Cameron Station
Alexandria, VA 22314

DISTRIBUTION LIST

Mr John Darrah
Senior Scientist and Technical Advisor
HQAfSPACOM/CN
Peterson AFB, CO 80914-5001

Dr Gary L Denman
Director
DARPA/DIRO
3701 North Fairfax Drive
Arlington, VA 22203-1714

Director, Ames Laboratory [2]
Iowa State University
Ames, Iowa 50011

Dr Nancy Dowdy
USACDA
320 21st Street NW
Washington, DC 20451

Professor Freeman J Dyson
Institute for Advanced Study
Olden Lane
Princeton, NJ 8540

Mr John N Entzminger
Chief Advance Technology
DARPA/DIRO
3701 North Fairfax Drive
Arlington, VA 22203-1714

Capt Kirk Evans
Director Undersea Warfare
Space & Naval Warfare Sys Cmd
Code PD-80
Department of the Navy
Washington, DC 20363-5100

Dr Norval Fortson
Department of Physics
FM-15
University of Washington
Seattle, WA 98195

Dr David Galas
Associate Director for Health
& Environmental Research
Office of Energy Research
ER-70/GTN
U S Department of Energy
Washington, DC 20585

Dr Richard L Garwin
IBM TJ Watson Research Center
PO Box 218
Route 134 & Taconics State Prkwy
Yorktown Heights, NY 10598

Dr S William Gouse
Sr Vice President and General Manager
The MITRE Corporation
Mail Stop Z605
7525 Colshire Drive
McLean, VA 22102

Mr Thomas H Handel
Office of Naval Intelligence
The Pentagon, Room 5D660
Washington, DC 20350-2000

Maj G Hard
Director of Space and SDI Programs
Code SAF/AQS
The Pentagon
Washington, DC 20330-1000

DISTRIBUTION LIST

Dr Robert G Henderson
Director
JASON Program Office
The MITRE Corporation
7525 Colshire Drive
Mailstop Z561
McLean, VA 22102

Dr Barry Horowitz
President and Chief Executive Officer
The MITRE Corporation
202 Burlington Road
Bedford, MA 01730-1420

Dr William E Howard III [2]
Director
Space and Strategic Technology Office
Assistant Secretary of the Army
The Pentagon, Room 3E474
Washington, DC 20310-0103

Dr Gerald J Iafrate
US Army Research Office
PO Box 12211
4330 South Miami Boulevard
Research Triangle Pk, NC 27709-2211

JASON Library [5]
The MITRE Corporation
Mail Stop W002
7525 Colshire Drive
McLean, VA 22102

Dr George Jordy [25]
Director for Program Analysis
US Department of Energy
ER30 OER
Washington, DC 20585

Dr O' Dean P Judd
Los Alamos National Lab
Mail Stop A-110
Los Alamos, NM 87545

Dr Bobby R Junker
Office of Naval Research
Code 412
800 North Quincy Street
Arlington, VA 22217

Dr Steven E Koonin
Kellogg Radiation Laboratory
106-38
California Institute of Technology
Pasadena, CA 91125

Technical Librarian [2]
Argonne National Laboratory
9700 South Cass Avenue
Chicago, IL 60439

Research Librarian [2]
Brookhaven National Laboratory
Upton, NY 11973

Technical Librarian [2]
Los Alamos National Laboratory
P O Box 1663
Los Alamos, NM 87545

Technical Librarian [2]
Oak Ridge National Laboratory
Box X
Oak Ridge, TN 37831

Technical Librarian [2]
Pacific Northwest Laboratory
Battelle Boulevard
P O Box 999
Richland, WA 99352

DISTRIBUTION LIST

Technical Librarian [2]
Sandia National Laboratories
P O Box 5800
Albuquerque, 87185

Technical Librarian [2]
Sandia National Laboratories
P O Box 969
Livermore, CA 94550

Technical Librarian [2]
Lawrence Berkeley Laboratory
One Cyclotron Road
Berkeley, CA 94720

Technical Librarian [2]
Lawrence Livermore National
Laboratory
P O Box 808
Livermore, CA 94550

Dr Gordon Mac Donald
IGCC
UCSD/0518
9500 Gilman Drive
La Jolla, CA 92093-0518

Mr Robert Madden [2]
Department of Defense
National Security Agency
Attn: R-9 (Mr. Madden)
Ft George G Meade, MD 20755-6000

Dr Arthur F Manfredi Jr [10]
OSWR
Central Intelligence Agency
Washington, DC 20505

Mr Joe Martin
Director
OUSD(A)/TWP/NW&M
The Pentagon, Room 3D1048
Washington, DC 20301

Mr James J Mattice
Deputy Assistant Secretary
SAF/AQ
The Pentagon, Room 4D-977
Washington, DC 20330-1000

Dr Claire E Max
617 Grizzly Peak Boulevard
Berkeley, CA 94708

Mr. Ronald D Murphy
Director
DARPA/ASTO
3701 North Fairfax Drive
Arlington, VA 22203

Dr Julian C Nall
Institute for Defense Analyses
1801 North Beauregard Street
Alexandria, VA 22311

Dr Gordon C Oehler
Central Intelligence Agency
Washington, DC 20505

Dr Peter G Pappas
Chief Scientist
US Army Strategic Defense Command
PO Box 15280
Arlington, VA 22215-0280

DISTRIBUTION LIST

Dr Ari Patrinos
Director
Environmental Sciences Division
ER74/GTN
US Department of Energy
Washington, DC 20585

Dr Bruce Pierce
USD(A)D S
The Pentagon, Room 3D136
Washington, DC 20301-3090

Mr John Pollard
Night Vision & Electro Opns Directorate
Attn: AMSEZ-RD-NVD
Fort Belvoir, VA 22060

Mr John Rausch [2]
Division Head 06 Department
NAVOPINTCEN
4301 Suitland Road
Washington, DC 20390

Records Resource
The MITRE Corporation
Mail Stop W115
7525 Colshire Drive
McLean, VA 22102

Dr Sally Ride
UCSD
California Space Institute
9500 Gilman Drive
La Jolla, CA 92093-0221

Dr Malvin A Ruderman
29 Washington Square West
New York, NY 10027

Dr Fred E Saalfeld
Director
Office of Naval Research
800 North Quincy Street
Arlington, VA 22217-5000

Dr John Schuster
Technical Director of Submarine
and SSBN Security Program
Department of the Navy OP-02T
The Pentagon, Room 4D534
Washington, DC 20450-2000

Dr Barbara Seiders [2]
Chief of Research
Office of Chief Science Advisor
Arms Control & Disarmament Agency
320 21st Street NW
Washington, DC 20451

Dr Philip A Selwyn [2]
Director
Office of Naval Technology
Room 907
800 North Quincy Street
Arlington, VA 22217-5000

Superintendent
Code 1424
Attn: Documents Librarian
Naval Postgraduate School
Monterey, CA 93943

Dr Sam B Treiman
60 McCosh Circle
Princeton, NJ 8540

DISTRIBUTION LIST

U S Department Of Energy
Procurement/Contracts Division
(DOE IA No. DE-AI05-90ER30174)
Oak Ridge Operations Office
P O Box 2001
Oak Ridge, TN 37831-8757

Dr George W Ullrich [3]
Deputy Director
Defense Nuclear Agency
6801 Telegraph Road
Alexandria, VA 22310

Ms Michelle Van Cleave
Asst Dr/National Security Affairs Office
Science and Technology Policy
New Executive Office Building
17th and Pennsylvania Avenue
Washington, DC 20506

Dr John Fenwick Vesecky
1945 Cambridge Road
Ann Arbor, MI 48104

Mr Richard Vitali
Director of Corporate Laboratory
US Army Laboratory Command
2800 Powder Mill Road
Adelphi, MD 20783-1145

Dr Robert M Westervelt
52 Follen Road
Lexington, MA 02173

Dr Edward C Whitman
Deputy Asst Secretary of the Navy
C3I Electronic Warfare & Space
Department of the Navy
The Pentagon, Room 4D745
Washington, DC 20350-5000

Mr Donald J Yockey
U/Secretary of Defense For Acquisition
The Pentagon, Room 3E9333
Washington, DC 20301-3000

Dr Fredrik Zachariasen
California Institute of Technology
452-48
1201 East California Street
Pasadena, CA 91125

Dr Linda Zall
Central Intelligence Agency
Washington, DC 20505

Mr Charles A Zraket
Trustee
The MITRE Corporation
Mail Stop A130
202 Burlington Road
Bedford, MA 01730